DIE FORMING OF SHEET METAL USING DISCRETE SURFACES

by

BRUCE ALAN OLSEN

B.S. Worcester Polytechnic Institute
(1978)

SUBMITTED IN PARTIAL FULFILLMENT
OF THE REQUIREMENTS FOR THE
DEGREE OF

MASTER OF SCIENCE

at the

MASSACHUSETTS INSTITUTE OF TECHNOLOGY

June 1980

Signature of Author.....
Department of Mechanical Engineering
June 13, 1980

Certified by.....
David E. Hardt
Thesis Supervisor

Accepted by.....
Warren M. Rohsenow
Chairman, Department Commitee

DIE FORMING OF SHEET METAL USING DISCRETE SURFACES

by

BRUCE ALAN OLSEN

Submitted to the Department of Mechanical Engineering on June 13, 1980 in partial fulfillment of the requirements for the Degree of Master of Science.

ABSTRACT

A test program was carried out to evaluate the feasibility of a discrete die surface (DDS) for sheet metal forming. A DDS contains a positionable array of discrete elements which may be arranged to form a desired sheet shape. A DDS test fixture was designed, fabricated, and tested to determine its feasibility in terms of accuracy, repeatability, shape limitations, and surface quality. The fixture was a mated die configuration with spherically tipped pins as the discrete elements.

The results showed dimpling of the sheet surface did not occur. The nominal repeatability of the system was 1.5%, and the set up accuracy 6%. The DDS was determined feasible in the configuration used and recommendations were made for future work in the area.

Thesis Supervisor: Dr. David E. Hardt
Title: Assistant Professor of Mechanical Engineering

ACKNOWLEDGEMENTS

The author wishes to thank David Hardt, David Gossard, Kim Stelson, Blair Allison, and Charles Dimarzio for their contributions to the development of this research and the final report. Leslie Regan, David Stanton, and Leslie Bianchi are also gratefully acknowledged for their help in completing the final report. This research grew from work done for the Air Force under Contract #F33615-78-C-5111.

TABLE OF CONTENTS

LIST OF FIGURES

LIST OF TABLES

CHAPTER 1

INTRODUCTION

1.1 An Overview

A discrete die surface (DDS) appears to be an attractive replacement for a conventional forming die to reduce costs of sheet metal forming by simplifying or automating die design and fabrication. A DDS is a surface consisting of discrete elements that can be positioned to form a desired contour. The control and positioning aspects of a DDS system, as well as the mechanical feasibility of a one-dimensional die have been previously demonstrated (Hardt and Gossard (1980)). The next logical step in evaluating the DDS concept was to test the feasibility of the forming process using a two-dimensional DDS. To meet this objective, a DDS test fixture was designed, fabricated, and tested to determine its feasibility in terms of accuracy, repeatability, shape limitations, and surface quality. The complete program involved conceptual analysis, material considerations, experimentation, and data evaluation. It was determined that the DDS was feasible in the configuration used, with acceptable repeatability and no observable dimpling of the sheet metal surface. Also, some recommendations toward the goal of a working DDS system have been established in this report.

1.2 Background

Before beginning a detailed description of this test program, it may be worthwhile to review the subject of die forming in

general and prior work with the DDS which led to the present research.

Die forming is the most commonly used method of sheet metal forming of sheets with compound curvature (where the formed sheet has curvature in more than one direction). The four most frequently used methods for die forming are illustrated in Figure 1.1. These are: hydroforming, where the sheet is compressed between a die and a compliant pad; mated die forming, where it is compressed between two mated dies; stretch forming, where the material is stretched over a die; and spin forming, where it is pressed against a spinning die with a blunt tool. Manufacture of the dies themselves is an expensive process since they must be machined, then adjusted by a trial and error method to account for material springback (elastic recovery of the metal upon unloading). Also, they must be stored when not in use if they are to be used again. This makes the process quite costly for short production runs. The concept of the DDS arose to answer the problems of die design and storage. With a DDS, all of the die configurations could be programmed and stored in a computer.

One application of the DDS concept has been found in Japan, where ship hulls are formed in sections in a giant, 3 row press (Iwasaki et al. (1977)). In this machine, 30 hydraulic rams are located both above and below the hull sheet. The rams are displaced until the correct curvature of the sheet is reached.

FIGURE 1.1: CONVENTIONAL DIE FORMING METHODS

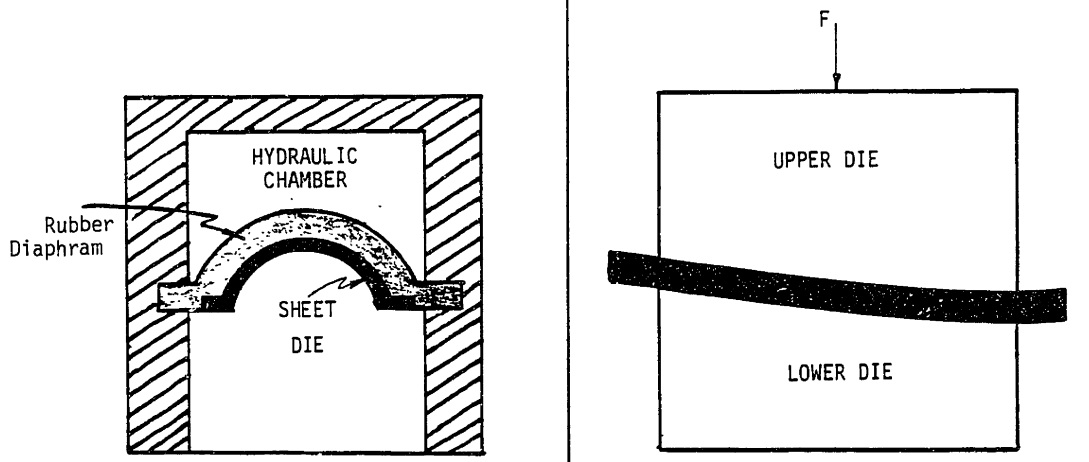

a) Hydro forming

b) Die forming

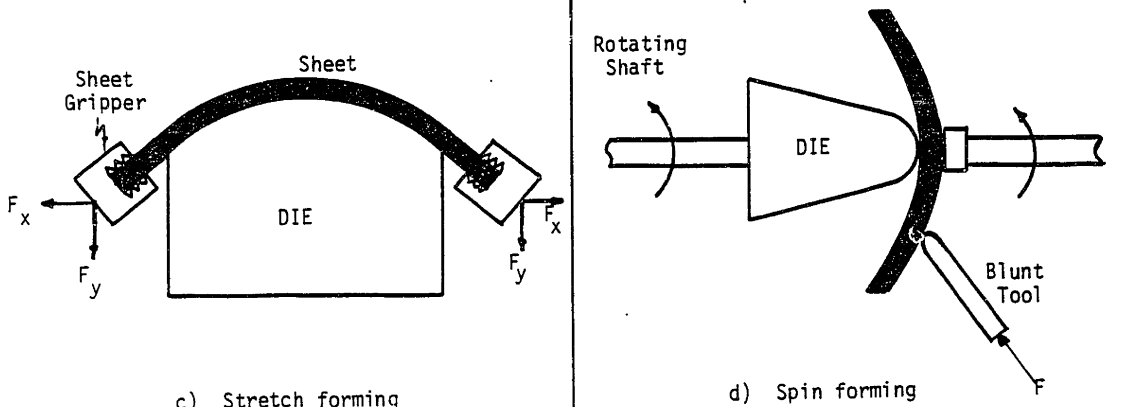

c) Stretch forming

d) Spin forming

Since the curvature is slight, and the material quite thick in this application, the discontinuities of the forming surface do not cause any problems in forming.

Original work on the DDS concept at M.I.T. began in the Fall of 1978. The initial work was with the control and positioning of a DDS (Gossard et al. (1980)). Appendix A contains details related to this work. After this initial stage, a one-dimensional 8 pin DDS was built and some experiments were performed (Hardt and Gossard (1980)). This was the first experimentation done with a DDS and showed that the control, positioning, and locking of the device worked well. Some results for one-dimensional forming (bending in one direction) were obtained and showed the concept worthy of further study.

The author of this thesis was closely involved with the initial developments of the DDS and it became apparent that a two-dimensional DDS had to be built to test the feasibility of the concept as it applied to forming sheets of compound curvature. This led to the design, fabrication, and testing of a DDS text fixture which was the subject of this research.

1.3 Organization

The remainder of this report is divided into five chapters which describe the complete research program. Chapter 2 describes the basic principles of a DDS system and some initial design con-

siderations. Chapter 3 examines material considerations and how they pertain to the design of a DDS. Chapter 4 covers the objectives and methods of an experiment performed using a DDS. Chapter 5 analyzes the results of this experiment in terms of four feasibility criteria. Finally, Chapter 6 draws conclusions on the basis of the analysis in Chapter 5, and makes some suggestions for future work.

CHAPTER 2

BASIC PRINCIPLES AND DESIGN OF A DISCRETE DIE SURFACE

2.1 Introduction

A discrete die surface (DDS) is a surface composed of discrete elements that can be positioned to form a desired contour. This type of die is different from a conventional die, in that these discrete elements are individually adjustable, and their positions may be programmable; and in that the forming surface is discontinuous. The basic principle is to replace the "one-shot" milled die with a die composed of individual components which may be easily rearranged to form different die surfaces. A control concept that could be expanded to a three-dimensional surface which could be programmed to form contours in sheet metal was the subject of the precursor to this work. Since the original interest was in the area of control, a prototype DDS was built to show that the control concept was feasible, as was described in Section 1.4.2 (Hardt and Gossard (1980)). From their original tests, the need arose to investigate the mechanical and material-properties parts of the process. To meet this need, a simple, manually-controlled machine that was adjustable, but not programmable, was built to investigate the various aspects of the forming process.

2.2 Types of Forming Where the DDS has Application

Three types of forming were investigated using the DDS surface concept. Some original work was done using rubber pads for forming. The problem that occurred with this type of forming was that the sheet metal was only supported at discrete points on one side and across the entire surface of the other side. (See Figure 2.1a). This resulted in a large amount of dimpling in the formed metal. (See Figure 2.1b) Another type of forming, that was considered but never implemented, was stretch forming. In this process, the material would have been stretched over the die. (See Figure 2.2). This method is commonly used in industry and is a prime subject for future work. For the present work, however, it was rejected because of the complexity of the machine design and the certainty that the dimpling problem would be exacerbated for reasons similar to rubber pad forming. The final type of forming considered, which was eventually implemented, was mated-die forming. With this technique, the pins contact both sides of the sheet and three point bending occurs at each pin tip, except at the outer rows of pins. (See Figure 2.3). This approach will be considered in detail in the following sections.

2.3 Design of a Test Fixture for DDS Forming

2.3.1 Introduction

Many choices were available in designing a machine to implement the discrete surface concept. The factors considered in the

FIGURE 2.1: RUBBER PAD FORMING WITH A DDS

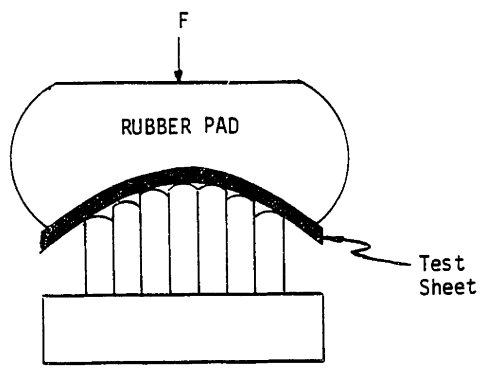

a) Rubber pad forming set-up

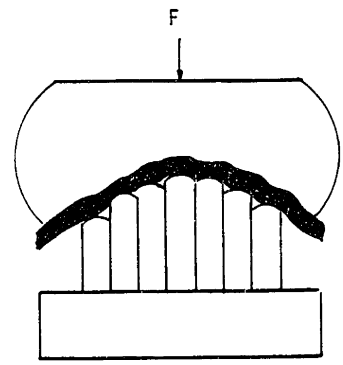

b) Dimpling occurring with rubber pad forming

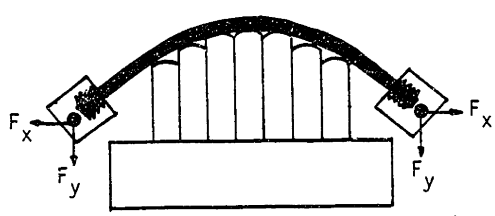

FIGURE 2.2: STRETCH FORMING WITH A DDS

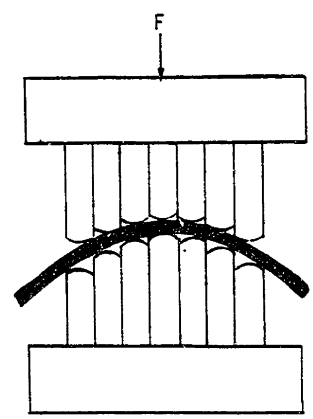

FIGURE 2.3: MATED DIE FORMING WITH A DDS

design of the DDS were: 1) Cost and ease of fabrication, 2) Ease of positioning, 3) Accuracy and 4) Minimization of discrete errors. Weighting the relative importance of these factors differently would result in many different designs. To minimize discretization errors, for example, a design was considered that would have used several different types of elements from which a set could be chosen to form the most accurate surface, as illustrated in Figure 2.4. The pins in this figure are square in cross-section. If they were rotated to match the appropriate angles and then positioned, a fairly accurate, nearly continuous surface could be produced. A problem with this concept is that to fabricate a different surface, the pins would need to be reassembled and totally rearranged. The surface that was eventually used was composed of identical pins which only required assembly once.

2.3.2 Pin Selection

After the approach of the identical pins was selected, the cross section and tip shape were determined. Incorporated into the design were considerations of accuracy, methods of securing the separate elements for forming, adaptation of the approach for automatic pin positioning and size. A small device was built originally with hexagonal pins to take advantage a "wedging" effect to lock them in place. These pins were hard to arrange so that they would all lock uniformly, and no apparent advantage was obtained over using less costly round pins. Thus the final design was fabricated using round pins in a "close-packed" arrangement to keep the pin

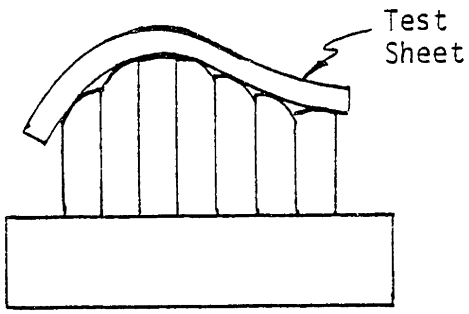

a) Forming set up

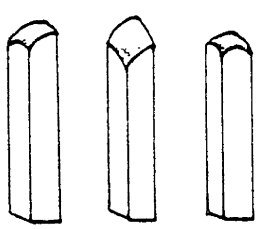

b) Pin types

FIGURE 2.4: POSSIBLE DDS CONFIGURATION

centers as close as possible. The tips of the pins were made spherical to minimize the dimpling effect over a wide variation in shapes. Selection of the tip radius was made on the basis of two competing considerations. A larger radius would produce less dimpling of the surface at the pin tip, while a smaller radius would allow a greater angle of bending without producing dimpling near the edges of the pins. Section 3.2.2 investigates this dimpling problem in detail and describes one method for choosing the proper pin tip radius.

2.3.3 Locking the Pins

Once the pin design was completed, a method for locking the pins rigidly together was established. The original work on the "automatic" DDS was done with the pins being locked by air plena. (See Figure 2.5). Problems with the arrangement for a prototype design were that the pin housing design was complex, and the packing of pins was limited by the plenum size. It was decided that if the pins could be individually positioned and then all of the pins locked at once, a simpler locking device could be designed. From this decision, a single locking device was chosen to hold the pins in place during the forming. The most important consideration in the design of this device was that after the pins were positioned they not be allowed to move relative to each other when the clamping device was activated. This problem is minimized when the pins are packed as tightly as possible. Another consideration was that the pins stay locked in place when the forming

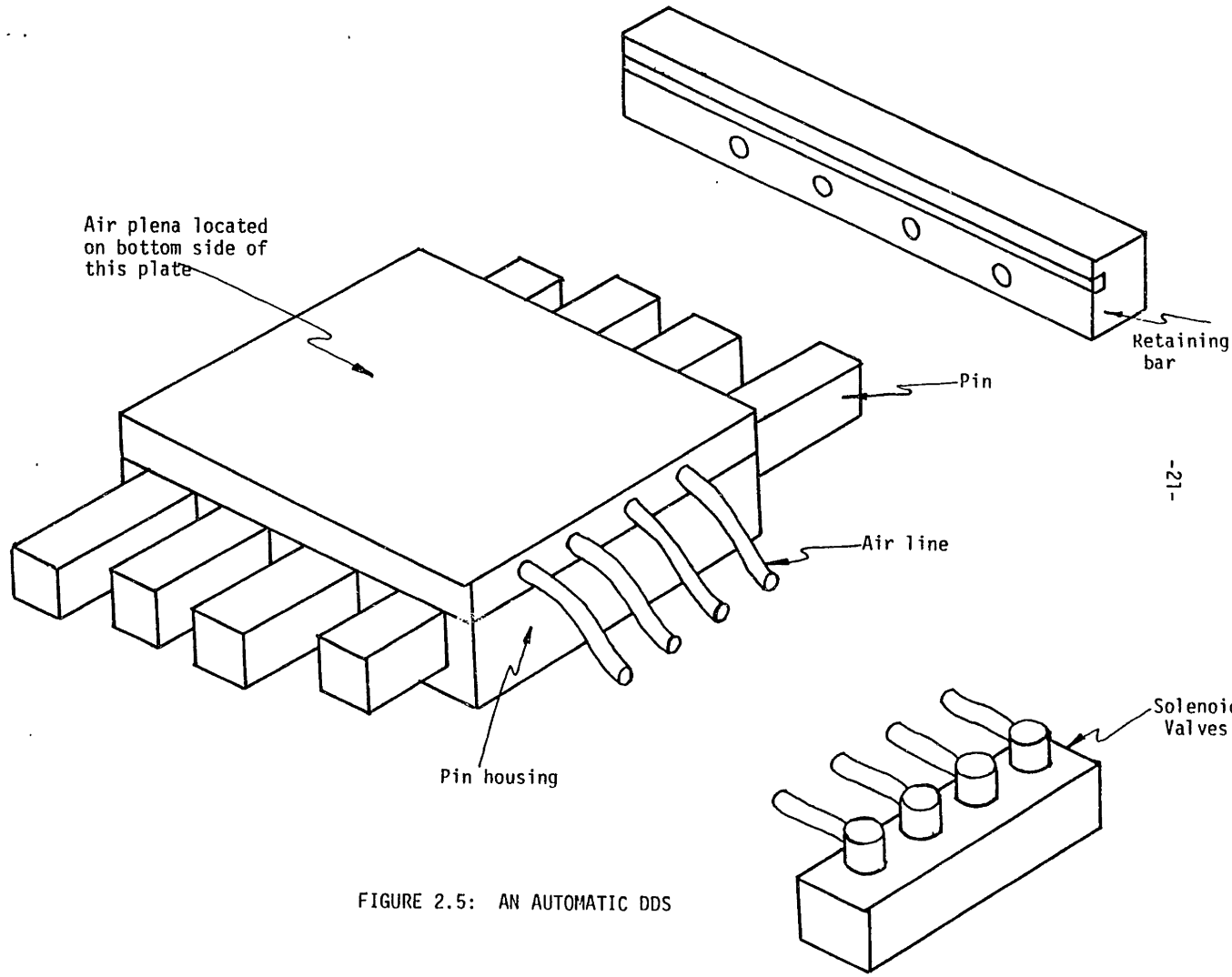

FIGURE 2.5: AN AUTOMATIC DDS

force was applied. The device described in Section 4.2.2 was able to withstand typical forming forces using a single locking device. This capability is dependent upon a sufficiently large clamping force.

2.3.4 Pin Positioning

The pins must be positioned before they are locked together for forming. Three different pin positioning concepts were considered: 1) individual pin positioning, 2) row positioning, and 3) surface positioning. The individual-pin positioning approach uses a 3-axis manipulator that positions each pin individually. For example, a three axis milling machine under servo control is sufficient to position the pins (see Figure 2.6). While this approach is attractive for use with automatic control, the calculations necessary for determining the pin positions are overly complicated for this experiment. The row-position approach uses a flat plate machined to the desired shape to position an entire row of pins. This approach in general would require a separate plate to position each row. However, for this experiment, a single shape was selected for all rows. The adjacent row positions were calculated mathematically and the row-positioner positioned accordingly. The surface positioning concept uses an entire surface which is machined to the shape desired for the die surface. Since this requires difficult fabrication techniques, the row-positioning concept was chosen as a compromise between the positioning ease afforded by the surface-positioning concept and the fabrication simplicity of the individual-pin concept.

FIGURE 2.6: PIN POSITIONING TECHNIQUES

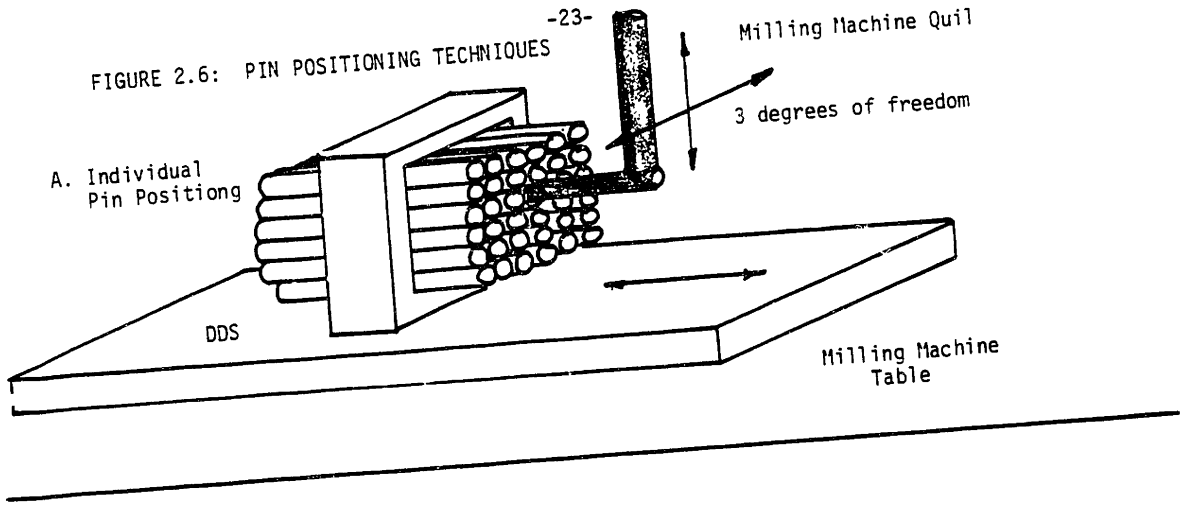

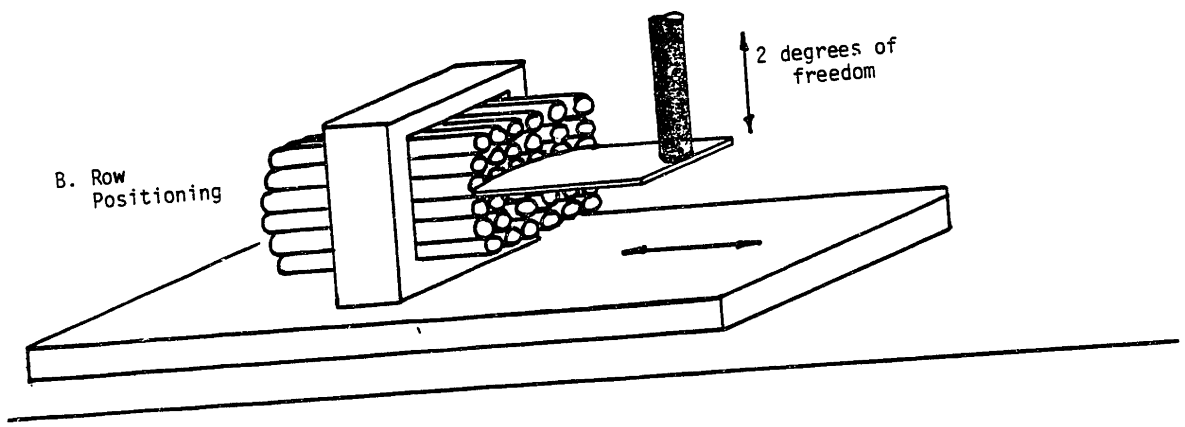

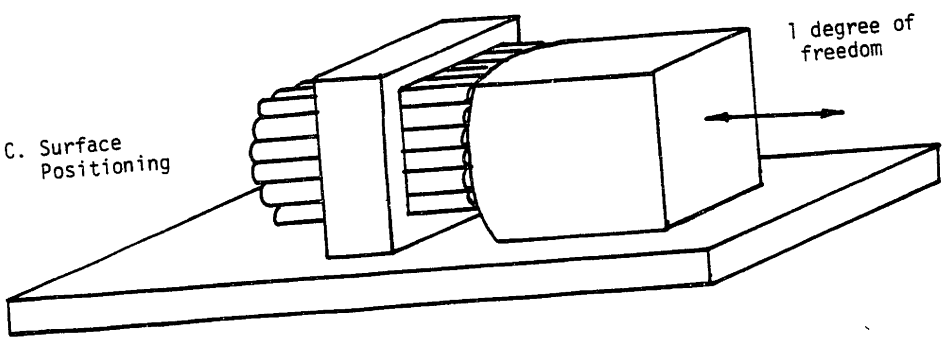

In all three cases, the thickness of the material and the pin tip radius were taken into account when calculating the mating die shape. If they were not taken into account, there would be no place for the material to go when the die was closed, and unknown stresses would be added to the sheet. The method used here for calculating the mating die pin positions is described in Section 4.4.3.

2.4 Summary

The DDS system is a positionable matrix of discrete elements that can be locked in place to form a surface suitable for die-forming sheet metal. The design chosen for experimental work was a mated-die set-up composed of spherically-tipped round pins with a single locking device. The pins were positioned by rows and locked in place. A device was built and experiments performed, which are described in Chapter 4. First, however, some of the material considerations were investigated analytically to determine what criteria need to be evaluated in the experiments. This is the subject of the next chapter.

CHAPTER 3

MATERIAL CONSIDERATIONS

3.1 Introduction

In order to implement the design of the DDS test fixture, it is necessary to examine the effects of a DDS on the material being formed. These effects include; springback, buckling, dimpling, anisotropic behavior, and end effects caused by positioning sensitivity. Analysis of these effects will provide some insight into the decisions behind selection of both the pin tips and material to be formed.

This chapter is divided into two sections. Section 3.2 describes each of the five forming effects, while Section 3.3 defines the significant conclusions drawn from consideration of these effects as they relate to the experiment.

3.2 DDS Forming Effects

3.2.1 Springback

Of utmost importance in the forming process is consideration for material springback upon unloading of the die. Springback is the elastic recovery of the metal upon unloading. A typical moment-curvature plot for simple bending where the moment is only applied along one axis of the sheet is shown in Figure 3.1. (The curvature, K, as shown in the Figure, equals the reciprocal of the radius of curvature of the metal). When the moment is decreased, the graph follows the slope of the elastic region, resulting in linearly decreasing curvature

FIGURE 3.1: TYPICAL MOMENT CURVATURE PLOT

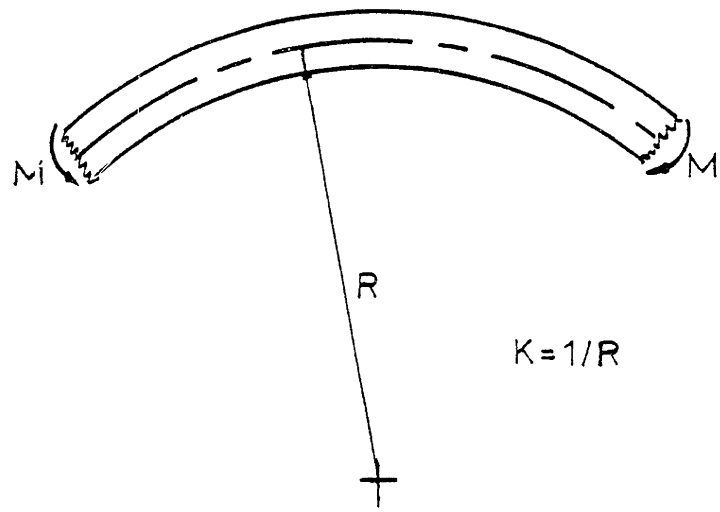

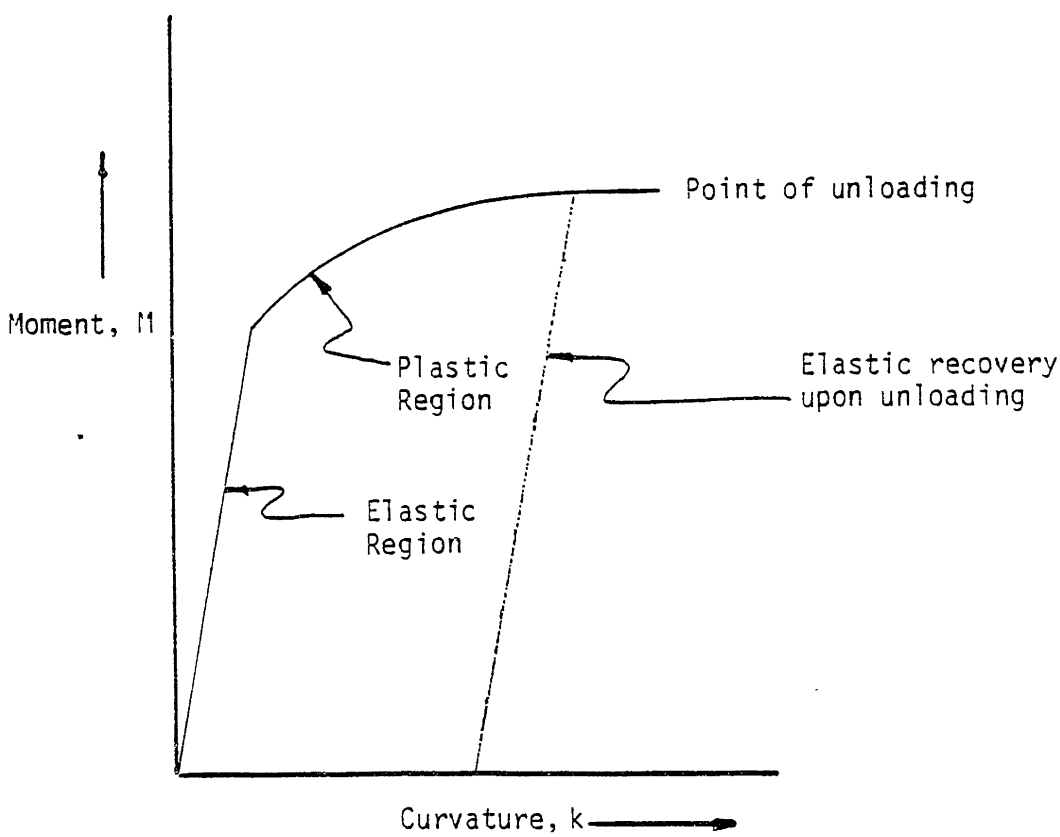

upon unloading. A formula for determining springback was developed in the M.I.T. report on "Sequential Forming of Sheet Metal Parts" (Gossard et al. (1980)). Using a piecewise-linear approximation of the moment-curvature relationship, and assuming the behavior of the material to be elastic-perfectly plastic (see Figure 3.2), a relationship between the loaded curvature and the predicted unloaded curvature was defined as follows:

$$\frac{R_L}{R_u} = 1 - 3\left(\frac{\sigma_y R_L (1-\nu^2)}{Et}\right) + 4\left(\frac{\sigma_y R_L (1-\nu^2)}{Et}\right)^3 \qquad (3.1)$$

where:

R_L = loaded curvature

R_u = unloaded curvature

σ_y = yield stress

ν = Poisson's ratio

E = modulus of elasticity

t = thickness of sheet

This formula only applies to simple curvature where the moments are applied about one axis only. In the rare cases where the DDS would be used for simple curvature, this formula could be used to account for the amount of overbend necessary to obtain the desired unloaded curvature.

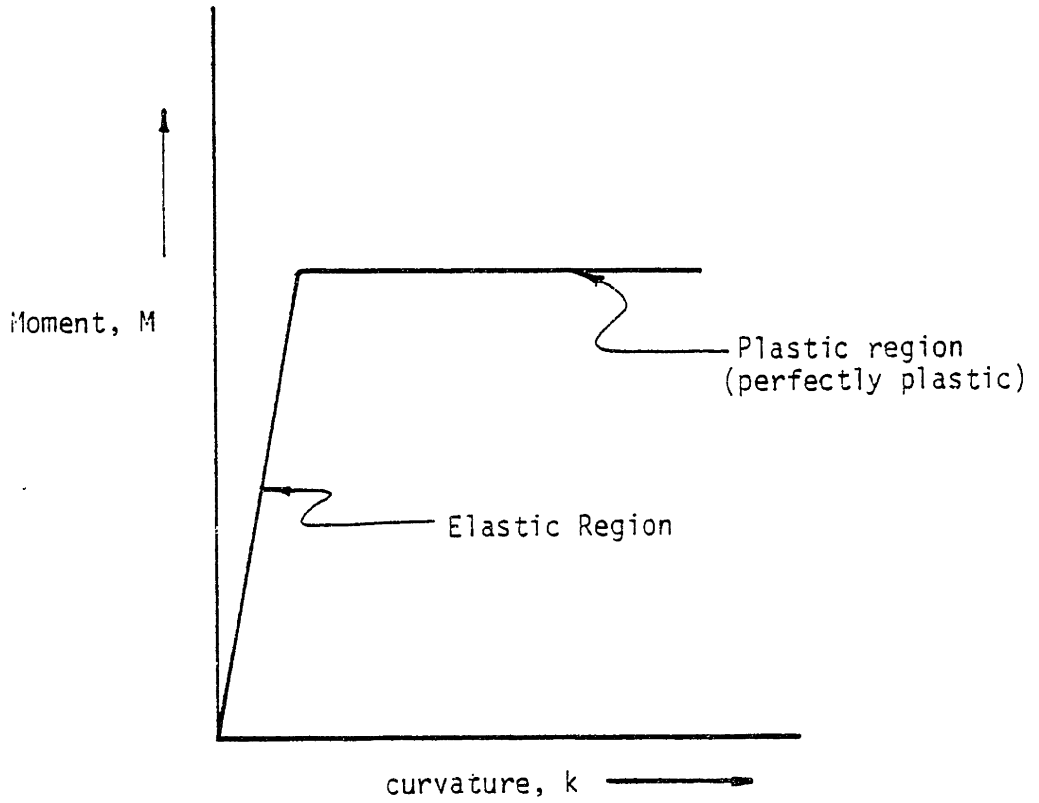

FIGURE 3.2: IDEALIZED MOMENT - CURVATURE PLOT

In the case of compound curvature, where moments are applied about two axes, springback determination becomes much more complicated. Compressive stresses in the plane of the sheet are induced during plastic deformation which distribute the springback across the sheet in a complex fashion, and the compressive stresses increase near the outer edges of the sheet. This may be seen by examination of Figure 3.3. In this figure, a disc is to be formed over a sphere with a radius of 1.5". Circumference lines are drawn at distances of 1" and 2" from the point "A" on both the surface of the sphere and the unformed disc. At 2" from point A, the circumference of the sphere is 8.6" while the circumference of the disc is 12.6". To have the disc fit on the sphere at this point, a compressive strain of:

$$\varepsilon_{2in.} = \frac{12.6" - 8.6"}{12.6"} = .32 \text{ in/in}$$

would be induced in the disc. This is a very high compressive strain and it is quite likely that buckling will occur unless some form of tensile stress is added to counteract the compressive stress caused by this strain. It is also seen that the strain increases with distance away from the center, as evidenced by the lower strain at the 1" circumference line.

$$\varepsilon_{1in.} = \frac{6.3 - 5.5}{6.3} = .13 \text{ in/in}$$

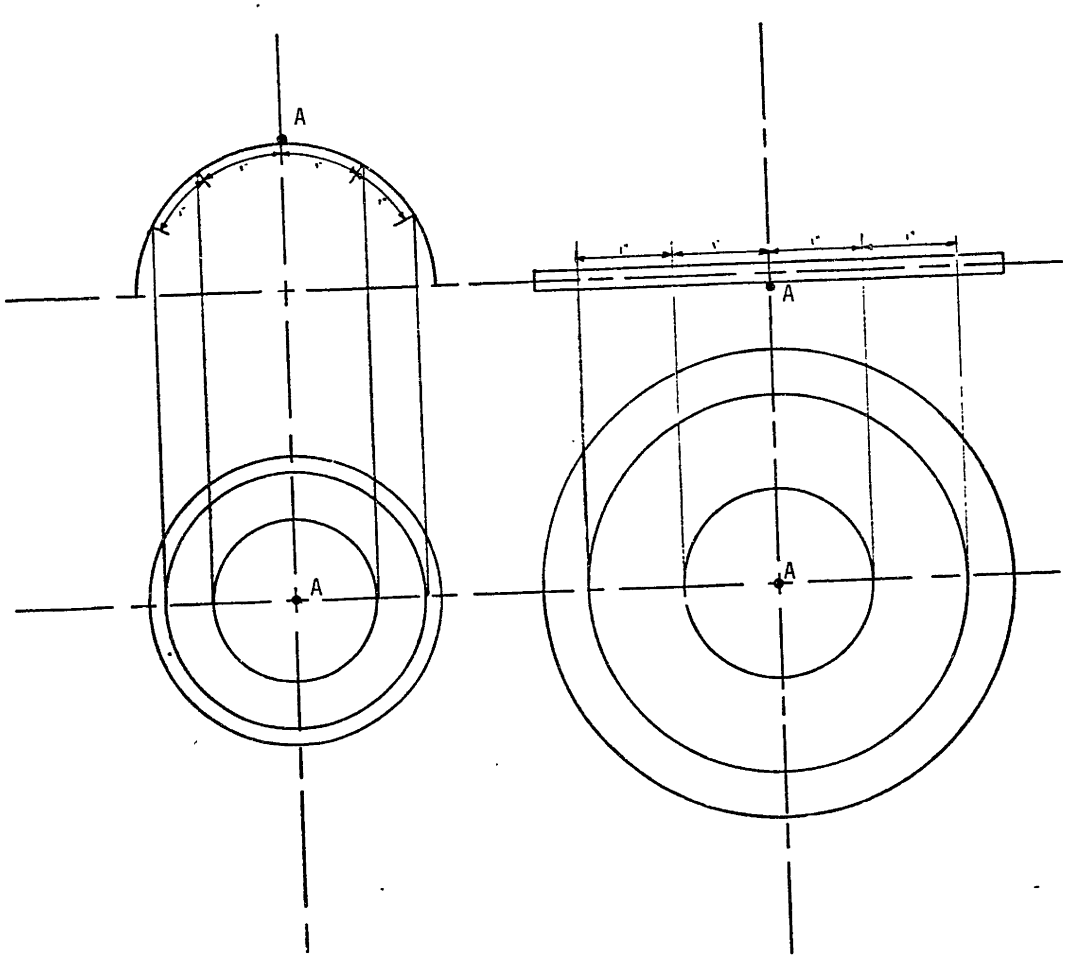

FIGURE 3.3: FORMING A DISC OVER A SPHERE

The combination of in-plane compressive stresses and axial bending stresses make the springback for compound curvature hard to predict. Presently, mostly trial and error methods are used to determine the overbend for compound curvature cases.

3.2.2 Buckling

The compressive strains described in the last section may be sufficiently large to cause buckling of the material to occur. This is a phenomenon which occurs in continuous-die forming and is dealt with by restraining the material in such a way as to cause counteractive tensile stress to occur during forming. Another method is to allow the material to buckle out near the ends and cut out the center portion for use.

With a DDS, the buckling problem may be more pronounced because of the discontinuities of the die surface. The smaller radius of the pin tip, as compared with the die radius, may cause localized bending moments which would initiate the buckling action. This subject will be studied in Section 5.3.4 where the results of DDS experimentation will be discussed.

3.2.3 Dimpling

A material forming effect of particular importance to the DDS is dimpling. Two types of dimpling may occur to the sheet during forming (See Figure 3.4). One is a surface effect, where the pin tip indents the material somewhat like a hardness tester does. This sur-

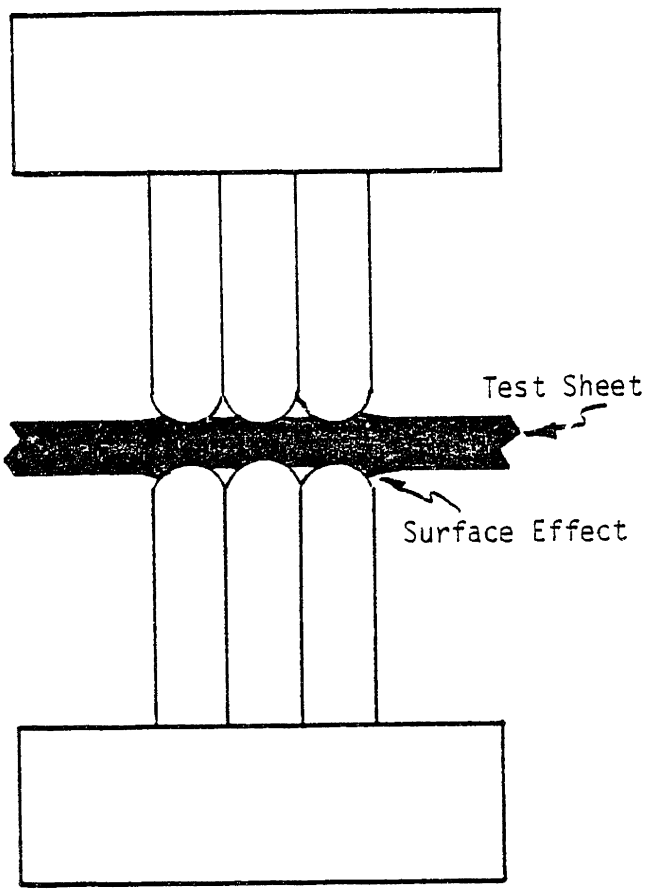

a) Surface dimpling

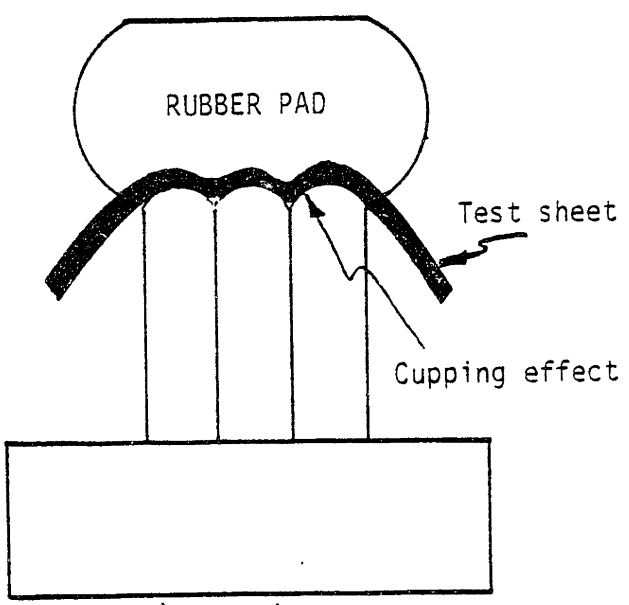

b) cupping

FIGURE 3.4: TYPES OF DIMPLING

face effect can occur in any DDS configuration where the contact stress of the pin tip on the material is high enough to cause plastic deformation of the sheet surface to take place. The other effect is "cupping" around the pin tip, where the material actually takes the shape of the pin tip itself. The latter effect will only occur in situations where the material is forced into the crevices between the pin tips. Hydroforming causes cupping to take place with thin material since it forces the material into these crevices. A thicker material would have a higher resistance to the cupping effect because of greater forces necessary to make it yield. The mated-die DDS may have some surface dimpling but no cupping will occur since the DDS only contacts the material at the pin tips. This was the reasoning behind the choice of a mated-die DDS for the experiments.

To minimize the dimpling effects, some type of interpolating surface can be used to distribute the load so that it is not all carried through the pin tips. For example, rubber sheets located between the specimen and the die would help produce this interpolating effect. A discussion of interpolators for the DDS is covered in Appendix B. Another way to minimize the dimpling effects is to choose an appropriate configuration for the geometry of the pin tip. The tip geometry should minimize the dimpling effect for all the different shapes to be formed. The ability of the system to form different shapes appears to be related to the smoothness of the forming surface for a particular shape, which affects the susceptibility to

dimpling. This is because when a pin tip must accomodate several different shapes, it cannot mate as well with a particular shape. Further discussion of the selection of appropriate tip geometries will be discussed later in this chapter (Section 3.3.3).

3.2.4 Anisotropy

Another phenomenon which may affect the material properties and hence, the forming accuracy, is anistropy of the material being formed. With sheet metal, the material is usually rolled to the desired thickness, which causes the grains of the metal to elongate along the direction of rolling. The differences in grain dimensions in different (orthogonal) directions causes variation in the mechanical properties in these directions (One way to reduce this problem is by proper heat treating of the metal). To assure repeatability of a given forming configuration, the rolling direction of the material should be oriented the same way in the die before each forming. Another precaution is to use metal from the same batch to minimize material property variations.

3.2.5 Sensitivity to Pin Position Errors

If the pins are not appropriately positioned in the DDS, the portions of the sheet that are at large angles to the reference plane of the die may have a reverse moment induced which would affect the unloaded shape of the sheet. This is illustrated in Figure 3.5. It can be seen from this figure that if the two end pins are

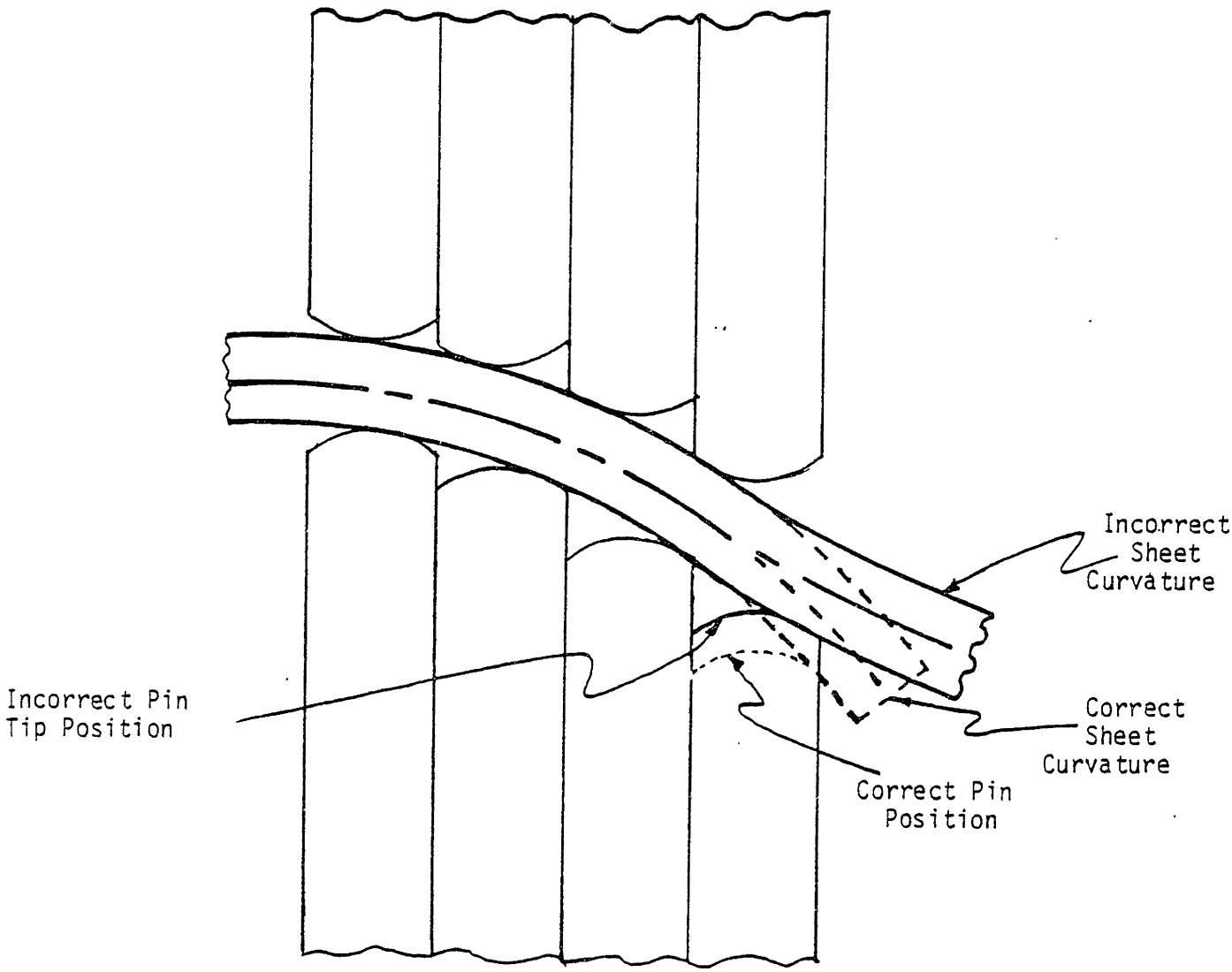

FIGURE 3.5: MATERIAL SENSITIVITY TO POSITIONING ERRORS

located too close together a moment will result which will bend the metal in the opposite direction from that desired. Appendix C analyzes the sensitivity of this effect to inaccuracy in pin positioning for the conditions of the experiment described in Chapter 4. The results show that a reverse moment large enough to cause the material to bend in the wrong direction will occur with a pin positioning error around .001 in. This effect was not observed in the experiment since rubber interpolators were used. The low modulus of elasticity of the rubber caused the material to be less sensitive to positioning errors.

3.3 DDS Design Based on Material Considerations

3.3.1 Relationship Between Pin Tip and Material Properties to Avoid Dimpling

A mathematical relationship was developed to relate the pin tip radius, sheet thickness, and material properties of the sheet so as to avoid dimpling. Appendix D develops this relationship to find a minimum size for the pin tip radius. The rubber interpolators used in the experiment (see Section 4.4.6) were not taken into account in this relationship, so it was not used to determine the pin tip radius. Further development of this relationship might be useful for designing future DDS systems.

3.3.2 Material Selection

The material chosen for the experiment to be performed in chapter four was selected on the basis of four considerations;

availability, low yield stress, low springback and a softness so that it would show dimpling effects without a very large load. The material chosen was 3003 H14 Aluminum, mostly because it was on hand, and preliminary tests showed the other considerations were well met. Some properties of the Aluminum sheet are:

Modulus of elasticity, $E \approx 10 \times 10^6$ psi

Yield stress, $\sigma_y \approx 21{,}000$ psi

Poisson's Ratio, $\nu \approx .33$

These values are used in Chapter 5 to predict the springback according to the method outlined in Section 3.2.1.

3.3.3 Pin Tip Selection

Two geometries were investigated for the tips of the pins in the DDS test fixture. These were variable curvature and spherical geometries (See Figure 3.6). For identical pins, the most adaptable shapes are continuous curves since any discontinuity would promote dimpling if the material contacted the discontinuity on the pin. The variable curvature tip could be chosen so as to minimize the dimpling for the variety of curvatures encountered in the DDS used. This would require an analysis of the die angles encountered, and the curvature of the tip would have to be made so that it best accomodated the most common angles. The spherical tip was chosen since it simplified calculations of pin positioning (pin positioning is dependent on tip geometry as shown in Section 4.4.3). Another reason for selecting the spherical

FIGURE 3.6: PIN TIP GEOMETRIES

a) Spherical Tip

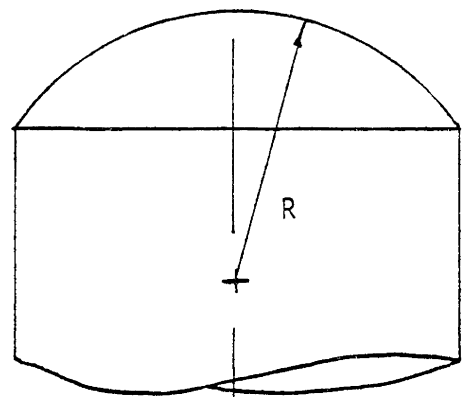

b) Variable curvature tip

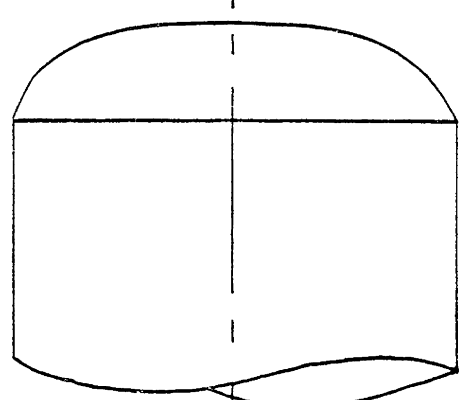

tip is that it is much easier to machine since round forming tools are available. When choosing a radius of curvature for the tip, the largest radius that would accomodate all of the shapes to form was selected. A loaded bend angle of 45° was selected as maximum for this experiment, so the radius was chosen to accomodate this angle. With pin diameter of 1/2", Figure 3.7 shows that:

$$R = \frac{1/4}{\cos 45^\circ} = .3536$$

The radius must be smaller than this to accomodate the 45° angle, thus, a 11/32" radius was chosen since it was the closest size forming tool to this radius (11/32" = .3438").

3.4 Summary

Five DDS forming effects have been considered in preparation for the experiment. A relationship was developed between the pin-tip radius and material dimensions, to avoid dimpling. This was not used because the relationship didn't account for rubber interpolators and early experimental results showed that the material selected was not subject to dimpling in the configuration used. Material selection was based primarily on availability with consideration for the forming effects. Finally, the spherical geometry was chosen because of its adaptability to different shapes. An 11/32 in. pin tip radius was selected as a compromise between the adaptability to different shapes of a small radius and the reduced dimpling effects of a large radius.

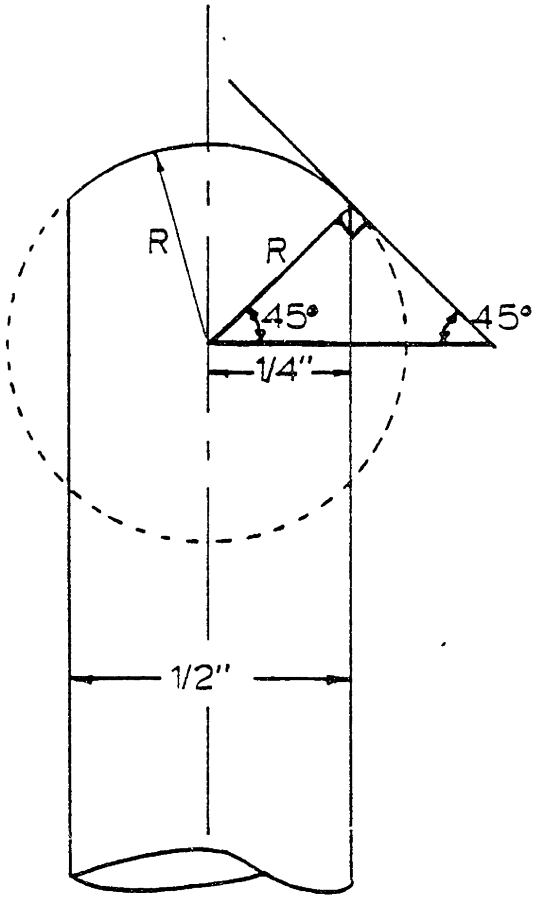

FIGURE 3.7: PIN TIP RADIUS SELECTION

CHAPTER 4

EXPERIMENTAL OBJECTIVES AND METHODS

4.1 Introduction

An experimental program was undertaken to determine the feasibility of the DDS principles for forming sheet metal discussed in Chapter 2. Sufficient data was collected to determine the limitations and surface quality of sheet metal formed by a DDS system. Some initial problems with the first design were resolved, and a final set of test pieces was produced which appeared to meet the above criteria for feasibility sufficiently well to warrant further analysis. For this experimental program, a DDS test fixture was built, and a method was developed for producing formed test samples. After this, there occurred a preliminary testing, redesign and modification period. From this test period, a final experimental method was developed, and a set of twelve test samples were produced. Finally, these test samples were measured to develop a data base for analysis of this implementation of the DDS concept. This chapter is divided into several subsections which discuss, respectively, the experimental equipment as it was originally configured, the preliminary testing, and the final experimental procedure.

4.2 Experimental Equipment

4.2.1 Introduction

A DDS system with spherically tipped pins was developed to

be used in this experiment. The design consisted of two manually operated locking devices, each containing 67 closely-spaced spherically-tipped pins, which were positioned and locked in place. The pins were separated by rubber sheets to aid in the independent positioning of each pin, and in locking them in place. In addition to the DDS system itself, a positioning device was fabricated. The locking device, the pins, and the positioning device will be discussed separately in the following sections.

4.2.2 Pin Housing

The first part of the fabrication was the pin housing, which also served as the locking device. This consisted of steel channels bolted and welded together to form a square housing, with a movable steel plate on top to compress the entire array of pins. Figure 4.1 shows this housing. The four pins extending from the housing were used to guide the mated die. Four bolts, two of which are visible, were used to provide the compressive force on the movable plate which is shown between the top channel and the pins. A simplified, dimensional drawing of the housing is shown in Figure 4.2.

4.2.3 Pins

The pins were fabricated from 1/2 inch hot-rolled steel bar stock. An 11/32 inch radius circular forming tool was used to turn the tips on a lathe, and the pins were cut to a seven inch length. They were packed as tightly as possible in the housing with staggered rows as illustrated in Figure 4.3. Rubber sheets were used as spacers

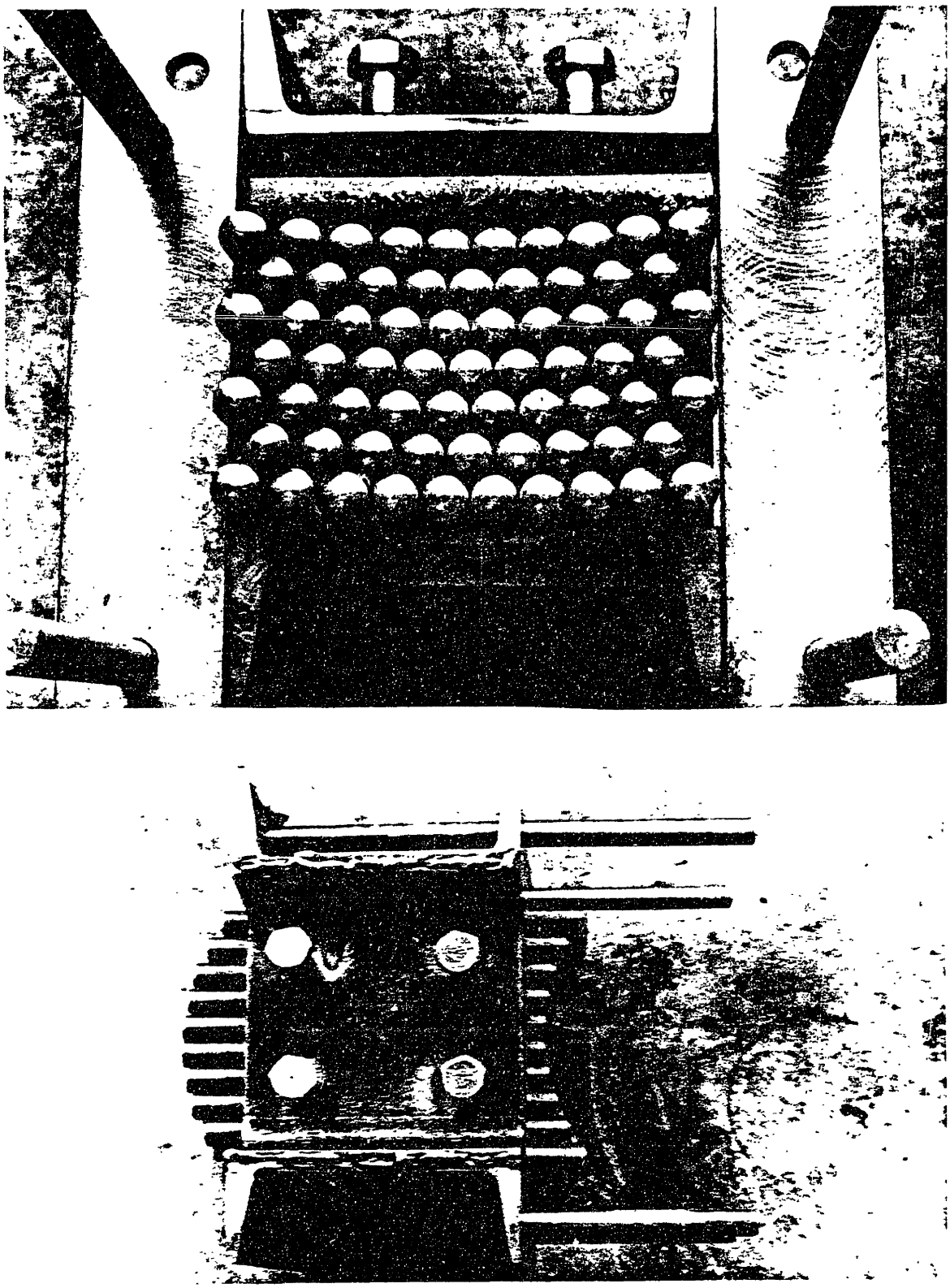

FIGURE 4.1 : PIN HOUSING PICTURE

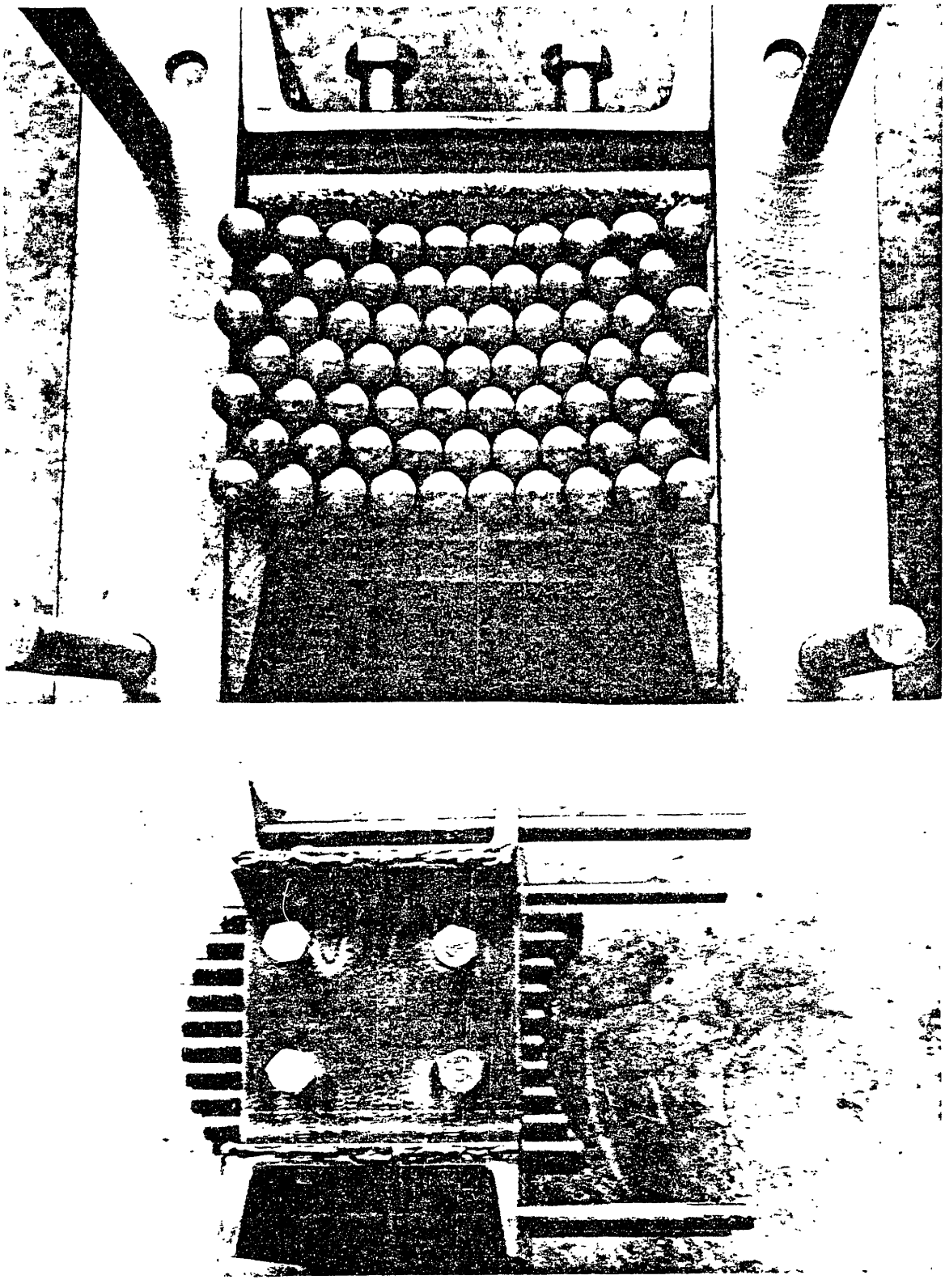

FIGURE 4.1 : PIN HOUSING PICTURE

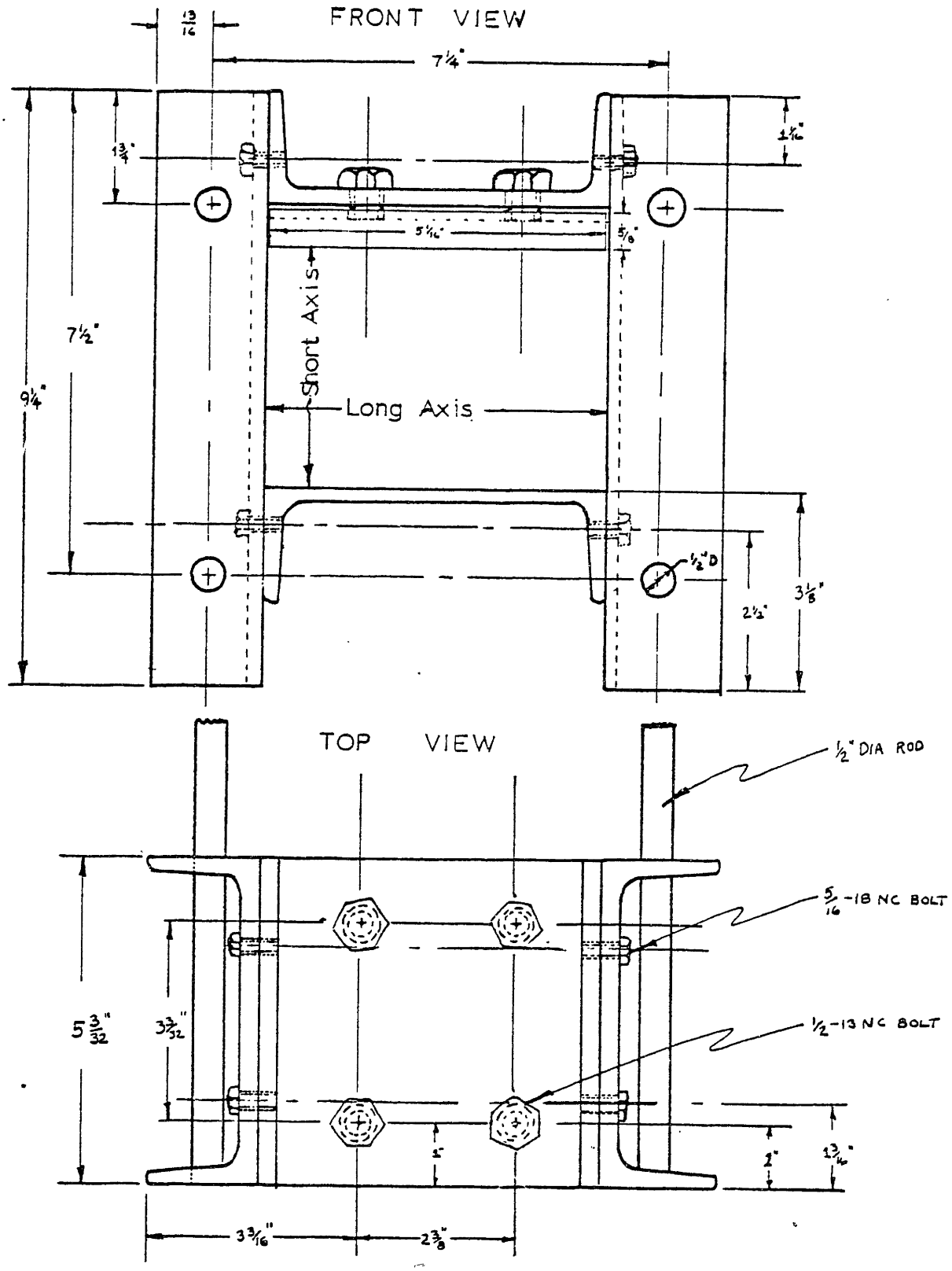

FIGURE 4.2: DIMENSIONED DRAWING OF PIN HOUSING

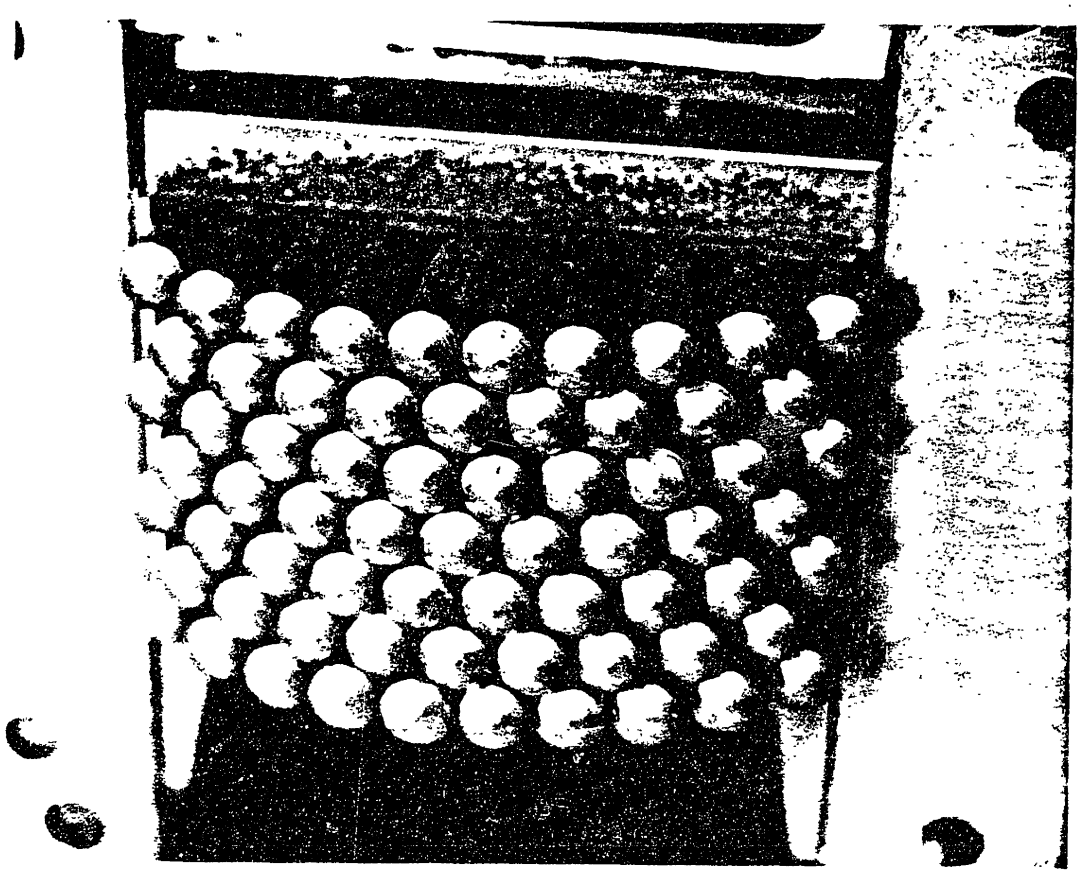

FIGURE 4.3: PIN PACKING IN HOUSING

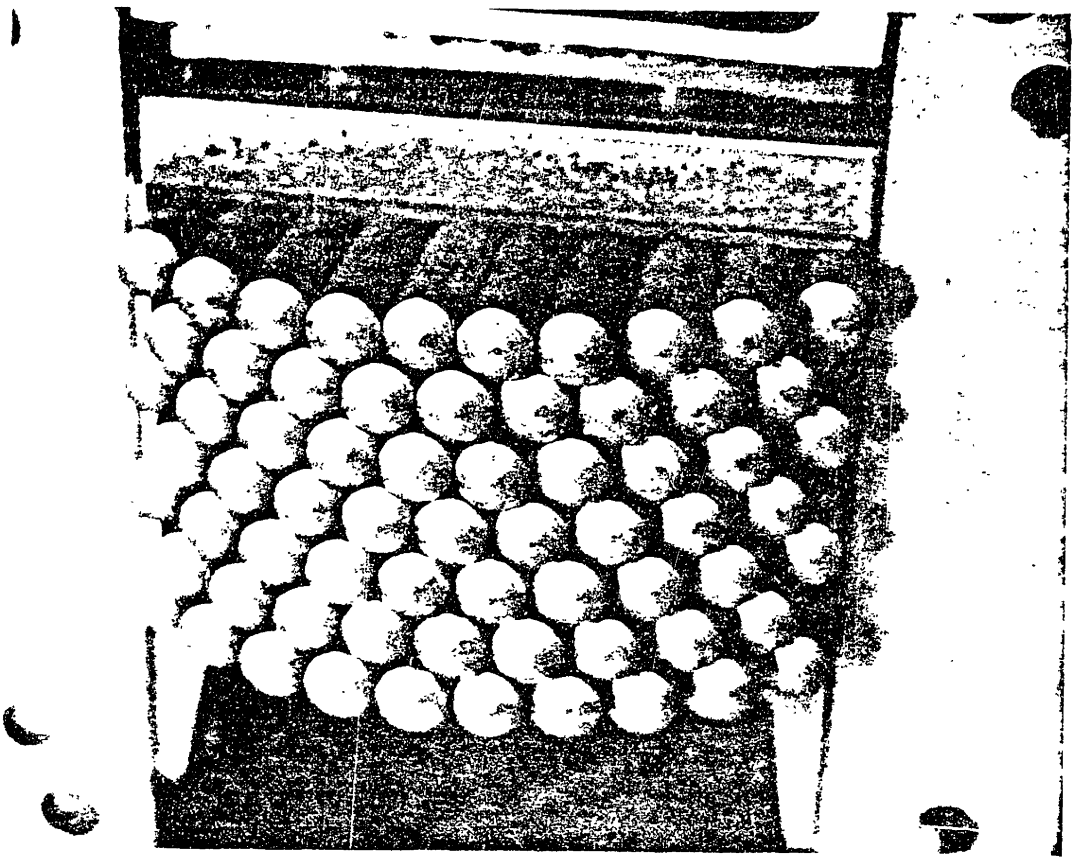

FIGURE 4.3: PIN PACKING IN HOUSING

between adjacent rows to limit the interaction of adjacent pins during positioning, and to compensate for any dimensional inaccuracies in the pins. Without the rubber spacers, when any pin was moved, the pins contacting it often moved due to frictional forces. With the rubber spacers in place, pin interaction was only possible when the spacer moved. Movement of the rubber spacer was inhibited by the gravitational force on all of the pins above it. The force acting on one pin by its own weight and the weight of the other pins above it was much less than that acting on the spacer. Therefore, motion of an individual pin was unlikely to cause motion of the spacer which could cause motion of the adjacent pins. The other advantage of the spacers is that it compensates for the static indeterminacy caused by varying pin sizes and spacing. The damping force will cause elastic deflection of the pins; and the larger pins, which will be deflected first, will receive most of the damping force. Because of the high modulus of the elasticity of the steel pins, it might not be possible to exert a strong enough force to lock the smaller pins in place without the spacer. A greater variability in pin diameters can be accomodated by the spacers because the modulus of elasticity of the rubber is lower than that of the steel for the loads used (with rubber, the modulus of elasticity varies with the load).

4.2.4 Positioning Device

The positioning devices used for the row positioning technique described in Section 2.3.4 consisted of aluminum sheets with a constant radius

cut on one end of each sheet. The sheets were milled using a rotary table on a vertical miller. The radius and sheet thickness was chosen and the positioners milled taking into account the sheet thickness. An example of how the radius was determined is shown in Figure 4.4. The radius, R_1, for the concave die is obtained by adding 1/2 the metal thickness and the thickness of one sheet of compressed rubber to the desired centerline radius, R. The positioner of this die is convex, with a radius of R_1. For the convex die, the positioner is concave with a radius of R_2, determined by subtracting 1/2 the metal thickness and one compressed rubber sheet thickness from the centerline radius, R. The centerline radii were selected to meet the objectives of the experiment as will be discussed in Section 4.4.3.

4.3 Preliminary Tests

4.3.1 Introduction

Before a formal experiment was formulated, a series of preliminary tests were performed and several decisions were made regarding the nature of this formal experiment. Also, modifications were made to the apparatus as suggested by the results of preliminary tests. Several different points will be discussed in this section starting with the establishment of the forming force in Section 4.3.2. Apparatus modifications will be discussed in 4.3.3, followed by adaption to a universal testing machine in Section 4.3.4. Finally, 4.3.5 will discuss material geometry selection.

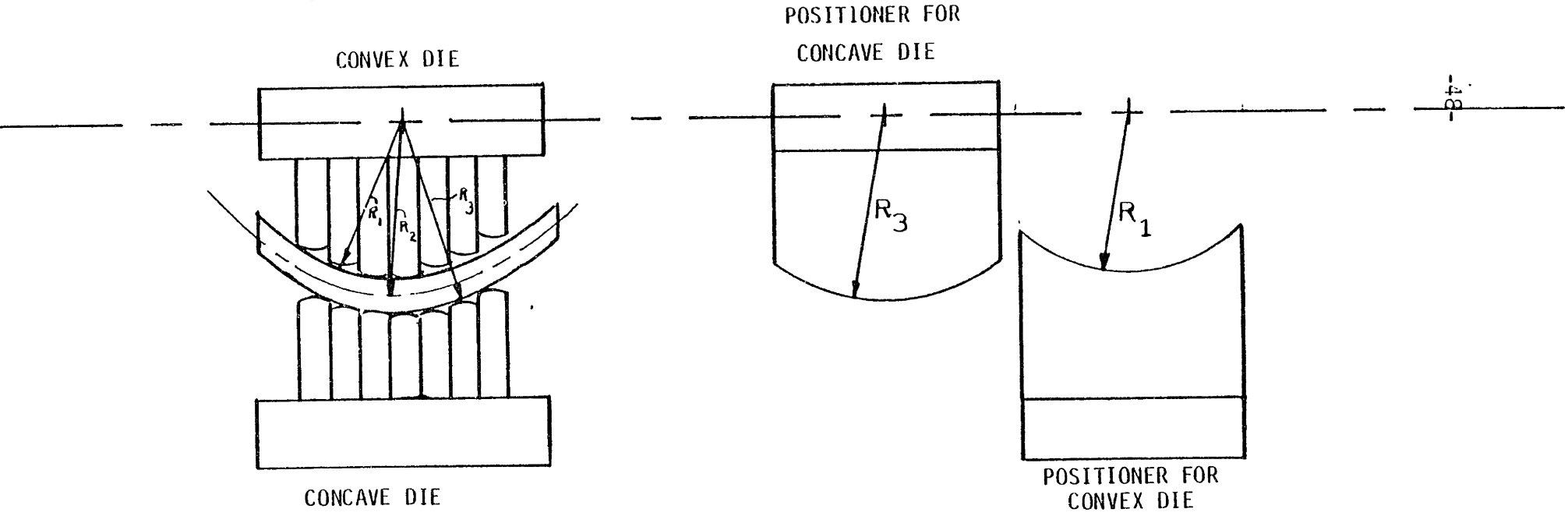

FIGURE 4.4: DETERMINING RADIUS FOR PIN POSITIONERS

4.3.2 Forming Force Experiment

A test was performed to determine whether the clamping force was sufficient to prevent pin slippage when a typical forming force was used. It was found that a forming force of 1500 pounds did not result in any pin slippage. At this force, however, dimpling of the sample material occurred. This demonstrated that the force was more than sufficient to form the metal. A forming force of 1000 pounds was chosen since it was demonstrated not to produce dimpling. To verify this, the dies were brougnt together at a constant rate and force was observed as a function of time. The typical behavior of this function is shown in Figure 4.5. The results suggest that between points A and B of the figure, plastic deformation of the sheet occurred, and the opposing pins contacted each other near point B. This also suggests that the 1000 pound force was sufficiently large for the forming in this experiment.

4.3.3 Apparatus Modifications

Three significant modifications were made to the apparatus. These were: welding to increase housing rigidity, machining to provide better reference surfaces for positioning, and the addition of shims to prevent lateral pin motion when the locking device was activated. During the initial tests, shifting of the housing occurred when either the forming or locking force was applied, causing some pin movement to occur. Since the position of the pins was referenced to the front side of the housing, the surface of the front side was milled flat and

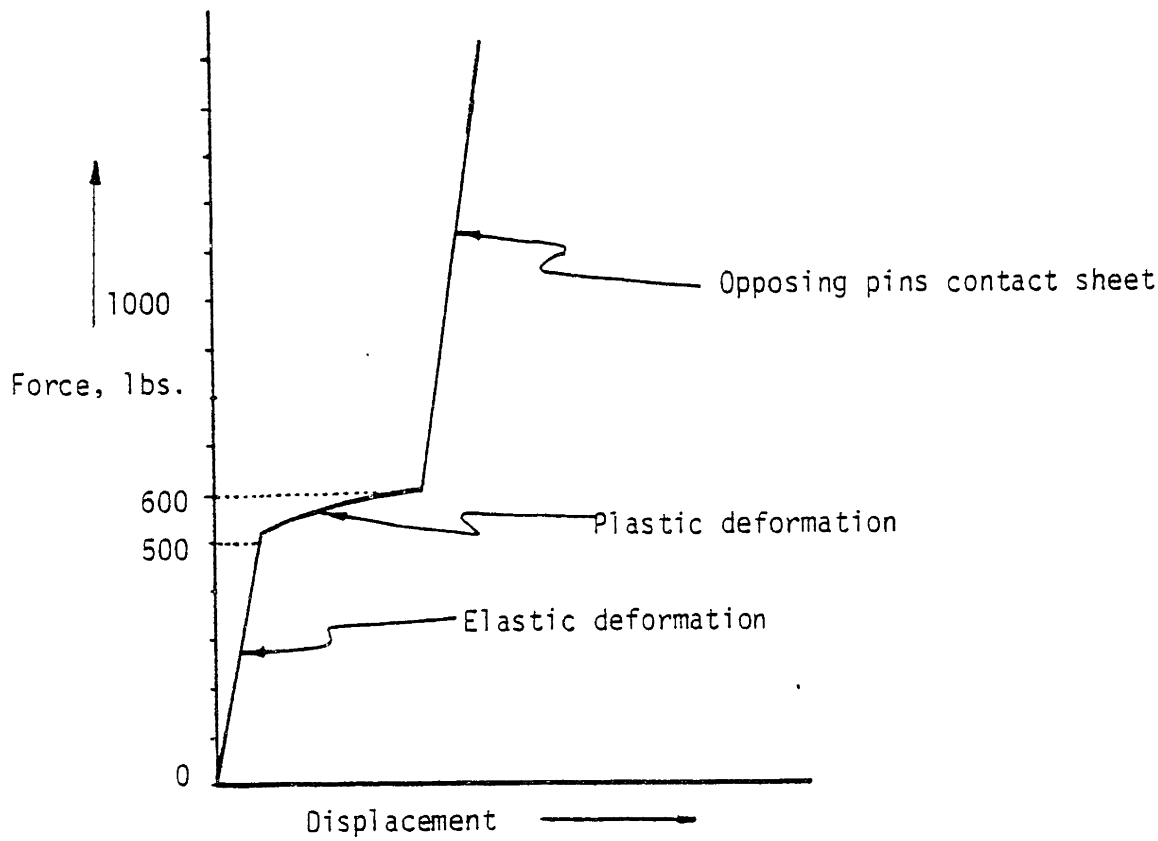

FIGURE 4.5: FORCE vs. DISPLACEMENT FOR GRIPPING HEAD OF TESTING MACHINE

perpendicular to the milling table during set-up to provide proper pin positioning. To flatten this surface, the housing was placed on a vertical miller and machined using a fly cutter. The base of the housing was then machined perpendicular to the front side. It was found that when the pins of a given row had spaces between them, they would laterally shift positions when the clamp was activated. Shims were added to the ends of the rows to eliminate the space between the pins, hence, greatly reducing lateral pin movement on clamping (see Figure 4.6).

4.3.4 Attachment Modifications

The initial forming tests were made by placing the upper die upon the lower die and setting wooden blocks above and below the dies. This was found to be unsatisfactory because the upper die did not mate the lower one correctly when a force was applied. To eliminate this problem, four guide pins were installed as described in the previous section, and the upper die was clamped to the gripping head of a Baldwin universal testing machine which was used to perform the forming experiments.

4.3.5 Material Geometry Selection

It was decided to use square sheet metal test pieces of a size that would fit the small axis of the die. These were chosen to be of dimensions 2 5/8 by 2 5/8 by 1/16 inches thick. The square configuration of the sample was selected since the length along a particular axis affects the final shape of the sheet along that axis.

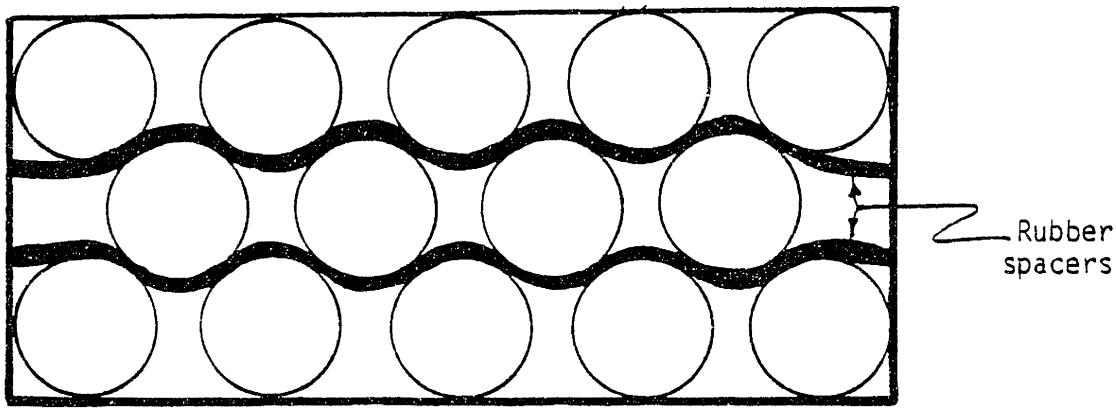

a) Loosely packed pins with no shim

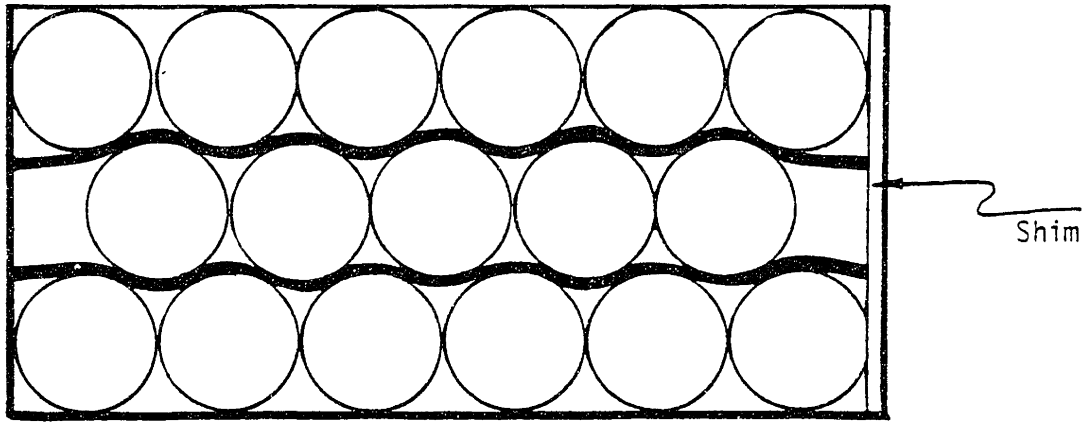

b) Tightly packed pins with shims

FIGURE 4.6: SHIM LOCATION TO MINIMIZE LATERAL PIN MOTION

4.4 Experimental Procedure

4.4.1 Introduction

After the preliminary testing was completed, a formal experiment was conducted. The dies were attached to the Baldwin universal testing machine and the samples inserted between the two rubber sheets in the die, compressed, removed, and measured. The following subsections describe chronologically the final experimental procedure from the radius selection through the measurement of the test pieces.

4.4.2 Die Radii Selection

Radii were chosen to address the objectives of the experiment which included repeatability and shape limitations. To address the repeatability question, it was decided to produce three samples for each shape for comparison. Four different shapes were used to determine if the degree to which the other objectives were met would be affected by the particular shape. Prior to the actual stamping process, radii of curvature were selected for each of the four set-ups, and two orthagonal radii were chosen for each piece. These choices for radii are listed in Table 4.1. The reason for selecting these radii was that they represent multiples of the smallest radius that can be used with this die surface (3.5 inches) on a full size sample. Use of a smaller radius would cause dimpling where pin edges contacted (see Figure 4.7).

4.4.3 Calculation of Pin Positions

The pins were positioned on the long axis of the dies using the

TABLE 4.1: RADII SELECTION

Set-up	x Short Axis of Die	y Long Axis of Die
1	3.5	3.5
2	3.5	5.25
3	7.0	3.5
4	∞	3.5

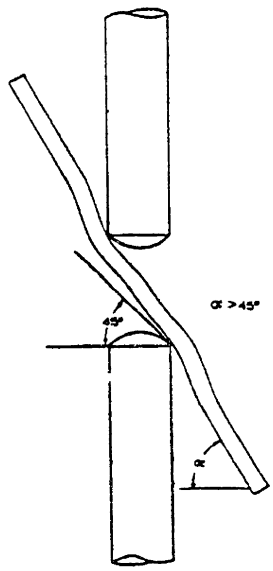

FIGURE 4.7: DIMPLING CAUSED BY LARGE CURVATURES

row positioner described in Section 4.2.4. The shorter axis was set by placing the row positioner in a precalculated position. The calculations were made to account for the radius of the pin tip and the thickness of the sheet metal and compressed rubber. When choosing the set-up for the concave and convex die, a sheet metal and compressed rubber thickness of 3/32 inches was allowed for. The sheet metal thickness was 1/16 inch and it was estimated that each of the 1/16 inch rubber pieces would compress to 1/64 inches with the 1000 pound load.

Having determined the desired die radius of curvature, the row locations were determined using trigonometric considerations. The principle of the calculation is illustrated in Figure 4.8, and can be explained as follows. It can be seen from Figure 4.8 that the distance from the center of curvature of the die to the center point of the tip radius for a particular pin in a convex die is

$$M = R-11/32 \text{ inches},$$

and for a concave die,

$$M = R+11/32 \text{ inches}.$$

The positions of each row correspond to the relative positions of each of these tip radius center points. The tip center distance in the X direction from the center of die curvature is:

$$\frac{X = n*L-1/2}{6}$$

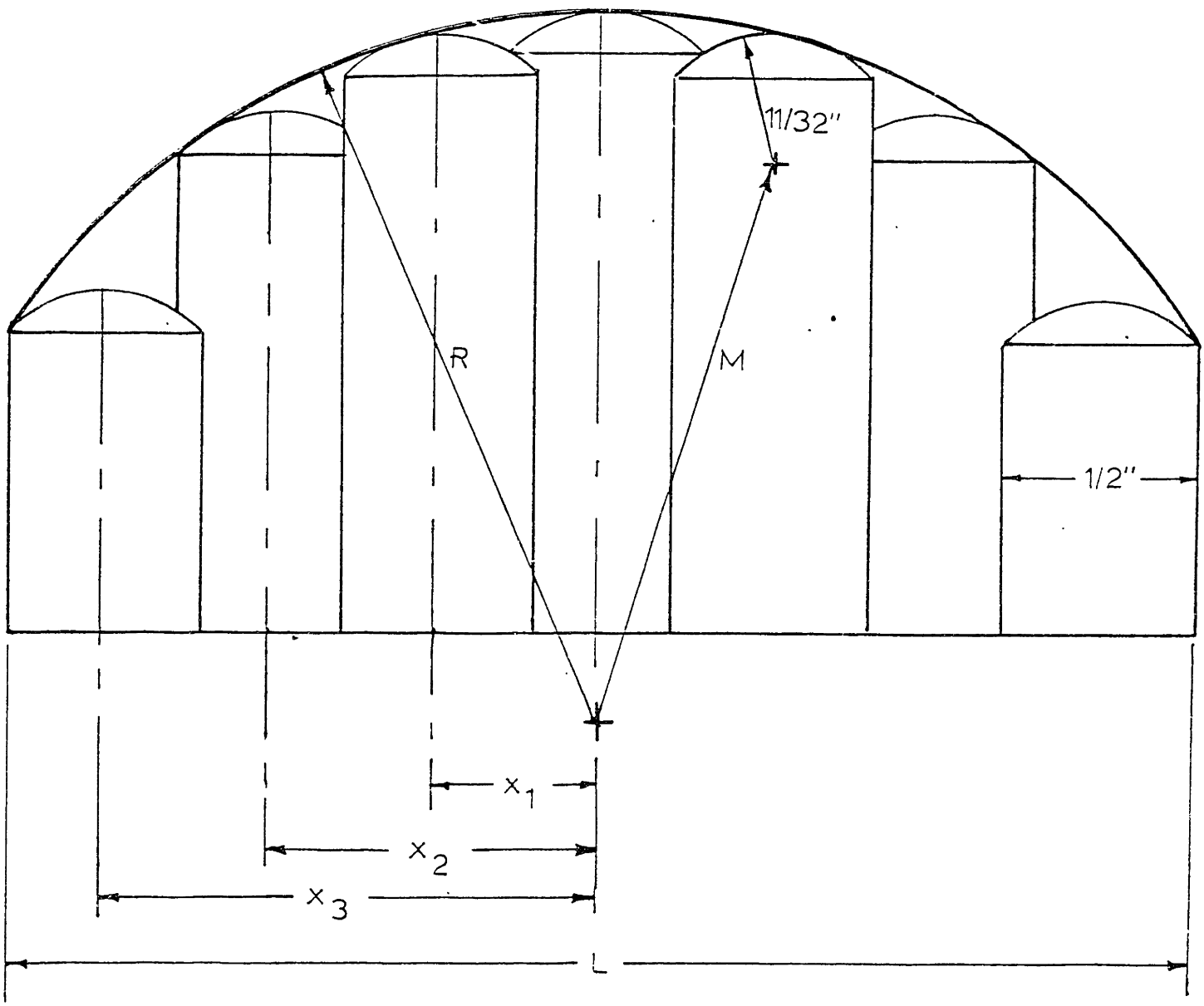

FIGURE 4.8: CALCULATION OF PIN POSITIONS

where

$$\frac{L-1/2}{6}$$

equals distance between pin centers, and n = number of pins away from the center pin. The Y distance from the center point for a particular pin is then

$$Y = \sqrt{n^2 - x^2}.$$

After the value of Y is found for all the pins, the Y values are found relative to the first row set.

$$Y_{rel} = Y_{calc} - Y_{first\ row\ set}$$

4.4.4 Positioning and Locking

After the calculations were made, each die was attached to the table of a vertical miller and the rows positioned with the positioning plates held in the quill of the miller. Since there were seven rows of pins to be positioned, and the die surface was symmetrical, three pairs of rows had identical positions, so only four positions were set. The clamp was then forced against the pins by tightening the four bolts on top. The bolts were tightened until the desired die opening, L, was achieved.

4.4.5 Attachment

When both dies were set and clamped, they were mated using the four alignment pins. Next they were attached to the universal testing machine by attaching the upper die to the gripping head and resting the lower die on two steel blocks on the bed of the testing machine. A picture of this set-up is shown in Figure 4.9.

4.4.6 Forming and Shape Measurement

The test sample, a 3003 H14 aluminum sheet which measured 2 5/8 inch by 2 5/8 inch by 1/16 inch, was inserted between two 1/16 inch rubber pads and carefully placed on the bottom die. The rolling lines on the aluminum sheets were oriented in the same direction (along the longer axis of the die) for all of the test specimens to avoid any forming variations arising from the anisotropy of the metal. The shape of the twelve test samples was then measured to establish a data base for subsequent analysis and evaluation of the process (see Figure 4.10). The measurements were performed as follows: A dial indicator was suspended above an X-Y table and an 11 by 11 array of points was measured on each sample. The samples were attached, convex side facing up, to the X-Y table using plasticene. Eleven points were measured in the X direction, separated by a 1/4 inch. The table was moved 1/4 inch in the Y direction, and the process was repeated in opposite direction in X. This continued until all eleven (11) rows were measured (121 points). The process was repeated for each of the remaining samples, and the data was entered into a computer for further analysis. Appendix E shows

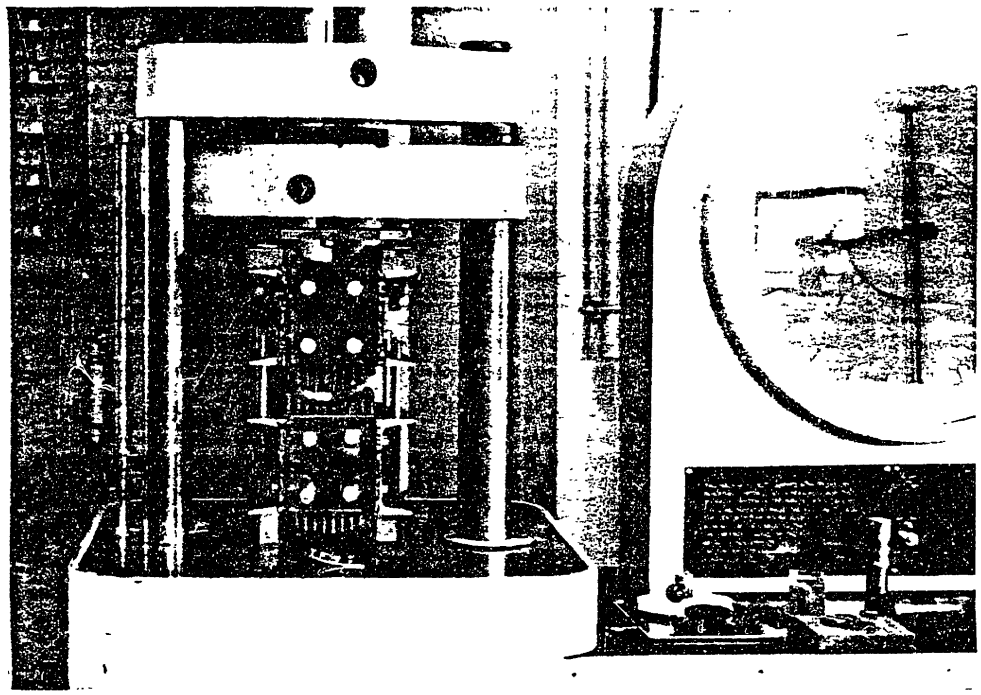

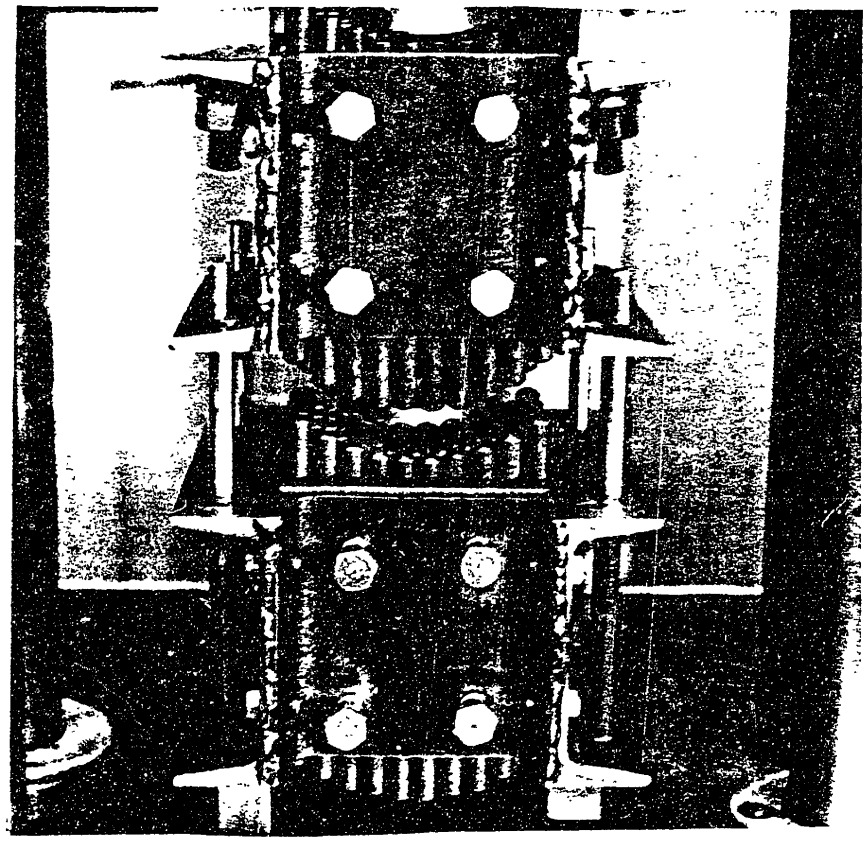

FIGURE 4.9: DDS EXPERIMENTAL SET-UP

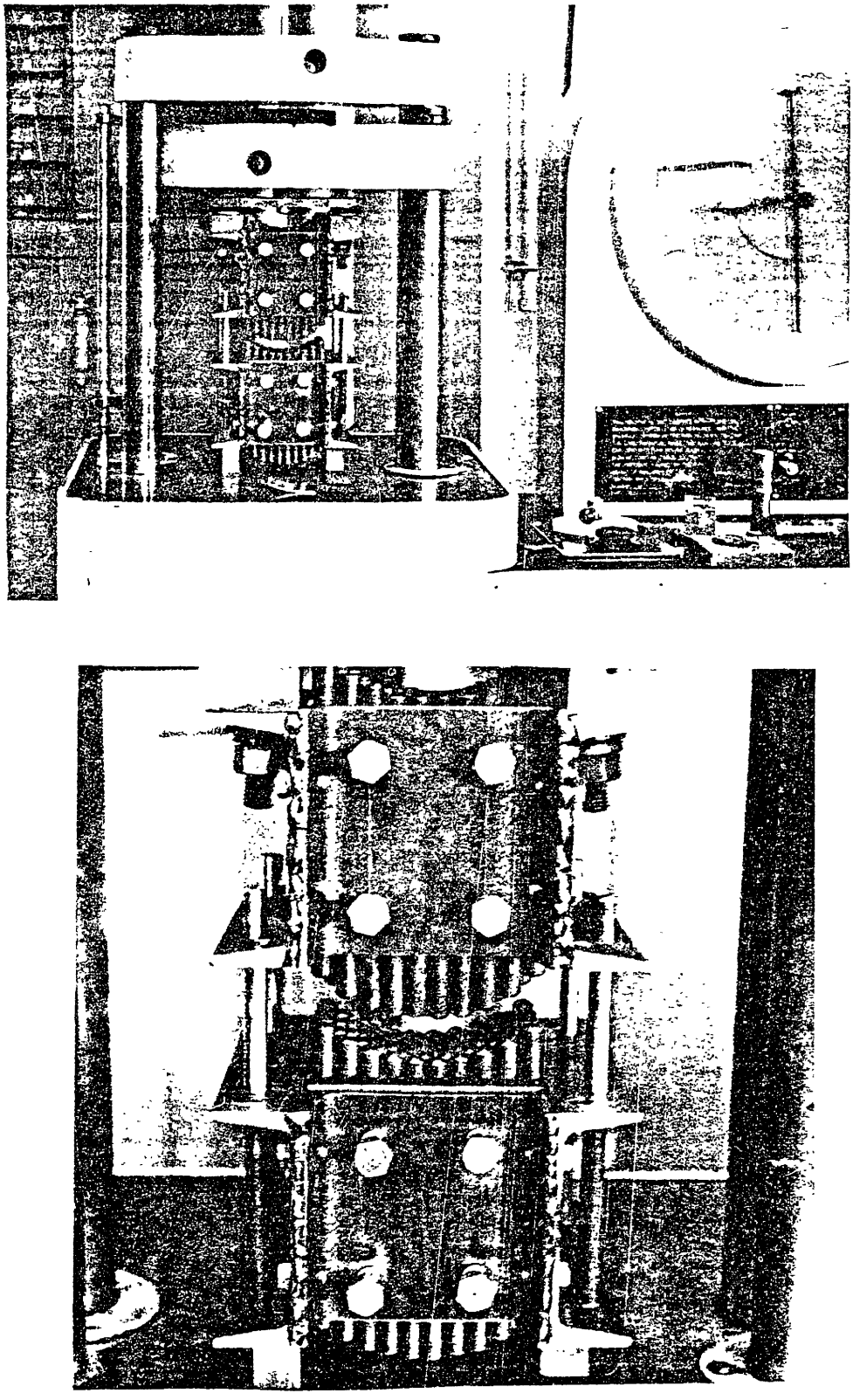

FIGURE 4.9: DDS EXPERIMENTAL SET-UP

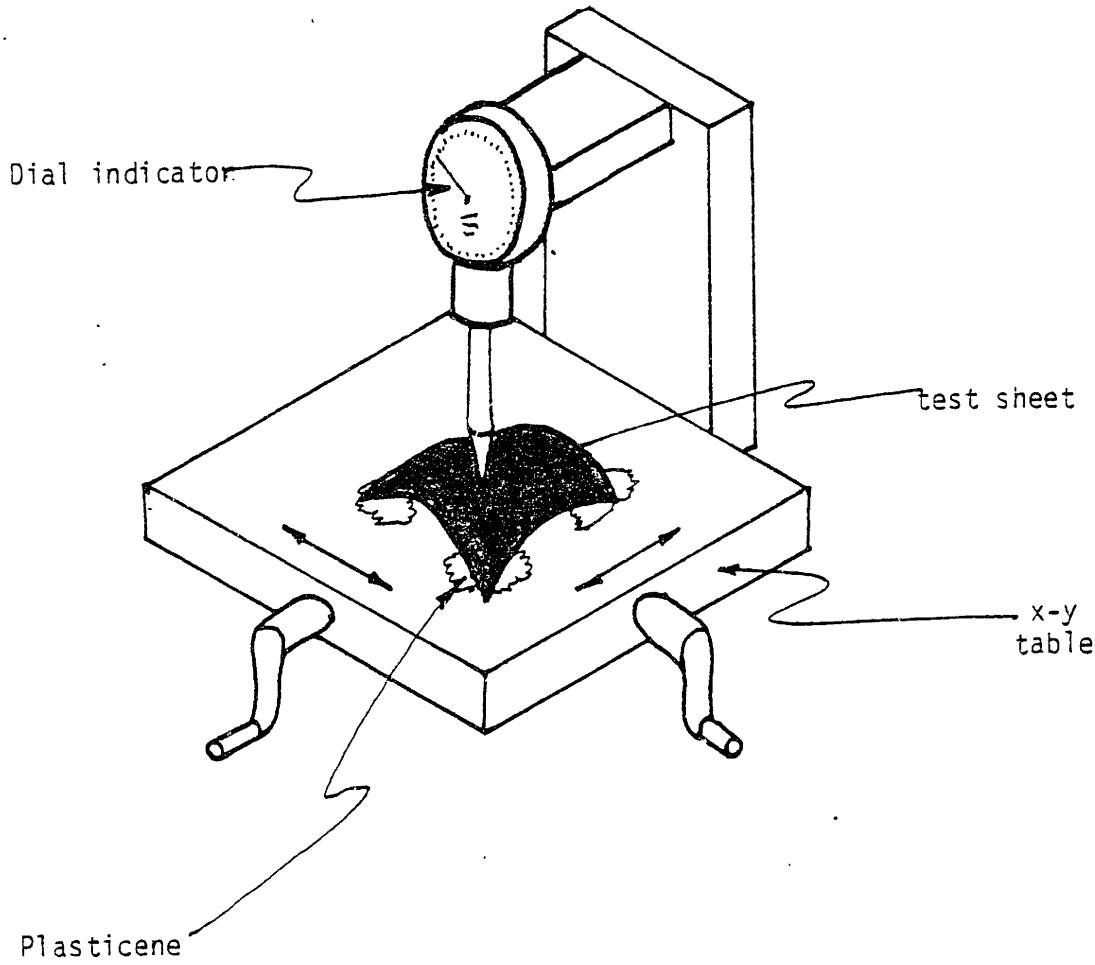

FIGURE 4.10: SHAPE MEASUREMENT METHOD

the raw data and the data file on the computer.

4.5 Summary

The experimental portion of the program consisted of the development and refinement of the necessary hardware to produce a set of test samples to establish a shape data base for further analysis. This data base was considered sufficient to answer the questions regarding accuracy, repeatability, shape limitations, and surface quality. As well as providing a data base for analysis, the experiment shed some light on the practical considerations that have to be taken into account when constructing a DDS system. Among these considerations were clamp stiffness and pin stacking. Now that the data has been gathered, an analysis to answer the questions about DDS forming may be undertaken. This is to be the subject of the next chapter.

CHAPTER 5

ANALYSIS OF RESULTS

5.1 Introduction

After the shape data was gathered, it was entered into the computer so that various analyses could be performed. The first step in analysis was the development of a program to calculate the unloaded shape, as described by the curvature of planar sections, from the data. The results of this analysis were then used to evaluate the DDS feasibility criteria by comparison of the various curvatures. Section 5.2 will discuss the curvature calculation, and Section 5.3 will discuss the evaluation of the results.

5.2 Calculation of Unloaded Curvature from Data

5.2.1 Unloaded Curvature Approximation

The unloaded curvature of the formed sheets can indicate the extent of material plastic flow and elastic springback, and the repeatability for a given set of forming conditions. Since the curvatures chosen in this experiment are constant along both axes of the die, it can be seen from the moment-curvature relationship that the curvature along those axes remains constant after springback Therefore, the unloaded curvatures of the test sheet along the two axes should be constants. With the data points given, arcs of constant curvature can be fit through these points. The unloaded centerline radius of curvature is the difference between the radius of one of these arcs

and 1/2 the sheet thickness (This is because the data points are taken on top of the sheet). Some methods for determining those arcs that most closely fit the data are described in Section 5.2.2.

5.2.2 Methods Used to Approximate Curvature

One method that may be used to fit a circle to the data is a least squares approximation. If it is assumed that the test piece is measured from an aribtrary origin, then the center of the circle is located a distance x_0, y_0 from the origin. Then the equation for the circle is:

$$(x - x_0)^2 + (y - y_0)^2 = R^2 \qquad (5.1)$$

Now, the measured value of y differs from the calculated value of y for a given R and x. The amount of error, e, is this difference. The least squares approximation is:

$$\frac{\partial(\text{variable})}{\partial E} = 0 \qquad (5.2)$$

where

$$E = \sum_{i=1}^{n} e^2 \qquad (5.3)$$

The variables in this case are R, x_0, and y_0. This gives three simultaneous equations with three unknowns. A detailed description of this derivation is given in Appendix F. This method was not chosen since it

involved solution of simultaneous non-linear equations. Iterative methods were used, but the results were unsatisfactory.

Another approach that may be used to approximate the circle that best fits the data points is the perpendicular bisector approach. Assuming that the data points lie on a circle, the perpendicular bisectors of the lines drawn between two sets of points should intersect at the center of the circle. (See Figure 5.1). The radius is the distance from this intersection to any of the points. By constructing several perpendicular bisectors, and determining the radii from the intersection points, an average radius can be found. This was the method implemented in a computer program which is discussed in the following section.

5.2.3 Computer Program

A FORTRAN program was implemented to perform the approximation described in 5.2.2. The average radius was calculated for each row of data points. Also, the standard deviation of the averaged radii was calculated as an indicator of how well the data points fit the circle. The values x_o and y_o (as described in 5.2.2) were printed for reference.

The radii were found using the following technique:

$$SL1 = \frac{x_A - x_B}{y_B - y_A} \qquad (5.2)$$

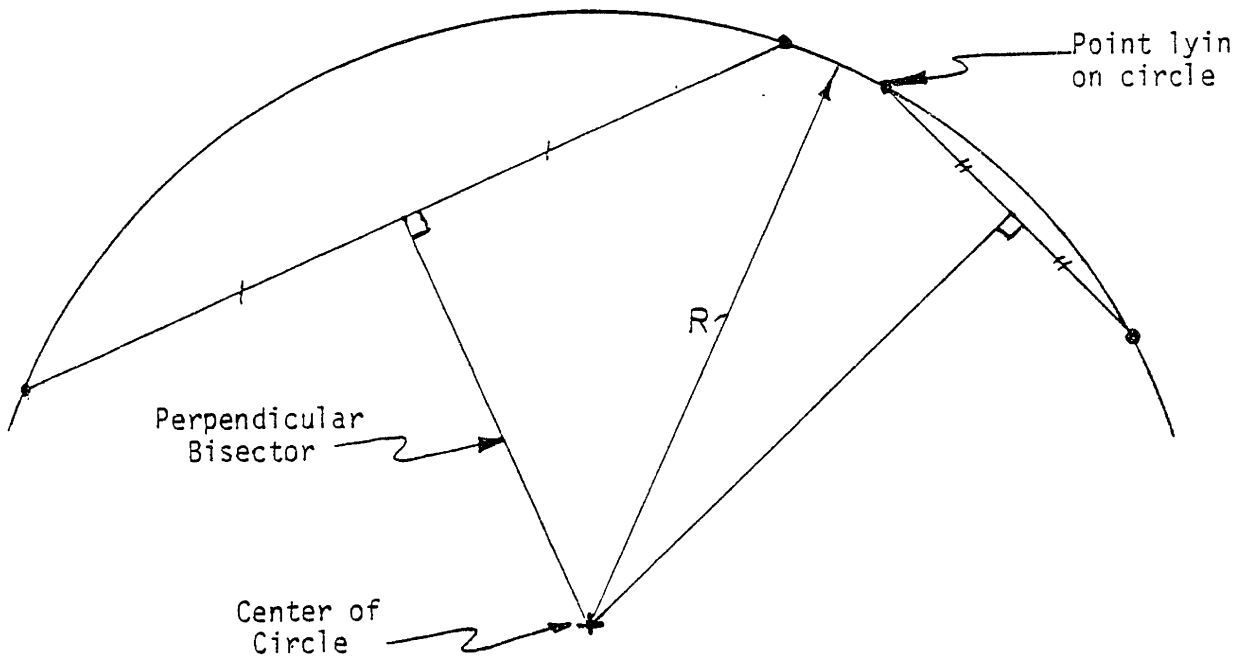

FIGURE 5.1: PERPENDICULAR BISECTOR APPROXIMATION

$$SL2 = \frac{x_C - x_D}{y_D - y_C} \tag{5.3}$$

where: SL1 = first perpendicular bisector slope

SL2 = second perpendicular bisector slope

y_B, y_A, x_A, x_B = first set of data points

y_D, y_C, x_C, x_D = second set of data points (see Figure 5.2)

To find the y-intersects:

$$y = mx + b \qquad b = y - mx$$

$$b_1 = \frac{y_A + y_B}{2} - SL1 * \frac{x_A + x_B}{2} \tag{5.4}$$

$$b_2 = \frac{y_C + y_D}{2} - SL2 * \frac{x_C + x_D}{2} \tag{5.5}$$

where b_1, b_2 are the 4 intersects of the perpendicular bisectors.

The intersection, x_o, y_o is

$$y_o = SL1 * x_o + b_1$$

$$y_o = SL2 * x_o + b_2$$

from these equations:

$$x_o = b_2 - b_1 / SL1 - SL2 \tag{5.6}$$

FIGURE 5.2: CONSTRUCTION OF PERPENDICULAR BISECTORS

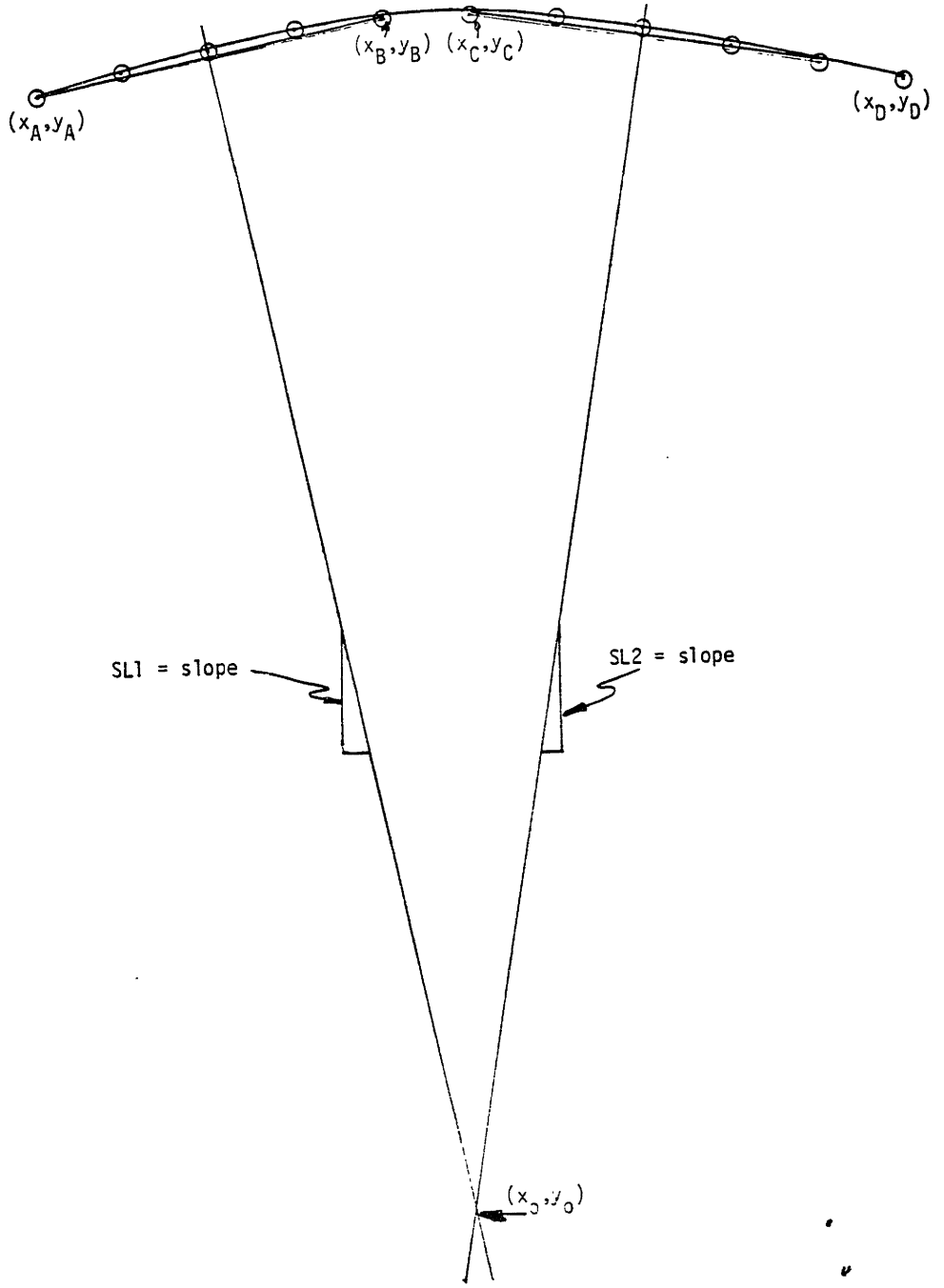

$$y_o = \frac{(SL2 * b_1 - SL1 * b_2)}{SL2 - SL1} \tag{5.7}$$

The radius is the distance from the center to one of the data points. In this experiment the radius was found by averaging these distances for all four data points.

$$R = \sqrt{(x_A - x_o)^2 + (y_A - y_o)^2} \tag{5.8}$$

A flowchart of the computer program is shown in Figure 5.3. The data was read into the array, CLEM. One row of CLEM was read into the array Y. The array X, consists of the distance between the rows, 1/4". The value for each X was:

$$X_n = \frac{1}{4}(n-1) \tag{5.9}$$

Next, four sets of points were selected from arrays X and Y and input into the subroutine, RAD, where the radius and center point were calculated by the method described above. The points selected were four points apart $(x_n, y_n, x_{n+4}, y_{n+4})$ for each perpendicular bisector. The points selected were separated by four points because it was found that the predicted center point wasn't as sensitive to errors in the y-values when the points selected were farther apart. There were fewer bisectors and hence less values for R to average with the selected points farther apart, so a compromise of 4 points separation was chosen. The intersections for all of these bisectors were found, and the radius

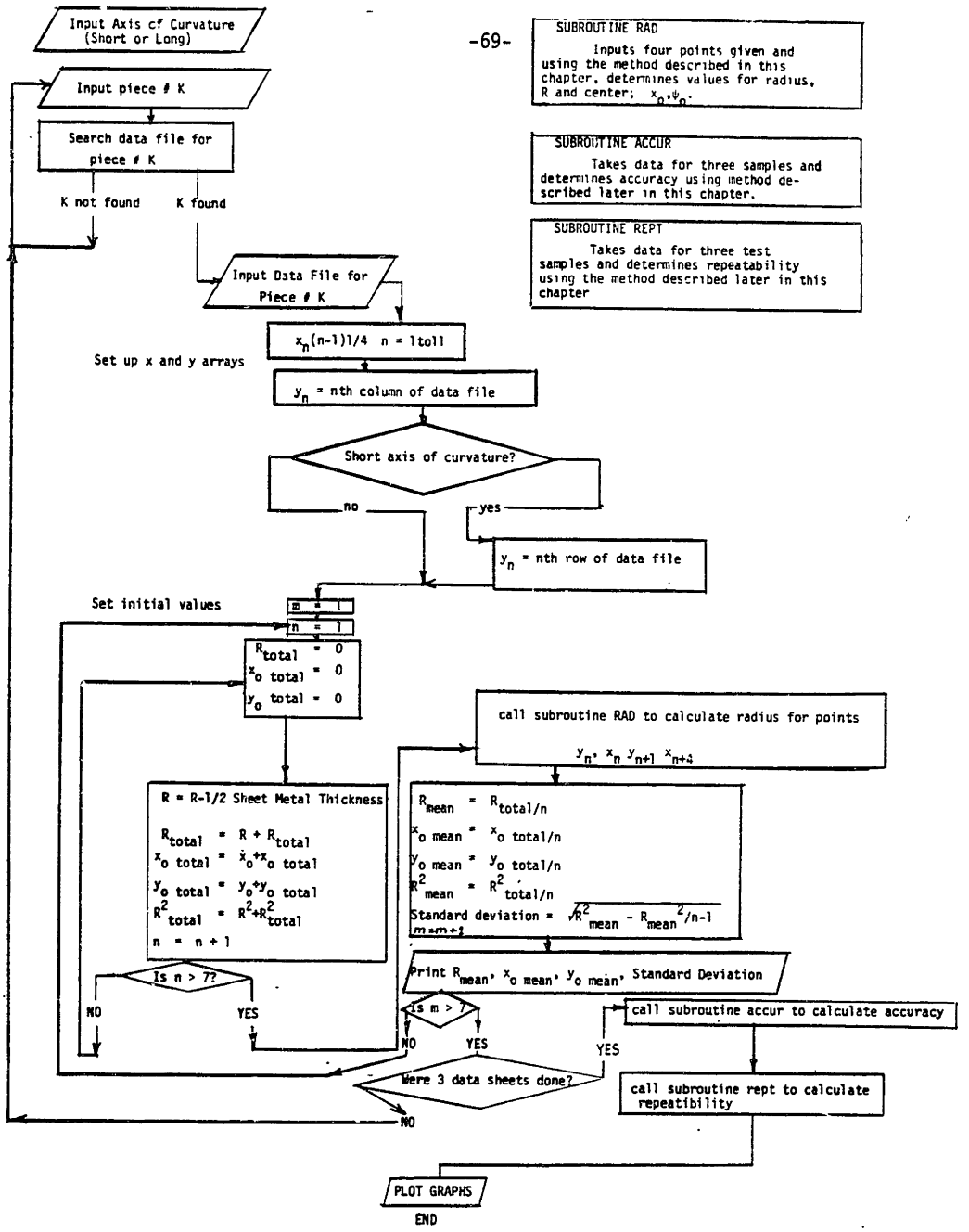

FIGURE 5.3: COMPUTER PROGRAM FLOWCHART

calculated for each. Finally, the average radius, standard deviation for the radius, and average x_o and y_o were printed out, repeated for the 11 rows in each test sheet and for all of the test sheets. From these values, some evaluations were made and are the subject of the next section. A listing of the program is included in Appendix G.

A complete listing of the results of this program is also shown in Appendix G.

5.3 Evaluation of the DDS Feasibility Criteria

With the unloaded sheet shape characterized by planar sheet radii, an evaluation of the four criteria for determining DDS feasibility can take place. These criteria are accuracy of forming, repeatability, shape limitations, and surface quality.

5.3.1 Accuracy

There are many factors that contribute to the accuracy of a forming operation. There is the accuracy of the die itself, variables such as forming force and material properties, as well as proper material flow and springback. In the sheets with simple curvature, the measured unloaded curvature was compared with a predicted value using the springback equation described in Section 3.2.1. Equation 3.1 is as follows:

$$\frac{R_L}{R_u} = 1-3\left(\frac{\sigma_y R_L (1-\nu^2)}{Et}\right) + 4\left(\frac{\sigma_y R_L (1-\nu^2)}{Et}\right)^3 \qquad (3.1)$$

where R_L = loaded radius of curvature

R_u = unloaded radius of curvature

σ_y = yield stress

ν = Poisson's ratio

E = modulus of elasticity

t = sheet thickness

From Section 3.3.2, the values for the material properties of 3003 H14 Aluminum are given for the test sheets:

t = 1/16"

ν = .33 (Poisson's ratio)

σ_y = 21,000 (yield stress)

E = 10×10^6 (modulus of elasticity)

Also, for the simple curvature cases, R_L = 3.5". This gives a spring-back ratio of

$$\frac{R_L}{R_v} = .681 \quad \text{or} \quad R_u = 5.14"$$

Averaging all of the measured values for radius of curvature of the three samples with simple curvature gives

$$\bar{R}_u = 6.02"$$

This variation in predicted and measured values for unloaded curvature could be attributed to two factors. First, the values for

yield stress and modulus of elasticity were handbook values which may vary significantly from the actual values of the sheet. Secondly, the curvature at the ends of the sheets were near zero since no moment was applied outside of the pin contact points. With the method used in this experiment for calculating curvature, this gave a larger radius of curvature than if the curvature continued to the ends, as was assumed in the springback formula.

It is not the purpose of this report to examine in depth the springback of sheet metal in contour forming; however, the data acquired may be sufficient to do preliminary analysis of springback in two directions. Until now, determination of overbend to account for compound curvature springback has been mostly by trial and error. Since the loaded sheet curvature is known, the springback can be evaluated for each curvature. Some empirical formulas for springback may be formulated from the data, which may find application in automated DDS systems where overbend can be determined by trial and error since it will be possible to change the die shape very easily.

The set-up accuracy of the die may be checked by observing the symmetry of the formed piece about its center. For each of the three trials in each die configuration, a method was used to find the average accuracy. The equation used in this method is shown below:

$$\% \text{ accuracy} = \frac{200}{11} \sum_{n=1}^{5} \frac{\bar{R}_n - \bar{R}_{12-n}}{\bar{R}_n - \bar{R}_{12-n}} \qquad (5.10)$$

where n = row #

$\bar{R}_n$ = average radius of curvature of three trials for one row

First, the average radii for each row (R_n) was calculated from the three pieces. Next, the difference between symmetrical points ($\bar{R}_n - \bar{R}_{12-n}$) was found and its percentage of the average of these two points calculated. Finally, these percentages were averaged for all of the rows. Table 5.1 shows quantitatively the values for this accuracy. The average for all of the pieces was 6% with a maximum of 14%. These numbers correspond to a lack of symmetry which may be caused by poor pin positioning or die misalignment. (see Figure 5.4) This problem may be easily eliminated in future experiments with more accurate die construction (the guide pins, for example, may be causing misalignment) and accurate pin positioning.

TABLE 5.1: ACCURACY OF DIE

SHEET NO.'S	Loaded Radius of Curvature, in.		Axis in which radii were measured	% Accuracy
	LONG AXIS	SHORT AXIS		
1,2,3	3.5	3.5	Long	10.0
4,5,6	5.25	3.5	Long	13.9
7,8,9	3.5	7.0	Long	4.5
10,11,12	3.5	∞	Long	.65
1,2,3	3.5	3.5	Short	6.2
4,5,6	5.25	3.5	Short	.99
7,8,9	3.5	7.0	Short	6.1

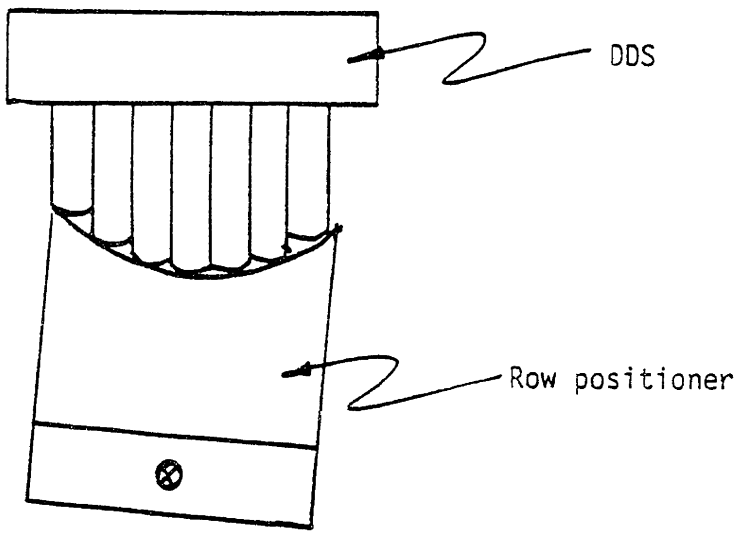

a) Positioner not aligned correctly during positioning

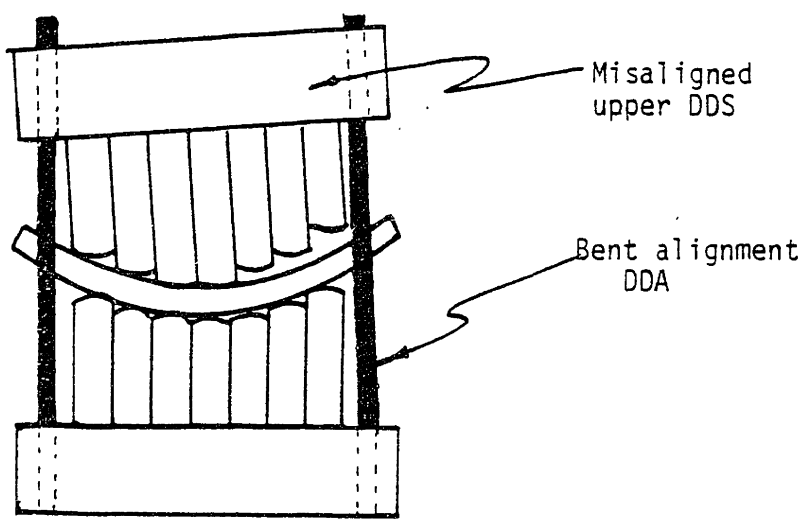

b) dies misaligned

FIGURE 5.4: PIN POSITIONING AND DIE MISALIGNMENT

5.3.2 Repeatability

Another criterion for feasibility is repeatability of forming. Factors which would affect the repeatability of the system are material property variations, correct positioning of the sheet in the die, change in the die surface with usage, and forming load variations. This section will analyze these factors and give quantitative values for repeatability of the DDS test fixture.

The test sheets used in this experiment were all cut from one sheet of 3003 H14 Aluminum. The rolling lines on the sheets were all lined up in the same direction in the die to eliminate anisotropy effects. These two considerations should have minimized the material property effects on repeatability. The forming force was measured to 1000 lbs, as precisely as possible. The forming force was applied with a precision of less than 3%, taking into account the operator's ability to observe sudden changes in force.

The repeatability of positioning the sheet in the die was expected to affect the repeatability of the formed sheet. The edge effects might have varied since the ends would take different positions with respect to the pin tips. Also, if the sheet was measured in a different position from that in which it was formed, the entire data set would have shifted. By careful indexing of the sheet when forming and measuring, this effect was kept to a minimum.

The surface of the die may have varied with successive forming

because of some pin slippage. Pin slippage is a cumulative error so that the curvature would have changed with successive formings. Since the load distribution is carried more equally with smaller die curvatures, pin slippage would tend towards decreasing the curvature in the sheet with successive formings, Figures 5.5a to 5.5g show plots of curvature in one direction with position in the orthogonal direction for the twelve samples. These figures showed no apparent successive curvature decrease with each trial, indicating that pin slippage was not a problem in this experiment.

As with die accuracy, a method was developed to determine the repeatability of each of the die configurations. The equation used in this method is shown below:

$$\frac{100}{11} \sum_{m=1}^{11} \frac{1}{\bar{R}_m} \sum_{n=1}^{3} [(R_{mn}-\bar{R}_m)^2/(n-1)]^{1/2} \qquad (5.11)$$

where n = trial # (3 trials for each configuration)

m = row # (11 rows on each sheet)

$\bar{R}_m$ = average radius of curvature of 3 trials for a single row

R_{mn} = radius of curvature of trial n, row m

The method was developed as follows. First, the mean and standard deviation of the three samples for each row was found. Next, the standard deviation was divided by the mean and multipled by 100 to obtain the percent standard deviation. Finally, the percent standard deviation was averaged over the 11 rows. Table 5.2 shows the results

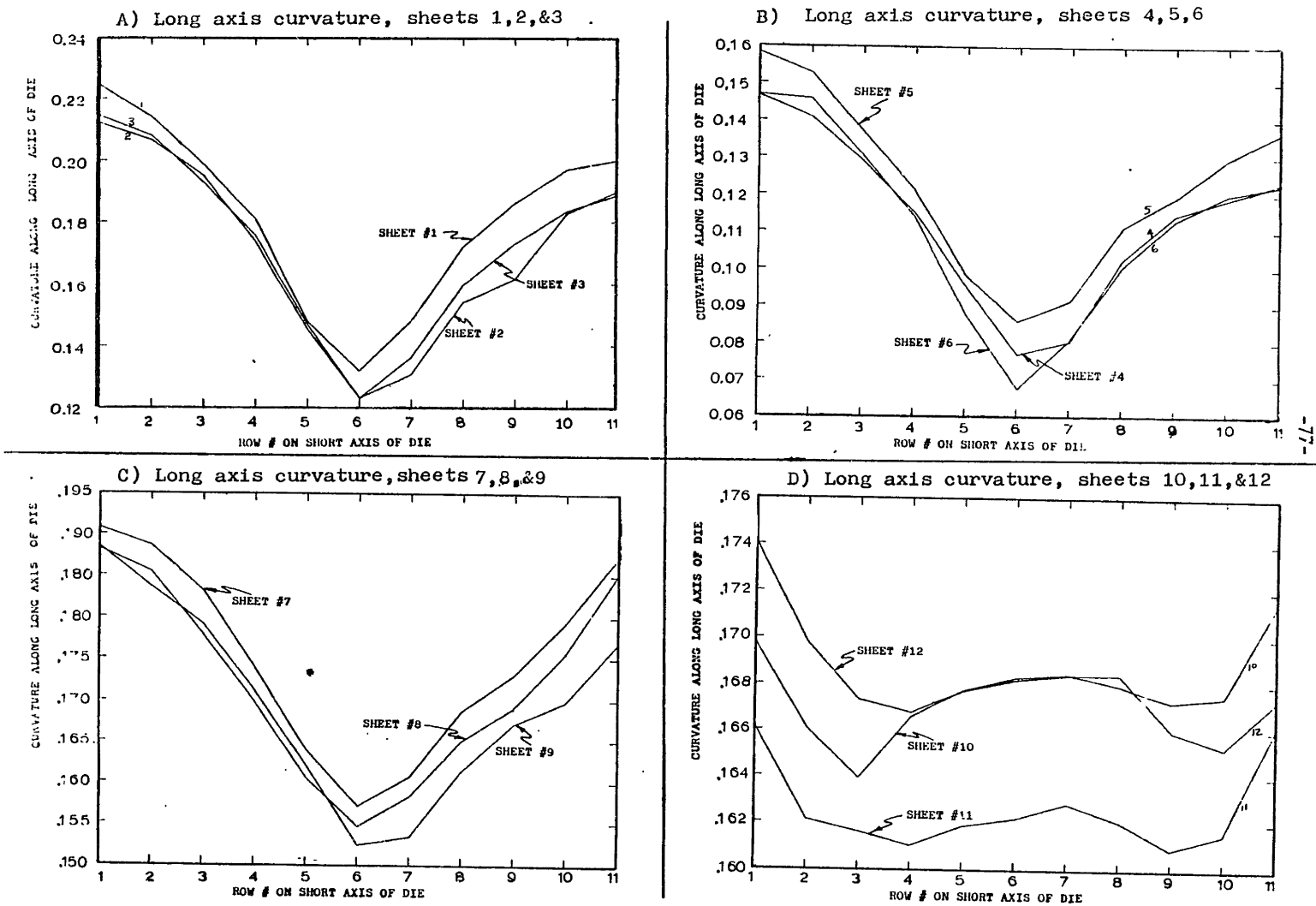

FIGURE 5.5: CURVATURE vs POSITION FOR 12 SAMPLES (Page 1 of 2)

E) Short axis curvature, sheets 1,2,&3

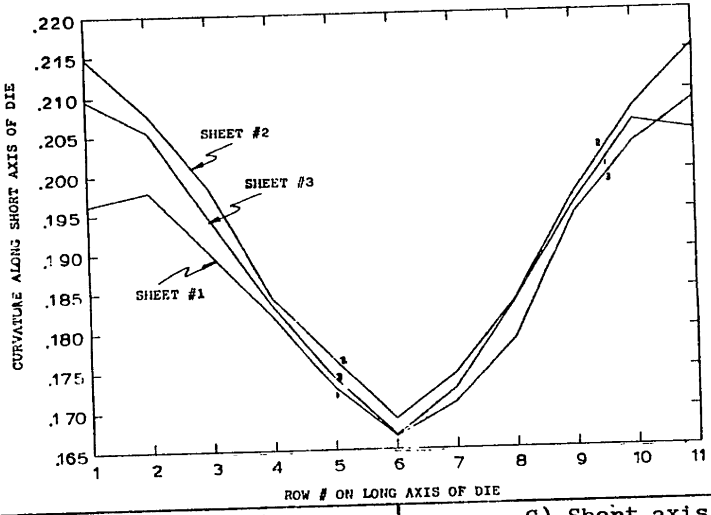

F) Short axis curvature, sheets 4,5,&6

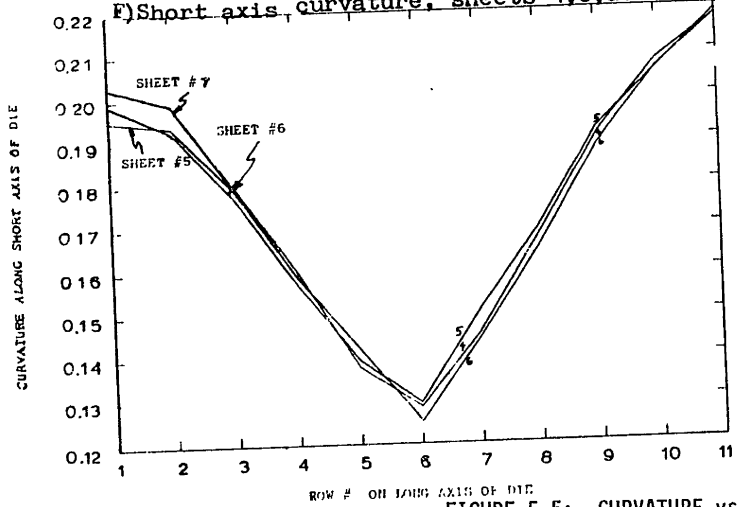

G) Short axis curvature, sheets 7,8,&9

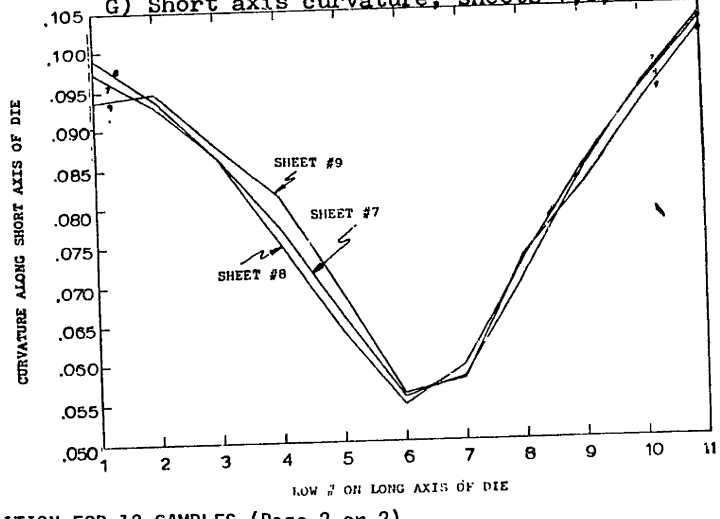

FIGURE 5.5: CURVATURE vs POSITION FOR 12 SAMPLES (Page 2 or 2)

of this calculation. The nominal repeatability of the system was found to be 1.5% with a maximum of 3.1%. These are determined to be reasonable values for repeatability and support the feasibility of the DDS concept.

TABLE 5.2: REPEATABILITY

SHEET NO.'S	Loaded Radius of curvature, in.		Axis whose curvature was measured	% Repeatability
	Long Axis	Short Axis		
1,2,3	3.5	3.5	Long	2.08
4,5,6	5.25	3.5	Long	3.07
7,8,9	3.5	7.0	Long	1.03
10,11,12	3.5	∞	Long	1.17
1,2,3	3.5	3.5	Short	0.75
4,5,6	5.25	3.5	Short	0.98
7,8,9	3.5	7.0	Short	1.10

5.3.3 Shape Limitations

The shape of a part formed on a DDS is ultimately limited by the mechanical constraints of a given DDS system as discussed in Section 2.3.2. When determining if a shape may be formed within these constraints, the effects of compound curvature on material flow and springback must be accounted for. The shape is also limited by the maximum curvature to avoid buckling (as described in Section 3.2.2),which may be more pronounced in a DDS than a conventional die. In this experiment, the buckling and apparent springback were found to be strongly related in

the sheets with compound curvature.

The experimental results showed that the curvature in one direction affected the apparent springback in the orthogonal direction. This is shown graphically in Figure 5.6. This graph shows the curvature along the long axis of the die as a function of position along the short axis for three different test samples. The loaded radius of curvature for all three samples on the long axis was 3.5". Sample 10 was made with no curvature along the short axis of the die. For this sample, the curvature along the long axis is nearly constant over all positions along the short axis. Sample number 2 was made with a loaded radius of curvature of 3.5" along both axes. Not only was the average radius of curvature of piece #2 smaller than that of piece #10 by about 0.3" (5.5%), but variation in the curvature by approximately a factor of two was observed with minimum curvature at the center. Sample no. 7 falls between these two curves in unloaded curvature, and had an intermediate value for the loaded radius of curvature in the orthogonal direction (5.25").

The apparent springback observed in these sheets did not coincide with what would be predicted, suggesting that buckling of the material occurred. With compound curvature, compressive stresses are introduced in the sheet as the material attempts to flow in-plane in such a way that higher compressive stresses occur away from the center of the sheet. Since the elastic compressive stress is a major contributor to springback, the distribution of springback is weighted towards the

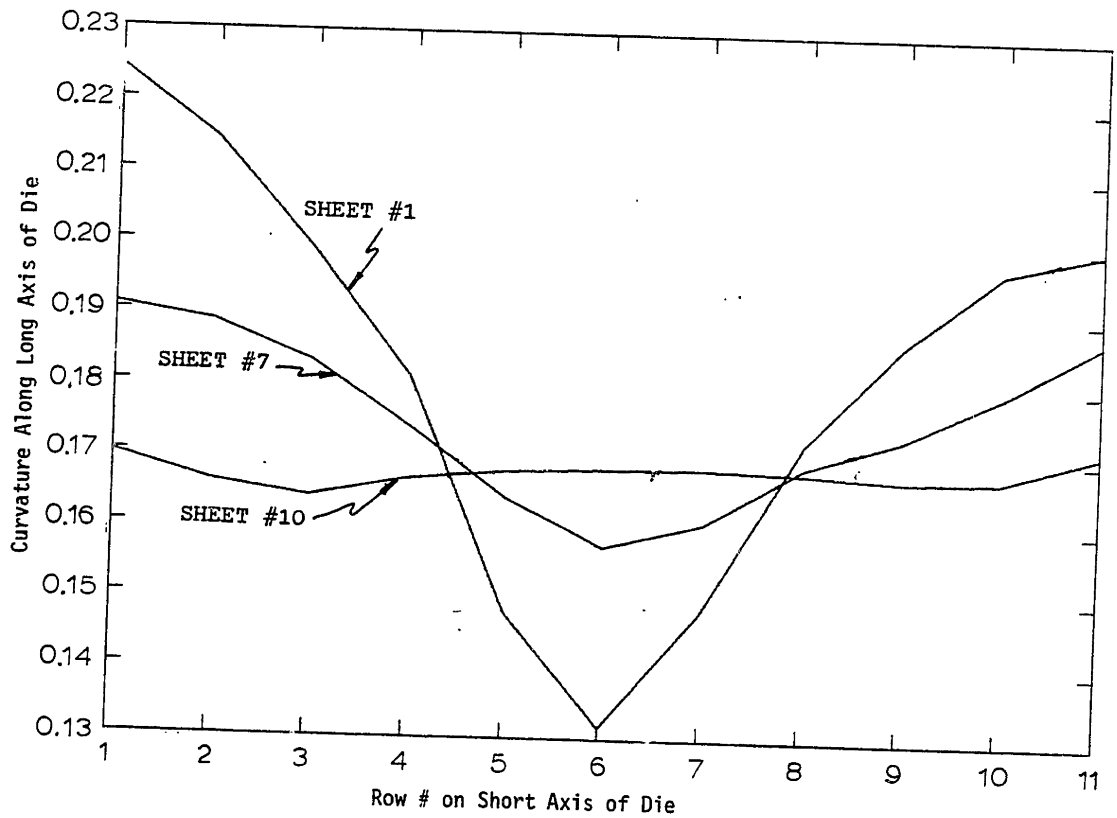

FIGURE 5.6: RELATIONSHIP BETWEEN LOADED CURVATURE AND SPRINGBACK

outside edges of the sheet. This was not observed, suggesting that some buckling or plastic flow took place.

The effect of buckling was to decrease the apparent springback along the edges of the sheet, especially with large compound curvatures. This effect is shown graphically in Figure 5.7. This graph shows the mapping of the first test sheet with loaded radii of curvature of 3.5" x 3.5". Along the edges of the sheet most of the curvature is located in the center, while there is hardly any curvature near the corners. This suggests that a small amount of buckling occurred, originating at the center of each edge. It appeared that the material bent over the four lines of pins connecting the center points of each edge so that the curvature was greatest along these lines (see Figure 5.8).

Quantitative information about buckling was not obtained in this experiment, although the effects were not found to be severe. Future experimentation could be undertaken to determine the relationship between springback and buckling, and how buckling effects can be minimized. Restraint of the edges of the sheet may be a way to counteract the compressive stresses which cause buckling.

5.3.4 Surface Quality

The primary consideration when evaluating surface quality of a DDS system is dimpling effects. In this experiment, rubber interpolators were used and no dimpling was observed by visual inspection. Since the surface of the aluminum is quite lustrous, and the spatial

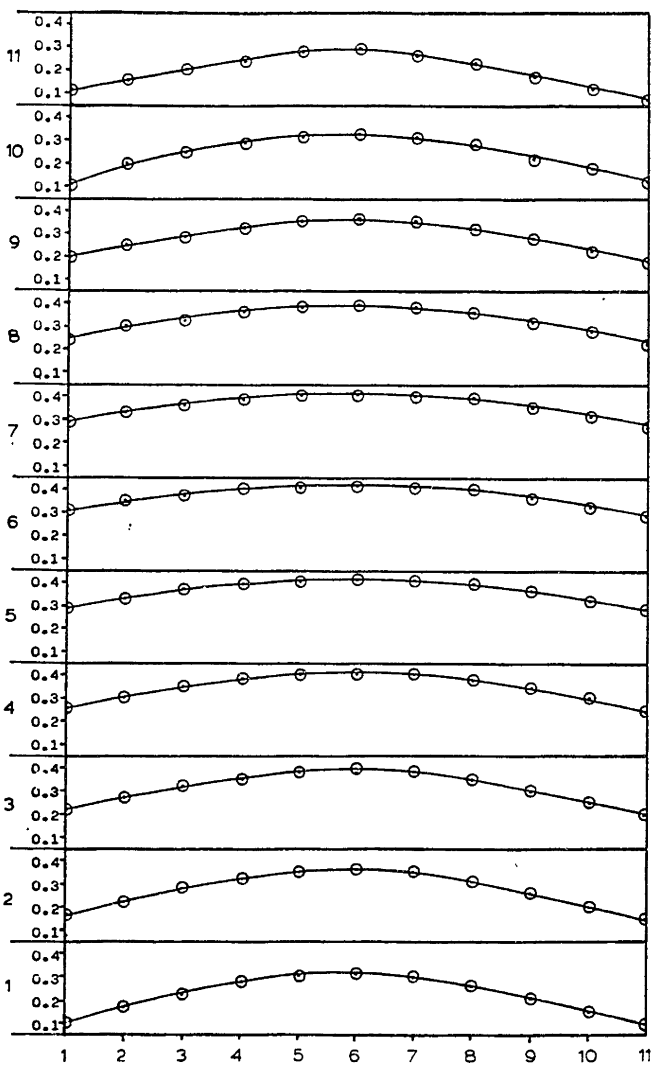

FIGURE 5.7: MAPPING OF TEST SHEET NUMBER 1

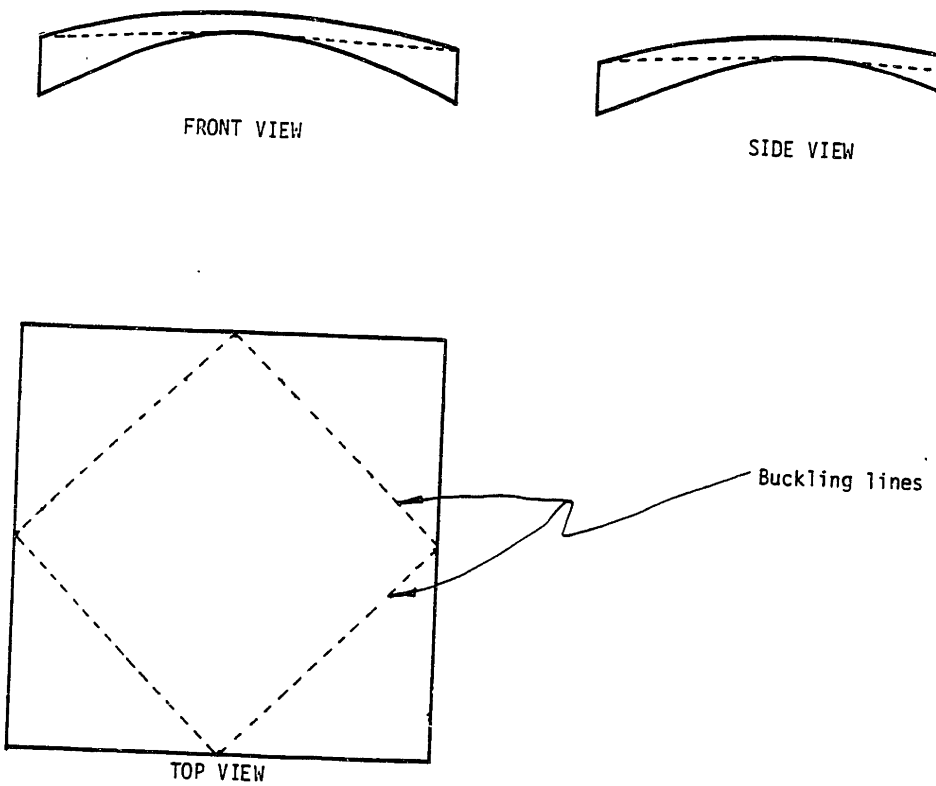

FIGURE 5.8: BUCKLING OF A TEST SHEET

frequency of the pins was relatively high, visual inspection was considered a satisfactory technique for determining surface quality. No indication was found by inspection which would indicate that the sheet was formed by a DDS as opposed to a continuous die surface. The reason for this result is probably the choice of a mated die configuration which eliminated the cupping effect as described in Section 3.2.3, and use of rubber interpolators and low forming forces to minimize surface dimpling.

Before it was realized that visual inspection was a satisfactory technique, a computer program for evaluating dimpling effects was begun. This program, using a Fast Fourier Transform, would have evaluated the spatial frequency characteristics of surface variations. The intention was to measure the amplitude at spatial frequencies corresponding to the pin separations. A listing of this program as it currently exists, is included as Appendix H. The program has not yet been completely debugged, and is presently not operational. Although this program was not required in this experimentation, it might be useful in the future to quantify the dimpling effect in cases where visual inspection shows that this effect occurs.

5.4 Summary

A computer program was written and used to calculate the radii of curvature using the perpendicular bisector method. The results of this computer program were analyzed in terms of the DDS feasibility criteria discussed in Chapter 4. The significant observations made in

this chapter are as follows:

1) With simple curvature, the predicted unloaded curvature for the test sheets varied from the measured value by 16%. This variation could be caused by mis-measurement or material property variations.

2) Using symmetry about the center of the sheet as an indicator of die accuracy, the accuracy was found to be nominally 6% with a maximum of 14% of the curvature. The inaccuracy was probably caused by die and/or positioner misalignment.

3) With compound curvature, springback varied with a change in curvature in either direction, and with location on the sheet.

4) Buckling occurred to a small degree along the ends of the sheet and affected the measured unloaded radius. This was probably caused by lack of support on the outside edges.

5) The repeatability of the process was found to be nominally 1.5% with a maximum of 3.1% of curvature.

6) Dimpling was not a problem in this experiment primarily because of the opposed die configuration and the use of rubber interpolators.

These results suggest that the DDS concept is quite feasible for die-forming of sheet metal. The results also identify areas for future work which is to be the topic of the next chapter.

CHAPTER 6

CONCLUSIONS

6.1 Experimental Conclusions

The experimental procedure was successful in that it produced a set of test samples which provided useful information concerning the feasibility criteria. From analysis of these test samples the general conclusion was that the DDS concept is feasible for this configuration. In support of this statement several specific observations were made.

First, a visual inspection of the surfaces of the test sheets indicated that dimpling did not occur in any case, primarily because of the use of mated dies and rubber interpolators. With compound curvature, buckling or plastic flow observed to effect the unloaded shape of the test sheet more severely than springback, although it only occurred near the edges of the sheet. The repeatability was found to vary with different die set-ups, with a nominal value of 1.5%, and a maximum value of 3% of curvature. The set-up accuracy was estimated to be nominally 6% with a 14% maximum, as indicated by symmetry about the center of the test sheet. These values of accuracy were likely caused by die or pin positioner misalignment. Also, in sheets with compound curvature, the curvature in one direction was found to affect the springback in the orthogonal direction in a complex fashion. Finally, the springback equation for simple curvature was verified with a 16% difference between the measured and calculated radius of curvature.

6.2 Future Work

The data produced in this experiment may still undergo further analysis. As a more precise method for determining the curvature of the formed piece, the least squares approach described in Section 5.2 and Appendix F could be used. Also, some quantitative measure of buckling could be developed and related to springback in such a way that an empirical method for predicting the unloaded shape could be formulated.

In this experiment, the measurement method used was rather tedious. An automatic measuring system which could send data directly to a computer for analysis would greatly speed up the process of measurement, so a larger data bank could easily be produced. This could be used to more accurately determine the repeatability of the system. Also, an experiment could be conducted which compared different methods of restraint on the edges of the test sheet to reduce the buckling effect. If a conventional die could be obtained, and a DDS positioned to approximate its shape, a comparison could be made of the accuracy and repeatability of a DDS as compared with a conventional die. An experiment where a particular set-up was repositioned several times could be undertaken to determine the repeatability of die set-up. Finally, different die shapes and test materials should be experimented with, and if dimpling occurs, different interpolrators investigated to eliminate the dimpling. Future DDS design could incorporate the relationship between pin tip radius and material properties discussed in Section 3.3.1 and Appendix D. Spectral analysis described in Section 5.3.5 and Appendix H could be utilized to quantify the dimpling effects.

REFERENCES

1. Brook, M.P., Chan, Y.N., Lepper, M., "Selecting An Interpolator for a Variable Geometry Die", M.I.T. Course 2.30 Final Report April 24, 1980.

2. Gossard, D.C., Hardt, D.E., McClintock, F.A., Allison, B.T., Stelson, K.A., Olsen, B.A., and Gu, I., "Sequential Forming of Sheet Metal Parts", Final Report to Air Force Materials Lab. WPAFB, Contract #F33615-78-C-5111, January 1980.

3. Hardt, D.E. and Gossard, D.C., "A Variable Geometry Die for Sheet Metal Forming: Machine Design and Control", JACC, June 1980.

4. Iwasaki, Y., Shiota, H., Taura, Y., Seko, N., Kumamoto, M., "Development of a Triple-Row-Press", Mitsubishi Heavy Industries, Technical Review, June 1977.

5. Lindberg, R.A., Materials and Manufacturing Technology, Allyn and Bacon, Inc., Boston, MA 1968, pp. 341-375.

6. McClintock, F.A. and Argon, A., Mechanical Behavior of Materials, Addison Wesley, Inc., Reading, MA, 1966, pp. 453-458.

7. Roark, R.J. and Young, W.C., Formulas for Stress and Strain, Fifth Ed., McGraw-Hill, Inc., 1975, pp. 516-517.

8. Shigley, J.E., Mechanical Engineering Design, McGraw-Hill, Inc., New York, 1977, pp. 26-93.

9. "Springback of Sheetmetal When Using Compressible Tools", Sheet Metal Industries, Vol. 5, November 11, 1974, pp. 695-698.

10. Stearns, S.D., Digital Signal Analysis, Hayden Book Co., Inc. 1975, pp. 249-255.

11. "Stresses in Sheet Metal Parts", Machine Design, Vol. 46 No. 27, November 14, 1974, pp. 186-187.

APPENDIX A

POSITIONING AND CONTROL OF A DDS

This appendix discusses the research the author was involved with in regards to the positioning and control of a DDS. For detailed information on experimentation related to the positioning and control aspects of a DDS see the Air Force report (Gossard et.al (1980)). The initial work on the control of a DDS grew out of a control concept used with a programmable backgage. Figure A.1 shows the set up for one row. The pins are held by a retaining bar and the housing is moved away from the retaining bar. As a pin reaches its correct position with respect to the housing, a locking device is activated and the pin moves along with the housing. The locking devices are air plena located in the housing above each of the pins. A computer controls solenoid valves connected to each of these plena. As mentioned, earlier in this report, this design is limited to the closeness of pin packing since the pins have to account for the thickness of the air plena.

Other methods were investigated to lock the pins. One method used wedging action to lock the pins (see Figure A.2). A wooden prototype was built and did not work so further work was not done. The next idea was to pack the pins together and lock them with one large damping device. The pins needed to move independently of each other for positioning before the clamp was activated. Spacers

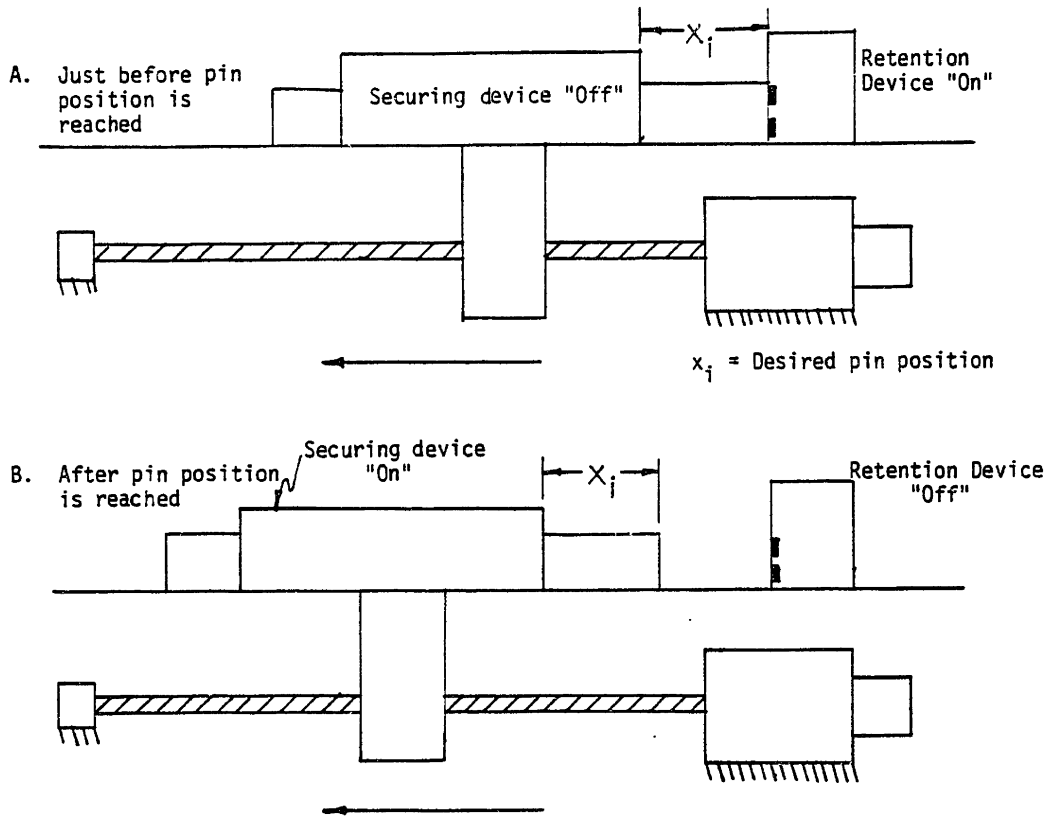

FIGURE A.1: AUTOMATIC PIN POSITIONING

FIGURE A.2: PIN LOCKING WITH WEDGES

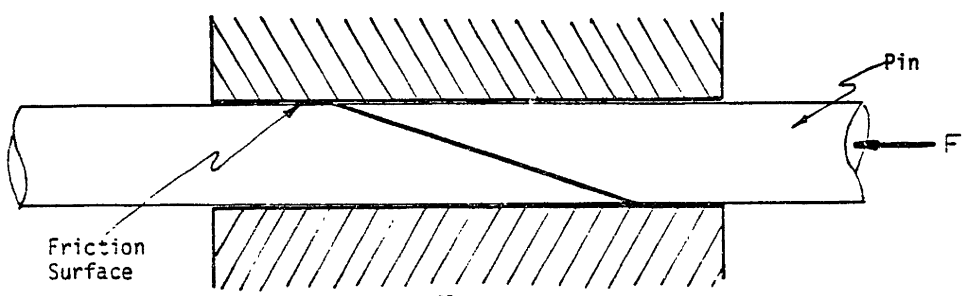

were inserted between rows to achieve this result. The proposed positioning concept for future work is a 3 axis manipulator that will position the pins individually before locking.

As DDS systems get larger, the problem of locking gets more complicated. One idea for larger systems is to have a locking device for each row of pins and use square pins. (See Figure A.3). This eliminates the problem of different pin locking forces caused by size differences in pins. With this configuration, an entire row may be positioned at once using a dummy pin-housing arrangement. The dummy pins could be positioned using the method described at the beginning of this appendix, then forces against the pins of the actual DDS.

The control and positioning concepts are important areas for future development if the DDS is to be used more extensively. The choice of control is dictated by the size of the DDS and larger systems will require more sophisticated control devices.

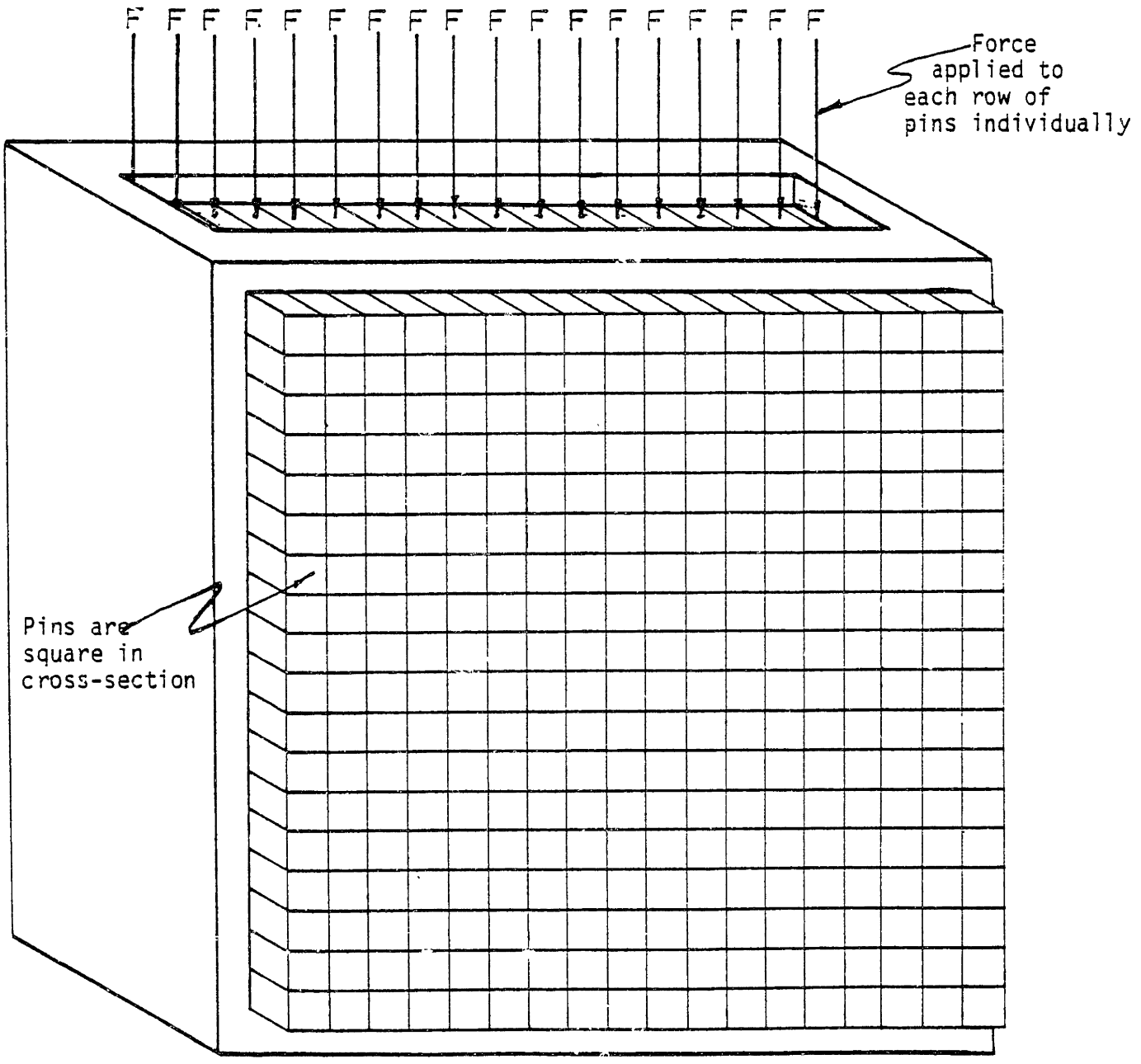

FIGURE A.3: DDS CONFIGURATION FOR A LARGE NUMBER OF PINS

APPENDIX B

INTERPOLATING SURFACES AND DEVICES

The purpose of an interpolating device in a DDS is to minimize the material effects (such as dimpling) caused by the discontinuities of the DDS surface. This may be achieved by supporting the material between the points where it is contacted (See Figure B.1). The two types of interpolators developed in this research project were surface interpolators and pin tip interpolators.

A group of M.I.T. undergraduate students (Brooks, M. (1980)) did some experiments with rubber tipped pins for use as interpolators. They found that the pin tip geometry shown in Figure B.2 worked the best. The concave shape of the pin tips cause them to provide more support out near the edges where surface discontinuities occur. This interpolator appears quite feasible and merits further investigation.

The type of interpolator used in the test fixture for this experiment was a surface interpolator composed of rubber sheets located on both sides of the sheet metal to be formed. The increased contact area caused by the use of the rubber sheet interpolator is comparable to increasing the pin tip radius, which decreases the chances of dimpling. This interpolator proved to be quite effective in this experiment, with no dimpling observed.

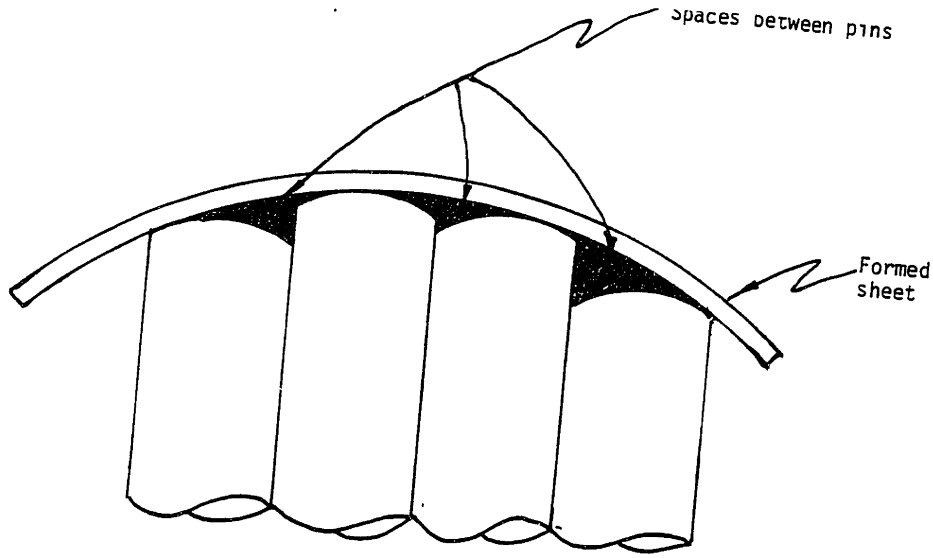

FIGURE B.1: SPACES BETWEEN PINS WHEN FORMING

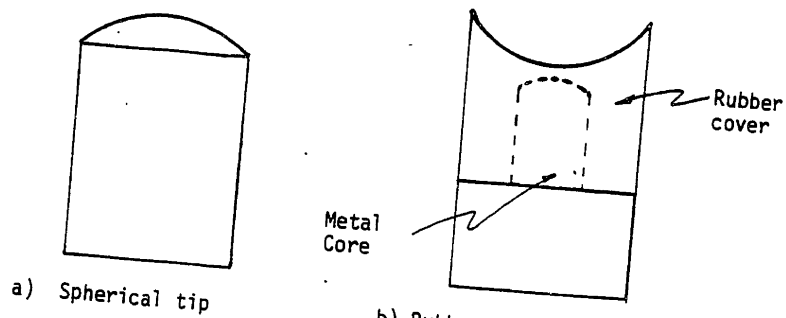

FIGURE B.2: RUBBER TIP INTERPOLATOR

Interpolating devices are an important subject for future work with the DDS. Other types of devices, such as a network of woven straps (see Figure B.3) could be used for interpolators, and experiments performed with them.

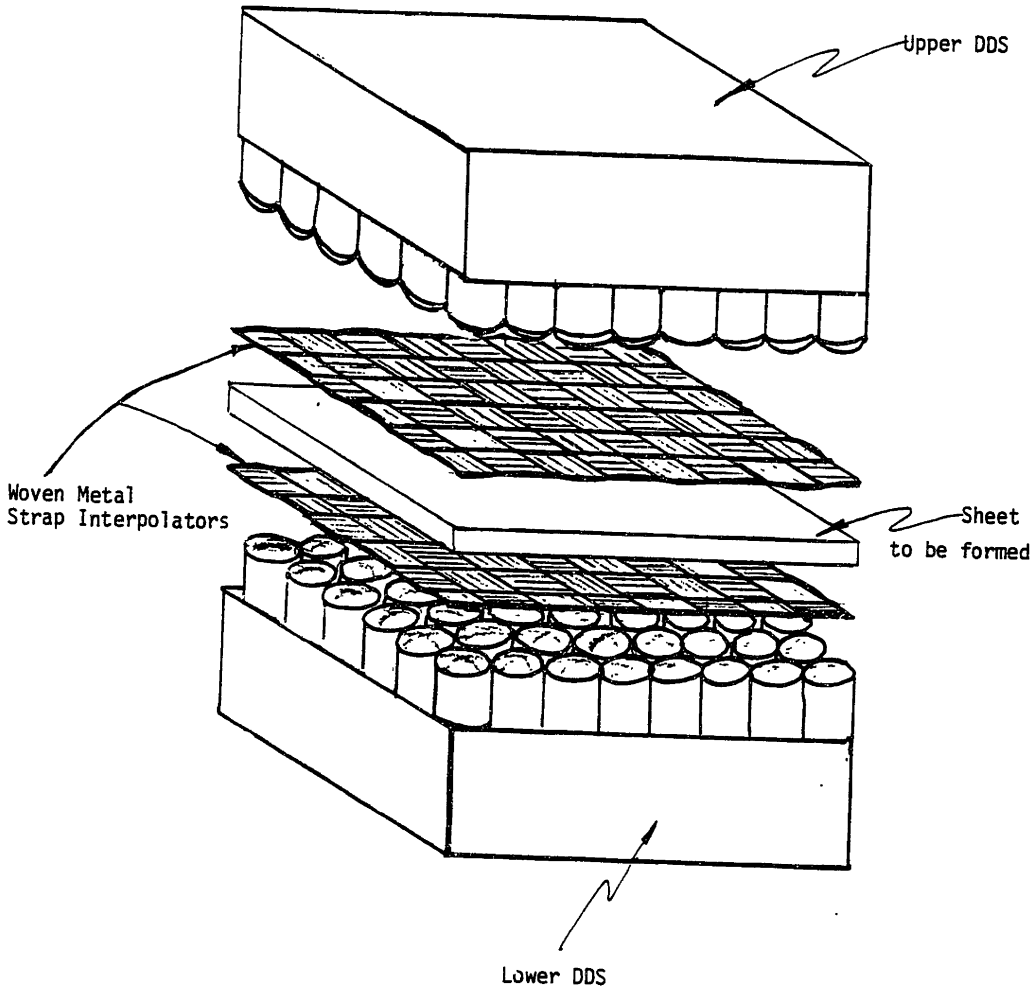

FIGURE B.3: WOVEN METAL STRAP INTERPOLATORS

APPENDIX C

MATERIAL SENSITIVITY TO PIN POSITIONING ERRORS

Section 3.2.5 discusses the sensitivity of the formed material to the positioning error of the pins. This Appendix determines the maximum sensitivity of the material to positioning for the DDS test fixture used in this experiment.

If the outside pins in the upper and lower dies are located too close together, a reverse moment results which will bend the metal in the opposite direction from that desired. A section of the sheet can be approximated to be a simply supported beam as shown in Figure C.1. In this Figure pins A and B are the pins on the outside rows and:

x_1 = distance between contact points of pins A and B

x_2 = distance between contact points of pins B and C

R = pin tip radius

D = pin diameter

t = sheet thickness

α = angle of sheet to reference angle of die

Using trigonometry, the distances x_1 and x_2 are:

$$x_1 = 2(R + t/2)\tan\alpha \qquad (C.1)$$

$$x_2 = \frac{D}{\sin\alpha} - x_1 \qquad (C.2)$$

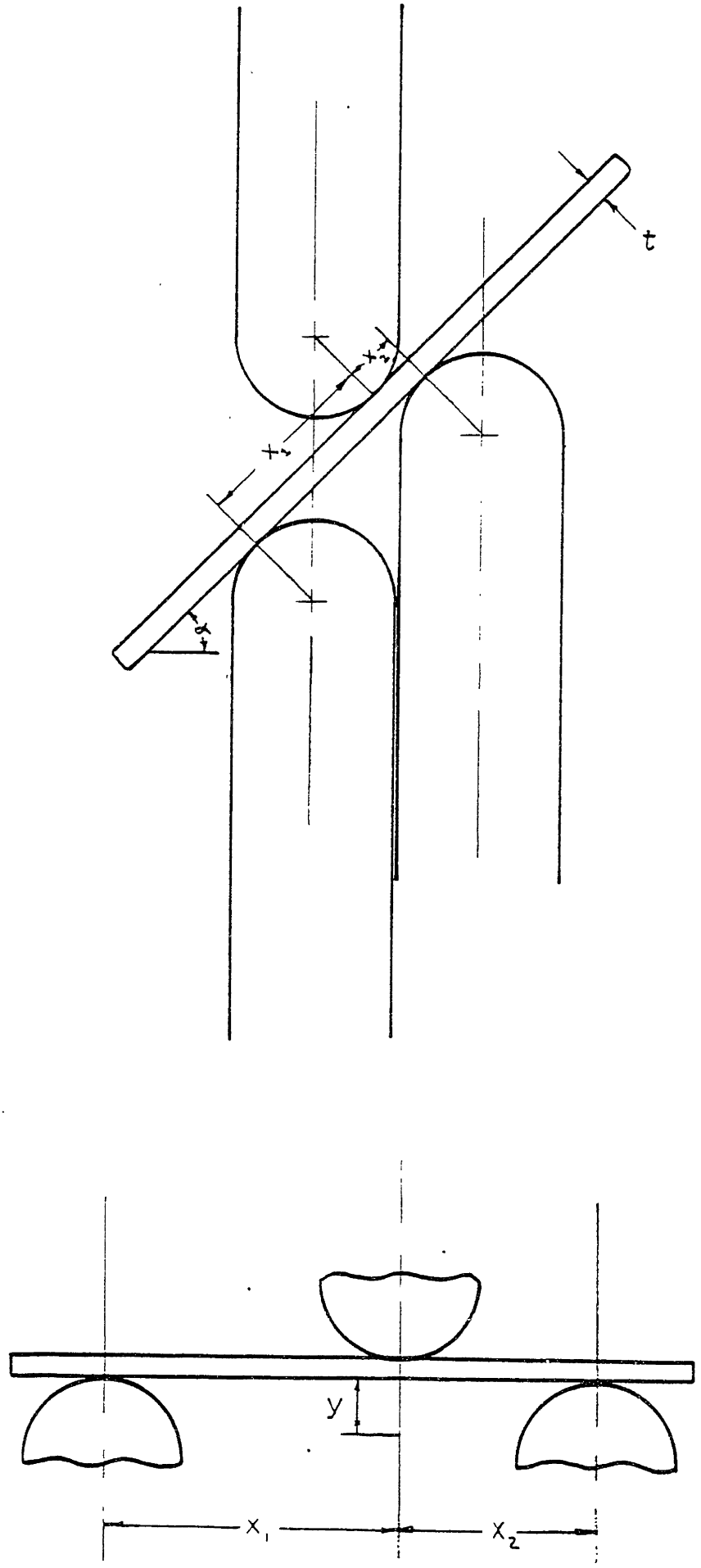

FIGURE C.1: SIMPLY SUPPORTED BEAM APPROXIMATION

The maximum deflection of a simply supported beam (max y) equals

$$\max y = - \frac{Ma^2}{(L-a)3EI} \left(\frac{L^2-a^2}{3}\right)^{3/2} \qquad (C.3)$$

where M = max moment

L = length of the beam (in this case, x_1+x_2)

a = distance from support to force (in this case, x_2)

E = modulus of elasticity of material

I = moment of inertia of material

To have bending occur, the stress in the sheet caused by the moment must be at least equal to the yield stress of the material

$$M = \sigma_y / I_c \qquad (C.4)$$

where σ_y = yield stress of material

C = one half the thickness of the sheet, t/2

Combining equations C.4 and C.3, and substituting x_1, x_2, and t:

$$\max y = \frac{-\sigma_y x_2^2}{3/2 t x_1 E} \left(\frac{x_1^2 + 2x_1x_2}{3}\right)^{3/2} \qquad (C.5)$$

In this experiment, the values for these variables are given as:

σ_y = 21,000 psi

E = 10×10^6 psi

t = 1/16"

R = 11/32"

D = 1/2"

Plugging these values into Equations C.1, C.2, and C.5, and equation in terms of y, x_1, and x_2 is formed.

$$\max y = - \frac{.0224\ x_2^2}{x_1} \left(\frac{x_1^2 + 2x_1x_2}{3} \right)^{1/2} \qquad (C.6)$$

where x_1 = .75 tanα

x_2 = .5/sinα-.75 tanα

with an angle (α) of 30°, this gives a max y value of .002" the pin movement is less than this mas y value so y < .002".

This number seems quite small considering the accuracy of the positioning method. In the experiment, this effect was not observed. This was probably because of the rubber interpolators with a lower modulus of elasticity which decreased the sensitivity. This approximation doesn't take into account that the moment arm on the sheet changes as the pins get closer together, and that the sheet is not really simply supported. In the future, a method could be developed to take these factors into account.

APPENDIX D

RELATIONSHIP BETWEEN PIN TIP RADIUS AND MATERIAL PROPERTIES TO AVOID DIMPLING

Section 3.3.1 discusses a relationship between the pin tip radius and material properties which may be used to avoid dimpling of the sheet surface. This appendix describes the development of this relationship in the case where interpolators are not used. If the modulus of elasticity of rubber which varies with force can be accounted for in the equation, this relationship will also be useful when using rubber interpolators.

For forming to occur without dimpling, the bending stress of the material must exceed its yield stress, and the contact stress of the pin tip on the sheet surface must be less than the yield stress of the material. As a crude approximation, the sheet may be modelled as a cantilever beam with a pin at one end (see Figure D.1). The maximum moment in the sheet is then:

$$M = FL \tag{D.2}$$

where M = moment
F = force of pin
L = distance between pins

This moment must be large enough to cause the material to yield, so

$$\sigma = \frac{Mc}{I} > \sigma_y \tag{D.3}$$

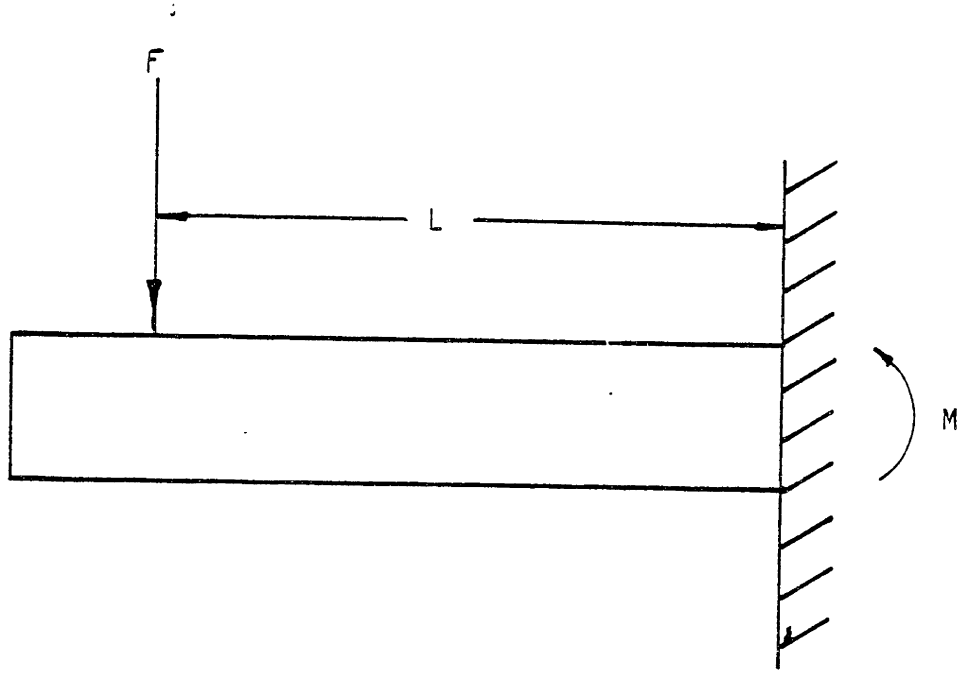

FIGURE D.1: CANTILEVER BEAM

where σ = forming stress

σ_y = yield stress

c = 1/2 sheet thickness (t)

I = moment of inertia

For this situation, $\frac{c}{I} = \frac{1/2t}{\frac{Lt^3}{12}} = \frac{6}{Lt^2}$

Combining Equation (D.2) and (D.3),

$$\sigma = \frac{6F}{t^2} > \sigma_y \qquad (D.4)$$

Now an equation can be used to find the contact stress of the pin tip on the sheet. Equation (D.5) was derived from an equation in "Formulas for stress and Strain" (Roark and Warren (1975)):

$$\text{Max. } \sigma_c = 1.5 \frac{F}{\pi a^2}$$

$$a = 0.721^3 \sqrt{FDC_E} \qquad (D.5)$$

$$C_E = \frac{1 - \nu_1^2}{E_1} + \frac{1 - \nu_2^2}{E_2}$$

where F = force on pin

σ_c = maximum contact stress

a = radius of circular contact area

D = tip diameter

ν_1 = Poisson's ratio for pin

E_1 = modulus of elasticity for Pin

ν_2 = Poisson's ratio for sheet

E_1 = modulus of elasticity for sheet

C_E = material properties constant

Simplifying and combining in Equation (D.5),

$$\sigma_c = .9185\ F^{1/3}\ D^{-2/3} C_E^{-2/3} \qquad (D.6)$$

To avoid dimpling, the contact stress must be less than the yield stress ($\sigma_c < \sigma_y$).

An inequality can be formed by substituting σ_y for σ_c.

Cubing both sides of this relationship and dividing through by σ_y^2 gives:

$$\sigma_y > \frac{.7749F}{\sigma_y^2 D^2 C_E^2} \qquad (D.7)$$

Equations (D.7) and (D.4) can now be related

$$\frac{6F}{t^2} > \sigma_y > \frac{.7749F}{\sigma_y^2 D^2 C_E^2} \qquad (D.8)$$

With more algebraic manipulation and substituting for C_E, the relationship can be formulated for the tip diameter, D.

$$D > \frac{.3594t}{\sigma_y\left(\frac{1-\nu_1^2}{E_1} + \frac{1-\nu_2^2}{E_2}\right)} \qquad (D.9)$$

This relationship gives a minimum size for the tip radius, D/2, in terms of material properties and thickness. In the future, the relationship might be modified to account for property and thickness variations when rubber interpolators are added.

APPENDIX E
DATA

The following pages are data recorded during the shape measurement described in section 4.4.6. All of the numbers are measured in inches and in all cases, the rows are data recorded along the long axis of the die and the columns are the data recorded along the short axis. Pages 110-119 are the raw data as it was recorded, and pages 120-122 are the data specifications for each sheet and the reference number for that sheet in the data file.

TABLE E.1 DATA SPECIFICATIONS

DATA SHEETS		DATA FILE	LOADED RADIUS OF CURVATURE, IN.	
TRIAL #	BATCH #	REFERENCE #	LONG AXIS OF DIE	SHORT AXIS OF DIE
1	1	1	3.5	3.5
2	1	2	3.5	3.5
3	1	3	3.5	3.5
1	2	4	5.25	3.5
2	2	5	5.25	3.5
3	2	6	5.25	3.5
1	3	7	3.5	7.0
2	3	8	3.5	7.0
3	3	9	3.5	7.0
1	4	10	3.5	∞
2	4	11	3.5	∞
3	4	12	3.5	∞

TEST SPECIMEN MAPPING

Date: 5-6
Forming Date: 5-1
R_1: 3.5
R_2: 3.5

Force: 1000#
Material: 3003 H14

Trial#: 1
Batch#: 1

Long axis of die (R_2)

.112	.170	.227	.273	.302	.315	.301	.262	.209	.150	.090
.172	.225	.280	.322	.348	.360	.349	.316	.262	.205	.149
.220	.270	.320	.355	.379	.388	.380	.350	.306	.253	.201
.258	.305	.356	.377	.402	.405	.402	.375	.340	.293	.245
.295	.334	.370	.391	.405	.411	.407	.383	.358	.321	.281
.315	.348	.374	.395	.404	.410	.404	.388	.360	.327	.285
.290	.329	.358	.384	.396	.404	.396	.379	.346	.310	.266
.251	.297	.327	.360	.379	.390	.384	.356	.319	.275	.226
.208	.251	.289	.326	.350	.364	.350	.321	.277	.231	.178
.159	.205	.246	.287	.315	.331	.310	.278	.229	.180	.126
.111	.155	.202	.243	.276	.291	.263	.228	.176	.124	.071

Short axis of die (R_1)

Notes:

TEST SPECIMEN MAPPING

Date: 5-5

Forming Date: 5-1

R_1: 3.5

R_2: 3.5

Force: 1000 #

Material: 3003 H14

Trial#: 2

Batch#: 1

Long axis of die (R_2)

.080	.136	.190	.240	.266	.290	.272	.241	.188	.133	.078
.136	.197	.244	.291	.311	.335	.321	.301	.243	.197	.134
.186	.239	.287	.327	.350	.364	.357	.332	.284	.242	.189
.224	.274	.312	.356	.369	.382	.380	.360	.329	.284	.236
.258	.303	.338	.364	.379	.389	.388	.374	.347	.312	.276
.281	.312	.346	.368	.380	.387	.386	.375	.352	.326	.293
.270	.302	.334	.358	.372	.380	.379	.365	.341	.310	.275
.239	.271	.308	.335	.357	.365	.364	.341	.314	.278	.239
.198	.231	.272	.304	.330	.340	.332	.307	.276	.238	.200
.147	.188	.232	.267	.301	.307	.292	.265	.229	.188	.141
.102	.143	.184	.227	.258	.269	.248	.216	.177	.135	.081

Short axis of die (R_1)

Notes:

TEST SPECIMEN MAPPING

Date: 5-5

Forming Date: 5-1 Force: 1000# Trial#: 3

R_1: 3.5 Material: 3003 H14 Batch#: 1

R_2: 3.5

Long axis of die (R_2)

.068	.128	.186	.240	.268	.294	.279	.251	.203	.151	.093
.122	.181	.237	.289	.314	.336	.325	.304	.255	.207	.151
.172	.228	.279	.323	.347	.364	.358	.340	.298	.255	.264
.206	.261	.308	.345	.366	.381	.381	.364	.331	.294	.248
.239	.290	.329	.359	.376	.387	.388	.377	.352	.324	.287
.268	.305	.337	.362	.376	.385	.385	.376	.356	.330	.301
.253	.288	.323	.350	.368	.377	.378	.365	.342	.311	.277
.214	.253	.293	.325	.350	.361	.364	.343	.315	.276	.237
.171	.211	.255	.291	.321	.337	.335	.310	.277	.234	.193
.124	.167	.212	.252	.286	.305	.296	.268	.230	.184	.141
.178	.121	.170	.212	.247	.269	.251	.219	.177	.130	.083

Short axis of die (R_1)

Notes:

TEST SPECIMEN MAPPING

Date: 5-7

Forming Date: 5-1

R_1: 3.5

R_2: 5.25

Force: 1000#

Material: 3003 H14

Trial#: 1

Batch#: 2

Long axis of die (R_2)

.077	.120	.156	.188	.208	.221	.210	.191	.161	.131	.103
.129	.171	.204	.236	.253	.265	.255	.241	.211	.185	.155
.183	.221	.252	.281	.296	.305	.296	.286	.260	.236	.207
.229	.262	.291	.317	.330	.337	.330	.321	.302	.280	.253
.265	.298	.321	.341	.352	.357	.351	.345	.330	.313	.290
.296	.317	.335	.350	.358	.364	.360	.353	.340	.326	.307
.290	.307	.326	.340	.351	.356	.352	.343	.330	.310	.292
.253	.275	.299	.316	.331	.334	.332	.319	.302	.277	.254
.212	.235	.261	.280	.299	.303	.301	.283	.262	.236	.212
.167	.189	.216	.238	.257	.264	.259	.240	.218	.189	.163
.118	.142	.170	.192	.212	.222	.214	.201	.170	.140	.111

Short axis of die (R_1)

Notes:

TEST SPECIMEN MAPPING

Date: 5-7

Forming Date: 5-1

R_1: 3.5

R_2: 5.25

Force: 10004

Material: 3003H14

Trial#: 2

Batch#: 2

Long axis of die (R_2)

.084	.128	.166	.203	.222	.240	.229	.212	.181	.146	.110
.145	.190	.224	.261	.275	.290	.279	.266	.233	.202	.165
.202	.242	.272	.303	.317	.327	.318	.308	.280	.252	.218
.244	.281	.310	.335	.347	.354	.348	.340	.319	.295	.262
.278	.311	.334	.353	.363	.370	.365	.359	.343	.326	.298
.296	.320	.340	.354	.367	.374	.370	.363	.350	.336	.311
.279	.302	.326	.342	.356	.361	.360	.350	.338	.318	.299
.241	.268	.297	.316	.333	.337	.338	.324	.308	.283	.259
.201	.226	.256	.278	.298	.302	.301	.285	.266	.239	.214
.146	.176	.208	.233	.253	.260	.257	.240	.218	.188	.162
.093	.124	.157	.184	.206	.216	.210	.192	.167	.137	.107

Short axis of die (R_1)

Notes:

TEST SPECIMEN MAPPING

Date: 5-6

Forming Date: 5-1

R_1: 3.5

R_2: 5.25

Force: 1000#

Material: 3003/H14

Trial#: 3

Batch#: 2

Long axis of die (R_2)

.075	.115	.161	.186	.204	.220	.209	.189	.159	.126	.098
.135	.174	.208	.241	.256	.268	.258	.242	.211	.182	.148
.192	.228	.252	.285	.298	.307	.298	.286	.260	.233	.201
.237	.270	.292	.321	.331	.337	.330	.321	.302	.279	.248
.275	.304	.321	.341	.349	.355	.349	.343	.329	.313	.289
.300	.318	.333	.347	.355	.361	.356	.349	.338	.325	.310
.284	.302	.325	.335	.345	.349	.347	.338	.324	.306	.286
.246	.268	.297	.309	.322	.327	.324	.311	.295	.270	.246
.204	.228	.258	.273	.289	.293	.291	.274	.254	.228	.203
.157	.181	.208	.231	.248	.254	.249	.232	.211	.181	.154
.109	.133	.153	.185	.204	.213	.205	.187	.162	.132	.104

Short axis of die (R_1)

Notes:

TEST SPECIMEN MAPPING

Date: 5-7

Forming Date: 5-2

R_1: 7

R_2: 3.5

Force: 1000#

Material: 3003H14

Trial#: 1

Batch#: 3

Long axis of die (R_2)

.066	.116	.163	.205	.235	.255	.245	.221	.181	.136	.087
.089	.141	.186	.229	.255	.271	.261	.240	.200	.158	.109
.112	.163	.208	.249	.273	.285	.275	.257	.219	.178	.131
.131	.180	.229	.261	.285	.292	.283	.266	.233	.195	.151
.147	.194	.239	.270	.291	.300	.289	.272	.242	.209	.167
.158	.200	.239	.272	.292	.301	.293	.277	.247	.212	.175
.153	.194	.234	.266	.289	.298	.292	.274	.243	.206	.169
.140	.181	.222	.255	.280	.291	.288	.265	.233	.192	.151
.128	.168	.208	.242	.270	.283	.278	.253	.217	.175	.132
.110	.151	.192	.228	.258	.272	.265	.238	.199	.155	.111
.084	.131	.174	.211	.243	.259	.247	.219	.178	.135	.089

Short axis of die (R_1)

Notes:

TEST SPECIMEN MAPPING

Date: 5-7

Forming Date: 5-2 Force: 1000# Trial#: 2

R_1: 7 Material: 3003 H14 Batch#: 3

R_2: 3.5

Long axis of die (R_2)

.079	.126	.171	.211	.238	.255	.241	.214	.173	.129	.081
.105	.153	.196	.238	.262	.275	.261	.239	.196	.155	.108
.130	.178	.220	.259	.280	.290	.277	.257	.218	.179	.134
.148	.196	.237	.272	.292	.300	.288	.269	.235	.198	.155
.165	.211	.248	.282	.300	.307	.296	.279	.247	.212	.172
.176	.218	.254	.286	.302	.310	.301	.285	.254	.219	.180
.172	.212	.250	.280	.300	.308	.301	.283	.252	.215	.175
.160	.200	.238	269	.292	.303	.299	.277	.244	.203	.161
.147	.187	.225	.258	.282	.295	.291	.267	.231	.188	.146
.130	.172	.211	.245	.272	.286	.279	.254	.216	.171	.123
.107	.153	.195	.231	.261	.276	.266	.238	.199	.154	.108

Short axis of die (R_1)

Notes:

TEST SPECIMEN MAPPING

Date: 5-6

Forming Date: 5-2 Force: 1000# Trial#: 3

R_1: 7 Material: 3003 H14 Batch#: 3

R_2: 3.5

Long axis of die (R_2)

.062	.112	.173	.199	.228	.250	.239	.212	.175	.131	.082
.086	.136	.192	.220	.246	.263	.253	.231	.192	.152	.105
.109	.157	.206	.241	.265	.279	.268	.249	.211	.172	.127
.128	.175	.221	.255	.278	.288	.278	.260	.227	.190	.148
.144	.192	.234	.267	.287	.295	.285	.269	.238	.204	.165
.160	.200	.238	.270	.289	.298	.290	.274	.245	.212	.176
.159	.195	.230	.266	.287	.297	.290	.273	.243	.208	.172
.143	.181	.212	.254	.279	.290	.287	.265	.239	.195	.157
.129	.167	.200	.240	.269	.282	.277	.253	.219	.178	.138
.112	.150	.178	.225	.256	.271	.264	.238	.201	.159	.117
.089	.131	.158	.210	.242	.259	.248	.220	.180	.140	.096

Short axis of die (R_1)

Notes:

TEST SPECIMEN MAPPING

Date: 5-7

Forming Date: 5-2 Force: 1000# Trial#: 1

R_1: ∞ Material: 3003-H14 Batch#: 4

R_2: 3.5

Long axis of die (R_2)

.072	.121	.168	.196	.212	.218	.208	.188	.161	.119	.068
.073	.121	.166	.196	.211	.218	.208	.188	.158	.122	.075
.075	.121	.165	.197	.213	.220	.209	.189	.158	.122	.081
.075	.122	.164	.198	.216	.223	.212	.191	.158	.123	.082
.076	.122	.164	.199	.218	.226	.215	.193	.160	.125	.084
.076	.122	.164	.200	.219	.229	.218	.202	.162	.129	.087
.077	.122	.164	.200	.220	.230	.220	.202	.166	.131	.089
.078	.124	.166	.200	.220	.231	.221	.202	.169	.134	.090
.080	.126	.166	.200	.221	.231	.224	.205	.172	.137	.093
.080	.127	.167	.201	.222	.233	.226	.209	.176	.140	.095
.080	.128	.170	.202	.226	.236	.230	.211	.180	.142	.094

Short axis of die (R_1)

Notes:

TEST SPECIMEN MAPPING

Date: 5-7

Forming Date: 5-2 Force: 1000# Trial#: 2

R_1: ∞ Material: 3003 H14 Batch#: 4

R_2: 3.5

Long axis of die (R_2)

.073	.117	.157	.192	.215	.225	.220	.201	.170	.131	.092
.074	.118	.156	.192	.212	.223	.216	.201	.168	.131	.092
.075	.118	.156	.192	.212	.223	.216	.201	.168	.131	.092
.076	.119	.156	.192	.212	.224	.216	.201	.168	.132	.092
.077	.119	.156	.192	.213	.225	.218	.201	.169	.132	.092
.078	.119	.156	.192	.214	.226	.220	.204	.170	.132	.092
.079	.121	.157	.192	.215	.227	.221	.205	.172	.133	.092
.080	.122	.158	.192	.215	.227	.221	.206	.173	.135	.092
.082	.126	.160	.193	.215	.227	.221	.206	.175	.136	.092
.082	.129	.165	.196	.216	.228	.222	.208	.178	.139	.092
.078	.129	.170	.199	.219	.230	.225	.210	.181	.140	.092

Short axis of die (R_1)

Notes:

TEST SPECIMEN MAPPING

Date: 5-7

Forming Date: 5-2 Force: 1000# Trial#: 3

R_1: ∞ Material: 3003 H14 Batch#: 4

R_2: 3.5

Long axis of die (R_2)

.072	.119	.161	.192	.214	.223	.215	.193	.160	.121	.071
.075	.120	.160	.191	.212	.221	.212	.191	.160	.120	.072
.077	.120	.159	.191	.211	.221	.212	.192	.161	.120	.074
.078	.121	.159	.191	.211	.222	.213	.193	.161	.119	.075
.078	.121	.158	.191	.212	.223	.215	.195	.163	.115	.075
.079	.121	.158	.191	.213	.225	.217	.198	.165	.118	.075
.080	.122	.158	.192	.214	.225	.218	.200	.167	.121	.075
.081	.122	.158	.192	.215	.225	.219	.201	.169	.123	.075
.083	.126	.160	.193	.214	.225	.219	.201	.171	.125	.076
.084	.130	.164	.195	.215	.225	.219	.202	.174	.127	.077
.085	.131	.169	.197	.218	.227	.221	.204	.175	.129	.077

Short axis of die (R_1)

Notes:

1

.112	.170	.227	.273	.302	.315	.301	.262	.209	.150	.090
.172	.225	.280	.322	.348	.360	.349	.316	.262	.205	.149
.220	.270	.320	.355	.379	.388	.380	.350	.306	.252	.201
.258	.305	.350	.377	.402	.405	.402	.375	.340	.293	.245
.295	.336	.370	.391	.405	.411	.407	.388	.358	.321	.291
.315	.348	.374	.395	.404	.410	.404	.388	.360	.327	.295
.290	.329	.358	.384	.396	.404	.396	.379	.346	.310	.266
.251	.297	.327	.360	.379	.390	.381	.356	.319	.275	.226
.208	.251	.289	.326	.350	.364	.350	.321	.277	.231	.178
.159	.205	.246	.287	.315	.331	.310	.278	.229	.180	.126
.111	.155	.202	.243	.276	.291	.263	.228	.176	.124	.071

2

.080	.136	.190	.240	.266	.290	.272	.241	.189	.133	.078
.136	.197	.244	.291	.311	.335	.321	.301	.243	.197	.134
.186	.239	.287	.327	.350	.364	.357	.332	.289	.242	.189
.224	.274	.312	.350	.369	.382	.380	.360	.324	.284	.236
.258	.303	.338	.364	.379	.389	.388	.374	.347	.312	.276
.281	.312	.346	.368	.380	.387	.386	.375	.352	.326	.293
.270	.302	.334	.358	.372	.380	.379	.365	.341	.310	.275
.234	.271	.308	.335	.357	.365	.364	.341	.314	.278	.239
.198	.231	.272	.304	.330	.340	.332	.307	.276	.238	.200
.147	.188	.232	.267	.301	.307	.292	.265	.229	.188	.141
.102	.143	.189	.227	.258	.269	.248	.216	.177	.135	.091

3

.068	.128	.186	.240	.268	.294	.279	.251	.203	.151	.093
.122	.181	.237	.289	.314	.336	.325	.304	.255	.207	.151
.172	.228	.279	.323	.347	.364	.358	.340	.298	.255	.204
.206	.261	.308	.345	.366	.381	.381	.364	.331	.294	.248
.239	.290	.329	.359	.376	.387	.388	.377	.352	.324	.287
.268	.305	.337	.362	.376	.385	.385	.376	.356	.330	.301
.253	.288	.323	.350	.368	.377	.378	.365	.342	.311	.277
.214	.253	.293	.325	.350	.361	.364	.343	.315	.276	.237
.171	.211	.255	.291	.321	.337	.335	.310	.277	.234	.193
.124	.167	.212	.252	.286	.305	.296	.268	.230	.184	.141
.078	.121	.170	.212	.247	.269	.251	.219	.177	.130	.083

4

.077	.120	.156	.188	.208	.221	.210	.191	.161	.131	.103
.129	.171	.204	.236	.253	.265	.255	.241	.211	.185	.155
.183	.221	.252	.281	.296	.305	.296	.286	.260	.236	.207
.229	.262	.291	.317	.330	.337	.330	.321	.302	.280	.253
.265	.298	.321	.341	.352	.357	.351	.345	.330	.313	.290
.296	.317	.335	.350	.358	.364	.360	.353	.340	.326	.307
.290	.307	.326	.340	.351	.356	.352	.343	.330	.310	.292
.253	.275	.299	.316	.331	.334	.332	.319	.302	.277	.254
.212	.235	.261	.280	.299	.303	.301	.283	.262	.236	.212
.167	.189	.216	.238	.257	.264	.259	.240	.218	.189	.163
.118	.142	.170	.192	.212	.222	.214	.201	.170	.140	.111

5

.084	.128	.166	.203	.222	.240	.229	.212	.181	.146	.110
.145	.190	.224	.261	.275	.290	.279	.266	.233	.202	.165
.202	.242	.272	.303	.317	.327	.318	.308	.280	.252	.218
.244	.281	.310	.335	.347	.354	.348	.340	.319	.295	.262
.278	.311	.334	.353	.363	.370	.365	.359	.343	.326	.298
.296	.320	.340	.356	.367	.374	.370	.363	.350	.336	.311
.279	.302	.326	.342	.356	.361	.360	.350	.338	.318	.299
.241	.268	.297	.316	.333	.337	.338	.324	.308	.283	.259
.201	.226	.256	.278	.298	.302	.301	.285	.266	.239	.214
.146	.176	.208	.233	.253	.260	.257	.240	.218	.188	.162
.093	.124	.157	.184	.206	.216	.210	.192	.167	.137	.107

6

.075	.115	.161	.186	.204	.220	.209	.189	.159	.126	.088
.135	.174	.208	.241	.256	.268	.258	.242	.211	.182	.148
.192	.228	.252	.285	.298	.307	.299	.286	.260	.233	.201
.237	.270	.292	.321	.331	.337	.330	.321	.302	.279	.249
.275	.304	.321	.341	.349	.355	.349	.343	.329	.313	.289
.300	.318	.333	.347	.355	.361	.356	.349	.338	.325	.310
.284	.302	.325	.335	.345	.349	.347	.338	.324	.306	.296
.246	.268	.297	.309	.322	.327	.324	.311	.295	.270	.246
.204	.228	.258	.273	.299	.293	.291	.274	.254	.228	.203
.157	.181	.208	.231	.248	.254	.249	.232	.211	.181	.154
.109	.133	.153	.185	.204	.213	.205	.187	.162	.132	.104

7

.066	.116	.163	.205	.235	.255	.245	.221	.181	.136	.087
.089	.141	.186	.229	.255	.271	.261	.240	.200	.158	.109
.112	.163	.208	.249	.273	.285	.275	.257	.219	.176	.131
.131	.180	.224	.261	.285	.292	.283	.266	.233	.195	.151
.147	.194	.234	.270	.291	.300	.289	.272	.242	.209	.167
.158	.200	.239	.272	.292	.301	.293	.277	.247	.212	.175
.153	.194	.234	.266	.289	.298	.292	.274	.243	.206	.169
.140	.181	.222	.255	.280	.291	.288	.265	.233	.192	.151
.128	.168	.208	.242	.270	.283	.278	.253	.217	.175	.132
.110	.151	.192	.228	.258	.272	.265	.238	.199	.155	.111
.084	.131	.174	.211	.243	.259	.247	.219	.178	.135	.089

8

.079	.126	.171	.211	.238	.255	.241	.214	.173	.129	.091
.105	.153	.196	.238	.262	.275	.261	.239	.196	.155	.108
.130	.178	.220	.259	.280	.290	.277	.257	.218	.179	.134
.148	.196	.237	.272	.292	.300	.288	.269	.235	.198	.155
.165	.211	.248	.282	.300	.307	.296	.279	.247	.212	.172
.176	.218	.254	.286	.302	.310	.301	.285	.254	.219	.180
.172	.212	.250	.280	.300	.308	.301	.283	.252	.215	.175
.160	.200	.238	.269	.292	.303	.299	.277	.244	.203	.161
.147	.187	.225	.258	.282	.295	.291	.267	.231	.188	.146
.130	.172	.211	.245	.272	.286	.279	.254	.216	.171	.128
.107	.153	.195	.231	.261	.276	.266	.238	.199	.154	.109

9

.062	.112	.173	.199	.228	.250	.239	.212	.175	.131	.082
.086	.136	.192	.220	.246	.263	.253	.231	.192	.152	.105
.109	.157	.206	.241	.265	.279	.268	.249	.211	.172	.127
.128	.175	.221	.255	.278	.288	.278	.260	.227	.190	.148
.144	.192	.234	.267	.287	.295	.285	.269	.238	.204	.165
.160	.200	.238	.270	.289	.298	.290	.274	.245	.212	.176
.159	.195	.230	.266	.287	.297	.290	.273	.243	.208	.172
.143	.181	.212	.254	.279	.290	.287	.265	.234	.195	.157
.129	.167	.200	.240	.269	.282	.277	.253	.219	.178	.138
.112	.150	.178	.225	.256	.271	.264	.238	.201	.159	.117
.089	.131	.158	.210	.242	.259	.248	.220	.180	.140	.096

10

.072	.121	.168	.196	.212	.218	.208	.188	.161	.119	.068
.073	.121	.166	.196	.211	.218	.208	.188	.158	.122	.075
.075	.121	.165	.197	.213	.220	.209	.189	.158	.122	.081
.075	.122	.164	.198	.216	.223	.212	.191	.159	.123	.082
.076	.122	.164	.199	.218	.226	.215	.193	.160	.125	.084
.076	.122	.164	.200	.219	.229	.218	.202	.162	.129	.087
.077	.122	.164	.200	.220	.230	.220	.202	.166	.131	.089
.078	.124	.166	.200	.220	.231	.221	.202	.169	.134	.090
.080	.126	.166	.200	.221	.231	.224	.205	.172	.137	.093
.080	.127	.167	.201	.222	.233	.226	.209	.176	.140	.095
.080	.128	.170	.202	.226	.236	.230	.211	.180	.142	.094

11

.073	.117	.157	.192	.215	.225	.220	.201	.170	.131	.092
.074	.118	.156	.192	.212	.223	.216	.201	.168	.131	.092
.075	.118	.156	.192	.212	.223	.216	.201	.168	.131	.092
.076	.119	.156	.192	.212	.224	.216	.201	.168	.132	.092
.077	.119	.156	.192	.213	.225	.218	.201	.169	.132	.092
.078	.119	.156	.192	.214	.228	.220	.204	.170	.132	.092
.079	.121	.157	.192	.215	.227	.221	.205	.172	.133	.092
.080	.122	.158	.192	.215	.227	.221	.206	.173	.135	.092
.082	.126	.160	.193	.215	.227	.221	.206	.175	.136	.092
.082	.129	.165	.196	.216	.228	.222	.208	.178	.139	.092
.078	.129	.170	.199	.219	.230	.225	.210	.181	.140	.092

12

.072	.119	.161	.192	.214	.223	.215	.193	.160	.121	.071
.075	.120	.160	.191	.212	.221	.212	.191	.160	.120	.072
.077	.120	.159	.191	.211	.221	.212	.192	.161	.120	.074
.078	.121	.159	.191	.211	.222	.213	.193	.161	.119	.075
.079	.121	.158	.191	.212	.223	.215	.195	.163	.115	.075
.079	.121	.158	.191	.213	.225	.217	.198	.165	.118	.075
.080	.122	.158	.192	.214	.225	.218	.200	.167	.121	.075
.081	.122	.158	.192	.215	.225	.219	.201	.169	.123	.075
.083	.126	.160	.193	.214	.225	.219	.201	.171	.125	.076
.084	.130	.164	.195	.215	.225	.219	.202	.174	.127	.077
.085	.131	.169	.197	.218	.227	.221	.204	.175	.129	.077

APPENDIX F

LEAST SQUARES FIT OF CIRCLES TO DATA

Section 5.2.2. describes a least squares fit of a circle to a set of data points so that the radius of curvature of these points may be approximated. Equation 5.1 is the equation for a circle with an arbitrary center point

$$(x - x_o)^2 + (y - y_o)^2 = R^2 \qquad (5.1)$$

where

R = radius

x,y = point lying on the circle

x_o, y_o = center point.

Now the measured y value differs from the calculated y value by an amount, e.

$$y_m = y + e \qquad (F.1)$$

where

y_m = measured value of y

y = calculated value of y

e = error

Substituting eq. F.1 into 5.1 and rearanging,

$$((y_m - y_o) - e)^2 = R - (x_m - x_o)^2 \qquad (F.2)$$

Which may be algebraically manipulated to form

$$e^2 - 2e\,(y_m - y_o)(y_m - y_o)^2 - R^2 + (x_m - x_o)^2 = 0 \qquad (F.3)$$

Using the quadratic equation and simplifying,

$$e = y_m - y_o \pm \sqrt{R^2 - (x_m - x_o)^2} \qquad (F.4)$$

Since the surface in this experiment is such that $y_o > y_m$ and the origin is on the same side of the curve as the center point (convex surface), the value for e is then:

$$e = y_m - y_o + \sqrt{R^2 - (x_m - x_o)^2} \qquad (F.5)$$

The total squared error, E, equals

$$E = \sum_{m=1}^{n} e_m^2 \qquad (F.6)$$

where

m = reference # for a particular point

n = number of points

e_m = error for a particular point

In this case, from eq's. F.5 and F.6, E equals

$$E = \sum_{m=1}^{n} e^2 = \sum_{m=1}^{n} y_m^2 - 2\, y_m\, y_o + y_o^2 + R^2 - x_m^2 + 2 x_x x_o - x_o^2$$

$$+2(y_m - y_o)\,(R^2 - x_m^2 + 2 x_m x_o - x_o)^{\frac{1}{2}} \qquad (F.7)$$

The closest fit is when the derivative of the total squared error with respect to each of the variables in the equation equals zero. In this case, the variables are x_o, y_o, and R.

$$\frac{\partial E}{\partial R} = 0 \qquad \frac{\partial E}{\partial x_o} = 0 \qquad \frac{\partial E}{\partial y_o} = 0 \qquad (F.8)$$

Taking these derivatives and simplifying:

$$\frac{\partial E}{\partial R} = 0 = \sum_{m=1}^{n} 2R\,\left(1 + \frac{y_m - y_o}{\sqrt{R^2 - (x_m - x_o)^2}}\right) \qquad (F.9)$$

$$\frac{\partial E}{\partial x_o} = 0 = \sum_{m=1}^{n} 2(x_m - x_o)\left(1 + \frac{y_m - y_o}{\sqrt{R^2 - (x_m - x_o)^2}}\right) \qquad (F.10)$$

$$\frac{\partial E}{\partial y_o} = 0 - \sum_{m=1}^{n} 2\left(y_o - y_m + \sqrt{R^2 - (x_m - x_o)^2}\right) \qquad (F.11)$$

It appears that these equations are not easily solvable in closed form because of the summations. Further work may be done to solve these equations so that values are given for x_0, y_0, and R. These values are likely to fit the data more closely than those obtained using the perpendicular bisector method.

APPENDIX G
COMPUTER PROGRAM LISTING AND RESULTS

A listing of the computer program described in section 5.2.3 and the results of this program are shown in this section. Pages 127-129 show the program listing with components. The results are print-outs of the radius of curvature for each of eleven rows for each sheet. Pages 134-136 show the radii of curvature of the sheet axis parallel to the short axis of the die for the first nine test sheets (the last three sheets have no curvature along the short axis). In addition to the radii of curvature, the standard deviation for these radii are given as an indicator of how well the circle fit the data (see section 5.2.2). The locations of the center point (x,y) are given for comparison of this analysis with other methods such as the least squares fit described in Appendix F. With the x,y, and R given, the error may be evaluated and compared with the value obtained using a least squares fit. This may be useful for future work.

```
C   THIS PROGRAM FITS A CIRCLE TO A SET OF DATA
C   POINTS USING THE PERPENDICULAR BISECTOR METHOD.
C   IT READS IN AN 11 X 11 ARRAY OF POINTS AND FINDS
C   THE CURVATURE OF EACH ROW.
        PROGRAM EDEN
        DIMENSION CLEM(11,11), X(11),Y(11),RR(3,11),RRM(11),ROW(11)
        COMMON X,Y
        IGY=1
C               DETERMINES WHICH AXIS TO CALCULATE CURVATURE FOR
        WRITE(6,99)
99      FORMAT(' OUTPUT FOR CURVATURE OF LONG AXIS(1) OR SHORT AXIS(2)?')
        ACCEPT*,NE
1       WRITE(6,100)
C   ASKS FOR PIECE # OF PIECE TO BE ANALYZED
100     FORMAT('  PIECE#, K=')
5       ACCEPT*,K
        IF(K.LE.0) GOTO 400
        IF(IGY.GT.3) GOTO 400
C   PROGRAM JUMPS THROUGH DATA TO FIND PIECE # REQUESTED.
        DO 10 I=1,150
        READ(12,112) L
        IF(K.EQ.L) GOTO 20
10      CONTINUE
112     FORMAT(I2)
        WRITE(6,103)
103     FORMAT('     PLEASE TRY ANOTHER VALUE FOR K'     )
        GOTO 5
C   READS IN DAT FOR PIECE REQUESTED
20      DO 30 J=1,11
        READ(12,104) (CLEM(J,N),N=1,11)
30      CONTINUE
104     FORMAT(11(3X,F4.3))
        WRITE(13,105) K
105     FORMAT('1  SHEET #',I2,' CALC. VALUES FOR RADIUS AND CENTER PT.')
        DO 300 J=1,11
C   INITIALIZES FOR A PARTICULAR PIECE
        LL=0
        RSQT=0.
        RT=0.
        YT=0.
        XT=0.
        DEV=0.
C   SETS UP X AND Y VALUES FOR A PARTICULAR ROW
        DO 150 I=1,11
        X(I)=(FLOAT(I)-1.)*.25
        Y(I)=CLEM(J,I)
150     IF(NE.EQ.1) Y(I)=CLEM(I,J)
        DO 180 I=1,6
        DO 181 M=I+1,7
C   CALCULATES RADIUS BASED ON FOUR POINTS
        CALL RAD(I,M,X0,Y0,R)
C   SUBTRACTS 1/2 SHEET THICKNESS FROM RADIUS
        R=R-.03125
        LL=LL+1
C   TOTALS R,R**2,X0,AND Y0 TO FIND AVERAGES AND STANDARD
C   DEVIATION FOR EACH ROW
        RSQT=RSQT+R**2
        RT=R+RT
        XT=X0+XT
        YT=Y0+YT
181     CONTINUE
```

THE ORIGINAL PRINT ON THE FOLLOWING PAGES IS ILLEGIBLE

```
190       CONTINUE
          SPA=FLOAT(LL)
C     FINDS MEAN AND STANDARD DEVIATION
          RM=RT/SPA
          XOM=XT/SPA
          YOM=YT/SPA
          RSOM=RSOT/SPA
          DEV=SQRT((RSOM-RM**2)/(SPA-1.))
          WRITE(13,106) J
C     PRINTS OUT RADIUS,STANDARD DEVIATION,AND CENTER POINT
106       FORMAT(' ROW#',I2)
          WRITE(13,107) RM,DEV,XOM,YOM
107       FORMAT('  R=',F8.3,'  ST. DEV.=',F12.4,'  X=',F8.3,'  Y=',F8.3)
          RR(IGY,J)=1./RM
300       CONTINUE
          IGY=IGY+1
          GOTO1
400       CONTINUE
          DO 410 JIK=1,11
          RR1=1./RR(1,JIK)
          RR2=1./RR(2,JIK)
          RR3=1./RR(3,JIK)
          RRM(JIK)=(RR1+RR2+RR3)/3.
          ROM(JIK)=(RR1**2+RR2**2+RR3**2)/3.
C     CENTER POINT
410       CONTINUE
C     FINDS THE ACCURACY, REPEATABILITY, AND PLOTS
C     THE CURVATURE (1/R) FOR THREE SAMPLES
          CALL ACCUR(RRM)
          CALL REPT(RRM,ROM)
          CALL OPICTR(RR,3,11)
          STOP
          END
```

```
          SUBROUTINE RAD(I,M,XO,YO,R)
C     THIS SUBPROGRAM CALCULATES THE RADIUS OF CURVATURE
C     FOR FOUR DATA POINTS
          COMMON X(11),Y(11)
          G=Y(I+4)-Y(I)
          H=Y(M+4)-Y(M)
          IF(H.EQ.0.) H=.001
          IF(G.EQ.0.) G=.001
C     SLOPES
          SL1=(X(I)-X(I+4))/G
          SL2=(X(M)-X(M+4))/H
C     Y-INTERCEPTS
          B1=(Y(I)+Y(I+4))/2.-SL1*(X(I)+X(I+4))/2.
          B2=(Y(M)+Y(M+4))/2.-SL2*(X(M)+X(M+4))/2.
          XO=(B2-B1)/(SL2-SL1)
          YO=(SL2*B1-SL1*B2)/(SL2-SL1)
C     AVERAGE RADIUS
          RA1=SQRT((X(I)-XO)**2+(Y(I)-YO)**2)
          RA2=SQRT((X(M)-XO)**2+(Y(I)-YO)**2)
          RA3=SQRT((X(I+4)-XO)**2+(Y(I+4)-YO)**2)
          RA4=SQRT((X(M+4)-XO)**2+(Y(I+4)-YO)**2)
          R=(RA1+RA2+RA3+RA4)/4.
          RETURN
          END
```

```
      SUBROUTINE ACCUR(RRM)
      DIMENSION RRM(11)
C   DETERMINES ACCURACY BY COMPARING AVERAGE VALUES
C   ON OPPOSITE SIDES OF THE CENTER LINE
      VLM=0.
      DO 420 JIK=1,5
      MIK=12-JIK
420   VLM=ABS(RRM(JIK)-RRM(MIK))*200./(RRM(JIK)+RRM(MIK))+VLM
      VLM=VLM/5.
      WRITE(13,430) VLM
430   FORMAT(' NOMINAL PERCENT ACCURACY IS:',F7.3,'%')
      RETURN
      END


      SUBROUTINE REPT(RRM,ROM)
C   DETERMINES REPEATABILITY BY FINDING THE PERCENT
C   STANDARD DEVIATION OF THE THREE SAMPLES AT EACH ROW
      DIMENSION RRM(11),ROM(11)
      REP=0.
      DO 500 J=1,11
500   REP=100*SQRT((ROM(J)-RRM(J)**2)/2.)/RRM(J)+REP
      REP=REP/11.
      WRITE(13,510) REP
510   FORMAT(' NOMINAL PERCENT REPEATABILITY:',F7.3,'%')
      RETURN
      END
```

Radius Along Long Axis

SHEET # 1 CALC. VALUES FOR RADIUS AND CENTER PT.

ROW# 1
R= 4.455 ST. DEV.= 0.1441E+00 X= 1.214 Y= -3.449
ROW# 2
R= 4.663 ST. DEV.= 0.1492E+00 X= 1.221 Y= -3.641
ROW# 3
R= 5.029 ST. DEV.= 0.1279E+00 X= 1.223 Y= -4.035
ROW# 4
R= 5.524 ST. DEV.= 0.7795E-01 X= 1.229 Y= -4.573
ROW# 5
R= 6.769 ST. DEV.= 0.7316E-01 X= 1.220 Y= -5.926
ROW# 6
R= 7.593 ST. DEV.= 0.1295E+00 X= 1.201 Y= -6.804
ROW# 7
R= 6.750 ST. DEV.= 0.1216E+00 X= 1.214 Y= -5.913
ROW# 8
R= 5.814 ST. DEV.= 0.1551E+00 X= 1.230 Y= -4.902
ROW# 9
R= 5.368 ST. DEV.= 0.2333E+00 X= 1.231 Y= -4.428
ROW#10
R= 5.074 ST. DEV.= 0.2699E+00 X= 1.267 Y= -4.138
ROW#11
R= 4.993 ST. DEV.= 0.3717E+00 X= 1.164 Y= -4.087

SHEET # 2 CALC. VALUES FOR RADIUS AND CENTER PT.

ROW# 1
R= 4.714 ST. DEV.= 0.2487E+00 X= 1.261 Y= -3.739
ROW# 2
R= 4.840 ST. DEV.= 0.1549E+00 X= 1.261 Y= -3.639
ROW# 3
R= 5.126 ST. DEV.= 0.1263E+00 X= 1.273 Y= -4.145
ROW# 4
R= 5.761 ST. DEV.= 0.1242E+00 X= 1.307 Y= -4.819
ROW# 5
R= 6.881 ST. DEV.= 0.8121E-01 X= 1.304 Y= -6.039
ROW# 6
R= 8.141 ST. DEV.= 0.1438E+00 X= 1.307 Y= -7.377
ROW# 7
R= 7.655 ST. DEV.= 0.1862E+00 X= 1.305 Y= -6.867
ROW# 8
R= 6.492 ST. DEV.= 0.1709E+00 X= 1.293 Y= -5.643
ROW# 9
R= 6.185 ST. DEV.= 0.3215E+00 X= 1.280 Y= -5.335
ROW#10
R= 5.465 ST. DEV.= 0.2258E+00 X= 1.227 Y= -4.605
ROW#11
R= 5.252 ST. DEV.= 0.2655E+00 X= 1.210 Y= -4.410

SHEET # 3 CALC. VALUES FOR RADIUS AND CENTER PT.

ROW# 1
R= 4.658 ST. DEV.= 0.2114E+00 X= 1.310 Y= -3.651
ROW# 2
R= 4.805 ST. DEV.= 0.1679E+00 X= 1.316 Y= -3.781
ROW# 3
R= 5.180 ST. DEV.= 0.1255E+00 X= 1.323 Y= -4.184
ROW# 4
R= 5.696 ST. DEV.= 0.7762E-01 X= 1.348 Y= -4.738
ROW# 5
R= 6.809 ST. DEV.= 0.4651E-01 X= 1.360 Y= -5.949
ROW# 6
R= 8.144 ST. DEV.= 0.9323E-01 X= 1.357 Y= -7.370
ROW# 7
R= 7.348 ST. DEV.= -0.1666E+00 X= 1.354 Y= -6.529
ROW# 8
R= 6.256 ST. DEV.= 0.2087E+00 X= 1.358 Y= -5.357
ROW# 9
R= 5.782 ST. DEV.= 0.3003E+00 X= 1.358 Y= -4.852
ROW#10
R= 5.444 ST. DEV.= 0.3335E+00 X= 1.332 Y= -4.515
ROW#11
R= 5.291 ST. DEV.= 0.4350E+00 X= 1.298 Y= -4.385

Radius Along Long Axis

SHEET # 4 CALC. VALUES FOR RADIUS AND CENTER PT.

POW# 1
R= 6.819 ST. DEV.= 0.4575E+00 X= 1.246 Y= -6.149
FCW# 2
R= 7.092 ST. DEV.= 0.3444E+00 X= 1.268 Y= -6.402
FCW# 3
R= 7.751 ST. DEV.= 0.3148E+00 X= 1.274 Y= -7.063
FCW# 4
R= 8.681 ST. DEV.= 0.2803E+00 X= 1.291 Y= -8.006
FCW# 5
R= 10.475 ST. DEV.= 0.3278E+00 X= 1.287 Y= -9.848
FCW# 6
R= 13.015 ST. DEV.= 0.3291E+00 X= 1.296 Y= -12.435
FCW# 7
R= 12.434 ST. DEV.= 0.5115E+00 X= 1.285 Y= -11.845
FCW# 8
R= 9.744 ST. DEV.= 0.2769E+00 X= 1.273 Y= -9.109
FCW# 9
R= 8.743 ST. DEV.= 0.3555E+00 X= 1.270 Y= -8.096
FCW#10
R= 8.422 ST. DEV.= 0.5248E+00 X= 1.279 Y= -7.790
FCW#11
R= 8.722 ST. DEV.= 0.5971E+00 X= 1.292 Y= -7.505

SHEET # 5 CALC. VALUES FOR RADIUS AND CENTER PT.

FCW# 1
R= 6.322 ST. DEV.= 0.3070E+00 X= 1.306 Y= -5.578
FCW# 2
R= 6.549 ST. DEV.= 0.2382E+00 X= 1.281 Y= -5.792
FCW# 3
R= 7.295 ST. DEV.= 0.2052E+00 X= 1.277 Y= -6.559
FCW# 4
R= 8.255 ST. DEV.= 0.1149E+00 X= 1.290 Y= -7.544
FCW# 5
R= 10.170 ST. DEV.= 0.1147E+00 X= 1.307 Y= -9.514
FCW# 6
R= 11.665 ST. DEV.= 0.1998E+00 X= 1.334 Y= -11.038
FCW# 7
R= 10.941 ST. DEV.= 0.2685E+00 X= 1.335 Y= -10.306
FCW# 8
R= 8.985 ST. DEV.= 0.1772E+00 X= 1.320 Y= -8.308
FCW# 9
R= 8.384 ST. DEV.= 0.2851E+00 X= 1.308 Y= -7.715
FCW#10
R= 7.711 ST. DEV.= 0.2945E+00 X= 1.300 Y= -7.051
FCW#11
R= 7.306 ST. DEV.= 0.3472E+00 X= 1.305 Y= -6.660

SHEET # 6 CALC. VALUES FOR RADIUS AND CENTER PT.

FCW# 1
R= 6.915 ST. DEV.= 0.4877E+00 X= 1.250 Y= -6.141
FCW# 2
R= 6.861 ST. DEV.= 0.2828E+00 X= 1.261 Y= -6.155
FCW# 3
R= 7.672 ST. DEV.= 0.2565E+00 X= 1.266 Y= -6.978
FCW# 4
R= 8.768 ST. DEV.= 0.1729E+00 X= 1.277 Y= -8.099
FCW# 5
R= 11.381 ST. DEV.= 0.2033E+00 X= 1.264 Y= -10.780
FCW# 6
R= 14.784 ST. DEV.= 0.6824E+00 X= 1.284 Y= -14.236
FCW# 7
R= 12.371 ST. DEV.= 0.3657E+00 X= 1.276 Y= -11.792
FCW# 8
R= 9.912 ST. DEV.= 0.3115E+00 X= 1.264 Y= -9.291
FCW# 9
R= 8.851 ST. DEV.= 0.2712E+00 X= 1.252 Y= -8.228
FCW#10
R= 8.330 ST. DEV.= 0.3886E+00 X= 1.269 Y= -7.713
FCW#11
R= 8.160 ST. DEV.= 0.5914E+00 X= 1.292 Y= -7.553

Radius Along Long Axis

SHEET # 7 CALC. VALUES FOR RADIUS AND CENTER PT.

ROW# 1
R= 5.242 ST. DEV.= 0.2282E+00 X= 1.324 Y= -4.354
ROW# 2
R= 5.301 ST. DEV.= 0.1663E+00 X= 1.299 Y= -4.425
ROW# 3
R= 5.456 ST. DEV.= 0.1487E+00 X= 1.263 Y= -4.600
ROW# 4
R= 5.750 ST. DEV.= 0.1470E+00 X= 1.269 Y= -4.928
ROW# 5
R= 6.098 ST. DEV.= 0.1810E+00 X= 1.264 Y= -5.305
ROW# 6
R= 6.364 ST. DEV.= 0.1925E+00 X= 1.275 Y= -5.585
ROW# 7
R= 6.223 ST. DEV.= 0.1867E+00 X= 1.265 Y= -5.426
ROW# 8
R= 5.926 ST. DEV.= 0.1901E+00 X= 1.305 Y= -5.092
ROW# 9
R= 5.780 ST. DEV.= 0.2476E+00 X= 1.306 Y= -4.933
ROW#1
R= 5.577 ST. DEV.= 0.2631E+00 X= 1.298 Y= -4.726
ROW#11
R= 5.340 ST. DEV.= 0.2377E+00 X= 1.276 Y= -4.483

SHEET # 8 CALC. VALUES FOR RADIUS AND CENTER PT.

ROW# 1
R= 5.311 ST. DEV.= 0.2461E+00 X= 1.267 Y= -4.461
ROW# 2
R= 5.393 ST. DEV.= 0.2093E+00 X= 1.248 Y= -4.548
ROW# 3
R= 5.622 ST. DEV.= 0.1902E+00 X= 1.235 Y= -4.799
ROW# 4
R= 5.889 ST. DEV.= 0.1818E+00 X= 1.230 Y= -5.088
ROW# 5
R= 6.228 ST. DEV.= 0.1896E+00 X= 1.229 Y= -5.452
ROW# 6
R= 6.464 ST. DEV.= 0.1666E+00 X= 1.244 Y= -5.696
ROW# 7
R= 6.317 ST. DEV.= 0.1590E+00 X= 1.262 Y= -5.529
ROW# 8
R= 6.057 ST. DEV.= 0.1961E+00 X= 1.292 Y= -5.228
ROW# 9
R= 5.914 ST. DEV.= 0.2423E+00 X= 1.298 Y= -5.071
ROW#1
R= 5.695 ST. DEV.= 0.2431E+00 X= 1.288 Y= -4.842
ROW#11
R= 5.399 ST. DEV.= 0.2212E+00 X= 1.277 Y= -4.532

SHEET # 9 CALC. VALUES FOR RADIUS AND CENTER PT.

ROW#
R= 5.304 ST. DEV.= 0.2483E+00 X= 1.306 Y= -4.442
ROW# 2
R= 5.446 ST. DEV.= 0.1876E+00 X= 1.286 Y= -4.604
ROW# 3
R= 5.582 ST. DEV.= 0.1899E+00 X= 1.279 Y= -4.744
ROW# 4
R= 5.843 ST. DEV.= 0.1786E+00 X= 1.269 Y= -5.033
ROW# 5
R= 6.169 ST. DEV.= 0.1946E+00 X= 1.253 Y= -5.392
ROW# 6
R= 6.561 ST. DEV.= 0.2069E+00 X= 1.273 Y= -5.800
ROW# 7
R= 6.518 ST. DEV.= 0.2577E+00 X= 1.299 Y= -5.736
ROW# 8
R= 6.196 ST. DEV.= 0.2744E+00 X= 1.333 Y= -5.371
ROW# 9
R= 5.984 ST. DEV.= 0.3048E+00 X= 1.330 Y= -5.143
ROW#10
R= 5.890 ST. DEV.= 0.3760E+00 X= 1.343 Y= -5.034
ROW#11
R= 5.655 ST. DEV.= 0.3518E+00 X= 1.325 Y= -4.795

Radius Along Long Axis

SHEET #10 CALC. VALUES FOR RADIUS AND CENTER PT.

ROW# 1
R= 5.891 ST. DEV.= 0.9594E-01 X= 1.221 Y= -5.178
ROW# 2
R= 6.023 ST. DEV.= 0.1274E+00 X= 1.220 Y= -5.324
ROW# 3
R= 6.101 ST. DEV.= 0.1923E+00 X= 1.215 Y= -5.408
ROW# 4
R= 6.004 ST. DEV.= 0.1585E+00 X= 1.217 Y= -5.298
ROW# 5
R= 5.961 ST. DEV.= 0.2034E+00 X= 1.225 Y= -5.243
ROW# 6
R= 5.942 ST. DEV.= 0.1962E+00 X= 1.247 Y= -5.219
ROW# 7
R= 5.936 ST. DEV.= 0.1850E+00 X= 1.256 Y= -5.194
ROW# 8
R= 5.953 ST. DEV.= 0.1613E+00 X= 1.263 Y= -5.214
ROW# 9
R= 5.980 ST. DEV.= 0.1329E+00 X= 1.277 Y= -5.235
ROW#10
R= 5.971 ST. DEV.= 0.1209E+00 X= 1.289 Y= -5.217
ROW#11
R= 5.831 ST. DEV.= 0.9555E-01 X= 1.292 Y= -5.058

SHEET #11 CALC. VALUES FOR RADIUS AND CENTER PT.

ROW# 1
R= 6.020 ST. DEV.= 0.1610E+00 X= 1.297 Y= -5.273
ROW# 2
R= 6.168 ST. DEV.= 0.1720E+00 X= 1.294 Y= -5.439
ROW# 3
R= 6.189 ST. DEV.= 0.1786E+00 X= 1.295 Y= -5.460
ROW# 4
R= 6.210 ST. DEV.= 0.1864E+00 X= 1.296 Y= -5.482
ROW# 5
R= 6.178 ST. DEV.= 0.1939E+00 X= 1.301 Y= -5.442
ROW# 6
R= 6.166 ST. DEV.= 0.2394E+00 X= 1.312 Y= -5.417
ROW# 7
R= 6.142 ST. DEV.= 0.1894E+00 X= 1.313 Y= -5.392
ROW# 8
R= 6.169 ST. DEV.= 0.1776E+00 X= 1.316 Y= -5.420
ROW# 9
R= 6.215 ST. DEV.= 0.1494E+00 X= 1.312 Y= -5.473
ROW#10
R= 6.190 ST. DEV.= 0.9812E-01 X= 1.306 Y= -5.459
ROW#11
R= 6.018 ST. DEV.= 0.5572E-01 X= 1.298 Y= -5.265

SHEET #12 CALC. VALUES FOR RADIUS AND CENTER PT.

ROW# 1
R= 5.746 ST. DEV.= 0.1023E+00 X= 1.255 Y= -4.994
ROW# 2
R= 5.890 ST. DEV.= 0.1154E+00 X= 1.254 Y= -5.155
ROW# 3
R= 5.978 ST. DEV.= 0.1433E+00 X= 1.259 Y= -5.246
ROW# 4
R= 5.997 ST. DEV.= 0.1637E+00 X= 1.260 Y= -5.264
ROW# 5
R= 5.962 ST. DEV.= 0.1908E+00 X= 1.263 Y= -5.218
ROW# 6
R= 5.945 ST. DEV.= 0.1951E+00 X= 1.279 Y= -5.188
ROW# 7
R= 5.938 ST. DEV.= 0.1716E+00 X= 1.287 Y= -5.177
ROW# 8
R= 5.938 ST. DEV.= 0.1669E+00 X= 1.294 Y= -5.172
ROW# 9
R= 6.024 ST. DEV.= 0.1521E+00 X= 1.292 Y= -5.268
ROW#10
R= 6.051 ST. DEV.= 0.1047E+00 X= 1.283 Y= -5.303
ROW#11
R= 5.976 ST. DEV.= 0.8113E-01 X= 1.277 Y= -5.224

Radius Along Short Axis

SHEET # 1 CALC. VALUES FOR RADIUS AND CENTER PT.

ROW# 1
R= 4.928 ST. DEV.= 0.3555E+00 X= -1.185 Y= -3.986
ROW# 2
R= 5.029 ST. DEV.= 0.2200E+00 X= -1.188 Y= -4.092
ROW# 3
R= 5.556 ST. DEV.= 0.2350E+00 X= -1.126 Y= -4.688
ROW# 4
R= 6.234 ST. DEV.= 0.1238E+00 X= -1.102 Y= -5.404
ROW# 5
R= 7.265 ST. DEV.= 0.1746E+00 X= -1.109 Y= -6.504
ROW# 6
R= 7.799 ST. DEV.= 0.1484E+00 X= -1.134 Y= -7.048
ROW# 7
R= 6.891 ST. DEV.= 0.1223E+00 X= -1.115 Y= -6.101
ROW# 8
R= 5.967 ST. DEV.= 0.9300E-01 X= -1.142 Y= -5.120
ROW# 9
R= 5.249 ST. DEV.= 0.1313E+00 X= -1.150 Y= -4.355
ROW#10
R= 4.819 ST. DEV.= 0.1570E+00 X= -1.176 Y= -3.887
ROW#11
R= 4.591 ST. DEV.= 0.1956E+00 X= -1.164 Y= -3.667

SHEET # 2 CALC. VALUES FOR RADIUS AND CENTER PT.

ROW# 1
R= 5.029 ST. DEV.= 0.2357E+00 X= -1.295 Y= -4.097
ROW# 2
R= 5.192 ST. DEV.= 0.1645E+00 X= -1.219 Y= -4.304
ROW# 3
R= 5.639 ST. DEV.= 0.1822E+00 X= -1.201 Y= -4.778
ROW# 4
R= 6.352 ST. DEV.= 0.1671E+00 X= -1.157 Y= -5.555
ROW# 5
R= 7.186 ST. DEV.= 0.1820E+00 X= -1.170 Y= -6.427
ROW# 6
R= 7.740 ST. DEV.= 0.1750E+00 X= -1.126 Y= -7.016
ROW# 7
R= 6.645 ST. DEV.= 0.1210E+00 X= -1.145 Y= -5.850
ROW# 8
R= 5.905 ST. DEV.= 0.1248E+00 X= -1.148 Y= -5.065
ROW# 9
R= 5.208 ST. DEV.= 0.1153E+00 X= -1.203 Y= -4.294
ROW#10
R= 4.876 ST. DEV.= 0.1555E+00 X= -1.223 Y= -3.923
ROW#11
R= 4.569 ST. DEV.= 0.1819E+00 X= -1.269 Y= -3.572

SHEET # 3 CALC. VALUES FOR RADIUS AND CENTER PT.

ROW# 1
R= 5.123 ST. DEV.= 0.3486E+00 X= -1.288 Y= -4.207
ROW# 2
R= 5.167 ST. DEV.= 0.2480E+00 X= -1.199 Y= -4.283
ROW# 3
R= 5.581 ST. DEV.= 0.2253E+00 X= -1.162 Y= -4.735
ROW# 4
R= 6.286 ST. DEV.= 0.1925E+00 X= -1.121 Y= -5.500
ROW# 5
R= 7.041 ST. DEV.= 0.1480E+00 X= -1.137 Y= -6.288
ROW# 6
R= 8.015 ST. DEV.= 0.1960E+00 X= -1.103 Y= -7.313
ROW# 7
R= 6.947 ST. DEV.= 0.1211E+00 X= -1.141 Y= -6.172
ROW# 8
R= 6.055 ST. DEV.= 0.1217E+00 X= -1.130 Y= -5.245
ROW# 9
R= 5.311 ST. DEV.= 0.1248E+00 X= -1.173 Y= -4.419
ROW#10
R= 4.864 ST. DEV.= 0.1862E+00 X= -1.169 Y= -3.938
ROW#11
R= 4.593 ST. DEV.= 0.2177E+00 X= -1.201 Y= -3.629

Radius Along Short Axis

SHEET # 4 CALC. VALUES FOR RADIUS AND CENTER PT.

ROW# 1
R= 5.095 ST. DEV.= 0.4113E+00 X= 1.399 Y= -4.084
ROW# 2
R= 5.054 ST. DEV.= 0.2304E+00 X= 1.306 Y= -4.086
ROW# 3
R= 5.266 ST. DEV.= 0.1945E+00 X= 1.286 Y= -4.375
ROW# 4
R= 5.499 ST. DEV.= 0.1556E+00 X= 1.244 Y= -4.596
ROW# 5
R= 5.786 ST. DEV.= 0.1176E+00 X= 1.255 Y= -4.903
ROW# 6
R= 6.000 ST. DEV.= 0.1457E+00 X= 1.238 Y= -5.140
ROW# 7
R= 5.853 ST. DEV.= 0.1305E+00 X= 1.264 Y= -4.970
ROW# 8
R= 5.593 ST. DEV.= 0.2120E+00 X= 1.227 Y= -4.705
ROW# 9
R= 5.145 ST. DEV.= 0.1670E+00 X= 1.255 Y= -4.204
ROW#10
R= 4.917 ST. DEV.= 0.2154E+00 X= 1.236 Y= -3.963
ROW#11
R= 4.790 ST. DEV.= 0.2246E+00 X= 1.265 Y= -3.815

SHEET # 5 CALC. VALUES FOR RADIUS AND CENTER PT.

ROW# 1
R= 4.655 ST. DEV.= 0.1915E+00 X= 1.240 Y= -3.689
ROW# 2
R= 4.811 ST. DEV.= 0.1917E+00 X= 1.186 Y= -3.880
ROW# 3
R= 5.045 ST. DEV.= 0.1547E+00 X= 1.189 Y= -4.128
ROW# 4
R= 5.430 ST. DEV.= 0.1588E+00 X= 1.153 Y= -4.562
ROW# 5
R= 5.669 ST. DEV.= 0.1254E+00 X= 1.177 Y= -4.803
ROW# 6
R= 5.924 ST. DEV.= 0.1655E+00 X= 1.150 Y= -5.085
ROW# 7
R= 5.732 ST. DEV.= 0.1079E+00 X= 1.190 Y= -4.861
ROW# 8
R= 5.447 ST. DEV.= 0.1508E+00 X= 1.165 Y= -4.566
ROW# 9
R= 5.076 ST. DEV.= 0.1448E+00 X= 1.203 Y= -4.143
ROW#10
R= 4.813 ST. DEV.= 0.2078E+00 X= 1.194 Y= -3.855
ROW#11
R= 4.642 ST. DEV.= 0.1634E+00 X= 1.244 Y= -3.655

SHEET # 6 CALC. VALUES FOR RADIUS AND CENTER PT.

ROW# 1
R= 4.770 ST. DEV.= 0.2593E+00 X= 1.287 Y= -3.783
ROW# 2
R= 4.864 ST. DEV.= 0.2171E+00 X= 1.234 Y= -3.912
ROW# 3
R= 5.148 ST. DEV.= 0.1606E+00 X= 1.278 Y= -4.193
ROW# 4
R= 5.460 ST. DEV.= 0.1676E+00 X= 1.195 Y= -4.585
ROW# 5
R= 5.745 ST. DEV.= 0.1470E+00 X= 1.207 Y= -4.887
ROW# 6
R= 5.995 ST. DEV.= 0.1935E+00 X= 1.187 Y= -5.160
ROW# 7
R= 5.795 ST. DEV.= 0.1293E+00 X= 1.219 Y= -4.932
ROW# 8
R= 5.451 ST. DEV.= 0.1673E+00 X= 1.200 Y= -4.568
ROW# 9
R= 5.110 ST. DEV.= 0.1875E+00 X= 1.221 Y= -4.185
ROW#10
R= 4.851 ST. DEV.= 0.2479E+00 X= 1.209 Y= -3.898
ROW#11
R= 4.881 ST. DEV.= 0.3682E+00 X= 1.242 Y= -3.904

Radius Along Short Axis

SHEET # 7 CALC. VALUES FOR RADIUS AND CENTER PT.

ROW# 1
R= 10.276 ST. DEV.= 0.5[illegible]E+00 X= -1.376 Y= -10.807
ROW# 2
R= 10.771 ST. DEV.= 0.4724E+00 X= -1.266 Y= -10.308
ROW# 3
R= 11.571 ST. DEV.= 0.5[illegible]E+00 X= -1.240 Y= -11.095
ROW# 4
R= 12.921 ST. DEV.= 0.6861E+00 X= -1.170 Y= -12.453
ROW# 5
R= 15.104 ST. DEV.= 0.6[illegible]E+00 X= -1.209 Y= -14.647
ROW# 6
R= 18.001 ST. DEV.= 0.[illegible]E+00 X= -1.219 Y= -17.564
ROW# 7
R= 17.229 ST. DEV.= 0.3[illegible]E+00 X= -1.213 Y= -16.771
ROW# 8
R= 14.173 ST. DEV.= 0.2844E+00 X= -1.239 Y= -13.708
ROW# 9
R= 11.922 ST. DEV.= 0.3[illegible]E+00 X= -1.255 Y= -11.439
ROW#10
R= 10.543 ST. DEV.= 0.4931E+00 X= -1.210 Y= -10.069
ROW#11
R= 9.643 ST. DEV.= 0.[illegible]E+00 X= -1.269 Y= -9.157

SHEET # 8 CALC. VALUES FOR RADIUS AND CENTER PT.

ROW# 1
R= 10.090 ST. DEV.= 0.4295E+00 X= 1.377 Y= -9.601
ROW# 2
R= 10.659 ST. DEV.= 0.5561E+00 X= 1.292 Y= -10.168
ROW# 3
R= 11.594 ST. DEV.= 0.6136E+00 X= 1.275 Y= -11.096
ROW# 4
R= 13.283 ST. DEV.= 0.1[illegible]E+01 X= 1.201 Y= -12.796
ROW# 5
R= 15.603 ST. DEV.= 0.9184E+00 X= 1.253 Y= -15.131
ROW# 6
R= 18.327 ST. DEV.= 0.8632E+00 X= 1.295 Y= -17.875
ROW# 7
R= 16.826 ST. DEV.= 0.2334E+00 X= 1.411 Y= -16.349
ROW# 8
R= 13.762 ST. DEV.= 0.2593E+00 X= 1.343 Y= -13.268
ROW# 9
R= 11.830 ST. DEV.= 0.3877E+06 X= 1.354 Y= -11.322
ROW#10
R= 10.593 ST. DEV.= 0.5420E+00 X= 1.298 Y= -10.096
ROW#11
R= 9.699 ST. DEV.= 0.4944E+00 X= 1.312 Y= -9.209

SHEET # 9 CALC. VALUES FOR RADIUS AND CENTER PT.

ROW# 1
R= 10.674 ST. DEV.= 0.1120E+01 X= 1.470 Y= -10.177
ROW# 2
R= 10.558 ST. DEV.= 0.5420E+00 X= 1.311 Y= -10.074
ROW# 3
R= 11.405 ST. DEV.= 0.6393E+00 X= 1.169 Y= -10.931
ROW# 4
R= 12.288 ST. DEV.= 0.6719E+00 X= 1.227 Y= -11.796
ROW# 5
R= 14.493 ST. DEV.= 0.5406E+00 X= 1.275 Y= -14.008
ROW# 6
R= 17.680 ST. DEV.= 0.5292E+00 X= 1.301 Y= -17.432
ROW# 7
R= 17.331 ST. DEV.= 0.6630E+00 X= 1.388 Y= -16.864
ROW# 8
R= 13.658 ST. DEV.= 0.2763E+00 X= 1.311 Y= -13.173
ROW# 9
R= 12.170 ST. DEV.= 0.7294E+00 X= 1.349 Y= -11.668
ROW#10
R= 10.809 ST. DEV.= 0.6117E+00 X= 1.306 Y= -10.316
ROW#11
R= 9.815 ST. DEV.= 0.7024E+00 X= 1.348 Y= -9.309

APPENDIX H

SPECTRAL ANALYSIS FOR DIMPLING

Section 5.3.4 refers to a program that was written (and never totally debugged) to analyze the spectral distribution of any set of eleven points on the test sheets. This appendix contains a listing of this FORTRAN program.

In the program, the eleven points were read in, the FFT of these points calculated, and the magnitude of the absolute value squared of the FFT found. This would give an approximation of the magnitude of spacial frequencies on the sheet. If dimpling occurred, there would be a peak around the frequency corresponding to the dimple size, and a comparative measure of its magnitude could be made. Dimpling was not observed in this experiment, so this program was not implemented.

The next few pages show a listing of the program. The FFT subroutine did not work when the program was run. With dimpling effects, a corrected version of this program, or another spectral density approximation method (such as periodogram averaging) could be used to quantify this effect.

```
      PROGRAM FITTY
C   THIS PROGRAM APPROXIMATES THE SPECTRAL DENSITY OF
C   THE SPATIAL FREQUENCY OF DATA POINTS FROM A DDS
C   FORMED SHEET METAL PART.
      DIMENSION CLEM(11,11),RLGA(16)
      LOGICAL CLEAR
      MN=0
1     WRITE(6,100)
5     CONTINUE
C   INPUT THE SHEETS TO BE AVERAGED AND ANALYZED
100   FORMAT('  PIECE #,AND # OF PIECES TO AVERAGE (K,M)')
      ACCEPT*, K,M
      IF(K.EQ.0) GOTO 200
      DO 10 I=1,150
      READ(12,112) L
      IF(K.EQ.L) GOTO 20
10    CONTINUE
112   FORMAT(I2)
      WRITE(6,103)
103   FORMAT('     PLEASE TRY ANOTHER VALUE FOR K'     )
      GOTO 5
C   READ ARRAY FROM DATA FILE FOR ONE PIECE
20    DO 30 J=1,11
      DO 31 N=1,11
      READ(12,104) CLEM(J,N)
31    CONTINUE
30    CONTINUE
104   FORMAT(11(3X,F4.3))
C   THE VARIABLE "CLEAR" DETERMINES HOW MANY POINTS TO AVERAGE
      CLEAR=.TRUE.
      MN=MN+1
      IF(MN.GT.M)GOTO 200
      IF(MN.GT.1) CLEAR=.FALSE.
C   "SPEC" IS THE SUBROUTINE TO CALCULATE THE SPECTRAL DENSITY
      CALL SPEC(CLEM,K,CLEAR,RLGA)
      GOTO 1
C   PLOT THE SPECTRAL DENSITY
200   CALL OPICTR(RLGA,1,16)
      STOP
      END
```

```
C   THIS SUPPROGRAM CALCULATES THE FFT, AND FIGURES THE MAG**2
      SUBROUTINE SPEC(CLEM,K,CLEAR,RLGA)
      LOGICAL CLEAR
      COMPLEX YAP(32)
      DIMENSION CLEM(11,11),RLG(16),RLGS(16),RLGA(16),F(16)
      NLP=13
      IF(.NOT.CLEAR) GOTO 100
      DO 110 I=1,16
      RLGS(I)=0.
110   CONTINUE
      NCOLS=0
100   CONTINUE
      DO 300 J=1,11
      DO 120 I=12,32
C   INPUT ARRAY TO FFT MUST BE COMPLEX
      YAP(I)=CMPLX(0.,0.)
120   CONTINUE
      DO 130 I=1,11
      YAP(I)=CMPLX(CLEM(I,J),0.)
130   CONTINUE
      CALL FFT(YAP,5,1)
      DO 140 I=1,16
C   MAGNITUDE SQUARED OF FFT IS CALCULATED
      RLG(I)=CABS(YAP(I))**2
      F(I)=FLOAT(I)/.25/32.
140   CONTINUE
      IF(J.EQ.1) WRITE(NLP,104)
      WRITE(NLP,103) J,K
      WRITE(NLP,102)(F(I),RLG(I),I=1,16)
102   FORMAT(5(F7.3,E11.3,3X))
103   FORMAT('  COLUMN',I4,'OF PIECE #',I4)
104   FORMAT('1  POWER SPECTRUM OF HEIGHT VARIATION')
      NCOLS=NCOLS+1
      DO 150 I=1,16
      RLGS(I)=RLGS(I)+RLG(I)
150   CONTINUE
300   CONTINUE
      DO 350 I=1,16
      RLGA(I)=RLGS(I)/FLOAT(NCOLS)
350   CONTINUE
      RETURN
      END
```